

Department of Natural Resources  
Resource Assessment Service  
MARYLAND GEOLOGICAL SURVEY  
Richard A. Ortt, Jr., Director

**REPORT OF INVESTIGATIONS NO. 88**

**EXPOSED TRIASSIC BASINS AS PROXIES FOR THE  
UNDERSTANDING OF  
BURIED RIFT SUCCESSIONS**

by

David K. Brezinski  
and  
Rebecca Kavage Adams



DNR 12-041720-225

January 2021



## EXECUTIVE SUMMARY

- Study of rocks exposed in the Culpeper and Gettysburg rift basins provides a foundation for the understanding of buried rift basin stratigraphic successions.
- Recurrent assemblages of rock types are interpreted as representing genetic packages of lithologies herein termed lithofacies associations.
- Five distinct lithofacies associations are recognized, each consisting of aggregated lithologies formed within overlapping depositional systems.
- Named Lithofacies Associations A through E, these groups of lithologies were interpreted to have formed in alluvial fan, braided stream, meandering fluvial, proximal, and distal lake settings.
- When the five lithofacies associations are applied to rocks of the buried Taylorsville basin a revised depositional architecture is elucidated.
- The lithofacies associations approach illustrates that deposition within Triassic rift basins did not form the layer cake geometries commonly portrayed, but rather laterally intergrading alluvial, fluvial, and lacustrine processes from basin margin to center.
- This revised internal stratigraphy provides insight as to areas suitable for long-term carbon dioxide (CO<sub>2</sub>) sequestration within the coarse-grained, fluvial lithofacies associations that are concealed beneath thick intervals of fine-grained lake strata.
- Thick intervals of concordant extrusive and intrusive mafic igneous rocks also provide potential CO<sub>2</sub> reservoirs owing to the primary porosity within lava flow vesicles, and fracture porosity produced by the rapid cooling and contraction of the lava flows and magmatic intrusions.



## TABLE OF CONTENTS

	Page
Abstract .....	1
Introduction .....	2
Triassic Basin Studies .....	2
Origin of Triassic Basins .....	4
Lithostratigraphy .....	4
Newark Supergroup Stratigraphy .....	4
Culpeper Basin Strata .....	4
Sub-Triassic Contact .....	4
Manassas Formation .....	4
Basal Conglomerate Member .....	5
Poolesville Member .....	5
Bull Run Formation .....	7
Leesburg Member .....	9
Groveton Member .....	10
Catharpin Creek Member .....	10
Goose Creek Member .....	11
Upper Culpeper Group .....	11
Gettysburg Basin Strata .....	12
Sub-Triassic Basement .....	12
New Oxford Formation .....	12
Irishtown Member .....	12
Post-Irishtown New Oxford .....	12
Gettysburg Formation .....	14
Unnamed lower member .....	14
Heidlersburg Member .....	14
Conewago Member .....	16
Unnamed upper member .....	16
Lithofacies Associations of the Culpeper and Gettysburg basins .....	19
Areal and temporal distribution of Culpeper and Gettysburg lithofacies associations .....	27
Taylorsville Basin Stratigraphy .....	33
Taylorsville Basin Cover Succession Thickness and Character .....	33
Taylorsville Basin Succession .....	34
Doswell Formation .....	35
Stagg Creek Member .....	35
Vanita Member .....	35
Newfound Member .....	38
Stagg Creek Lithofacies Associations .....	38
Taylorsville Basin Lithofacies Associations .....	39
Stratigraphic Architecture of Triassic Basins .....	41
Triassic Sandstone Characteristics .....	47
Methods .....	47
Results .....	51
Sandstone Composition and Present-day Porosity .....	51
Culpeper Basin, Poolesville Member and Gettysburg Basin, New Oxford Formation .....	51
Gettysburg Basin, Gettysburg Formation, Conewago Member .....	53
Taylorsville Basin, Doswell Formation .....	55
Porosity Types .....	55
Porosity Reduction .....	57
Cements .....	58

Compaction-----	63
Discussion -----	63
Carbon Sequestration Potential -----	68
Potential for Traditional CO <sub>2</sub> Reservoirs -----	69
Culpeper and Gettysburg Basins -----	69
Taylorsville Basin -----	70
Concordant Igneous Bodies as Reservoirs -----	72
Acknowledgements -----	75
References Cited-----	75
Appendix I-----	83
Appendix IA -----	83
Appendix IB-----	84
Appendix II Glossary of Geologic Terms -----	86

## LIST OF ILLUSTRATIONS

	Page
Figure 1. CAM Triassic rift basins of the United States -----	3
Figure 2. Idealized geologic and tectonic cross-section of Maryland -----	3
Figure 3. Generalized stratigraphic nomenclature of the Newark Supergroup -----	5
Figure 4. Geologic map and stratigraphy of the Culpeper Basin -----	6
Figure 5. Measured section of the Tuscarora Creek and Poolesville Members-----	7
Figure 6. Measured section of the Poolesville Member -----	8
Figure 7. Measured section of upper Poolesville and lower Balls Bluff Member-----	9
Figure 8. Measured section at Balls Bluff National Cemetery -----	9
Figure 9. Measured section of the Bull Run Formation, Culpeper Crushed Stone-----	10
Figure 10. Geologic map and stratigraphy of the Gettysburg Basin-----	13
Figure 11. Measured sections of the Irishtown Member -----	15
Figure 12. Measured section of the upper New Oxford Formation-----	15
Figure 13. Measured section of the New Oxford-Gettysburg Transition-----	16
Figure 14. Measured section of the lower Gettysburg Formtion-----	17
Figure 15. Measured section of the Heidlersburg Member -----	18
Figure 16. Measured section of the Conewago Member -----	18
Figure 17. Lithologies of Lithofacies Association A -----	21
Figure 18. Lithologies of Lithofacies Association B -----	23
Figure 19. Lithologies of Lithofacies Association C -----	24
Figure 20. Geologic map of the Emmitsburg Delta -----	26
Figure 21. Lithologies of Lithofacies Association D -----	28
Figure 22. Lithologies of Lithofacies Association E-----	29
Figure 23. Map of the distribution of lithofacies associations in the Culpeper Basin -----	30
Figure 24. Map of the distribution of lithofacies associations in the Gettysburg Basin -----	32
Figure 25. Location and extent of the Taylorsville Basin -----	34
Figure 26. Thickness of Coastal Plain sediments overlying the Taylorsville Basin -----	34
Figure 27. Geologic map of the Doswell Inlier -----	35
Figure 28. Lithologic character of the Doswell Formation -----	36
Figure 29. Graphic measured section along Stagg Creek -----	37
Figure 30. Interpreted vertical stacking of lithofacies association of the Stagg Creek Section ---	39
Figure 31. Examples of lithofacies association within subsurface of the Taylorsville Basin-----	42
Figure 32. Strike-oriented stratigraphic cross-section of the Taylorsville Basin -----	43
Figure 33. Stratigraphic cross-section of the Taylorsville Basin-----	44
Figure 34. Interpreted relations between stratigraphic and seismic cross-sections of the Taylorsville Basin-----	45
Figure 35. Differences in interpretations between geologic and lithofacies association within several CAM Basins -----	46
Figure 36. Location map of sandstone sampling in the Culpeper, Gettysburg, and Taylorsville basins for the report -----	49
Figure 37. Porosity based on hand-specimen and thin-section analysis-----	50
Figure 38. Thin-section porosity evidenced in JMicrovision-----	51
Figure 39. Ternary diagrams of sandstone composition-----	52
Figure 40. Ternary diagrams of sandstone provenance-----	53

Figure 41. Photomicrographs of the Poolesville Member-----	54
Figure 42. Stratigraphic variations in sandstone composition and texture in the Poolesville Member -----	56
Figure 43. Stratigraphic variations in sandstone composition and textures in the New Oxford Formation-----	57
Figure 44. Stratigraphic variations of sandstone texture in the Poolesville Member at Nolands Ferry -----	58
Figure 45. Stratigraphic variations of sandstone composition and texture in the Conewago Member of the Gettysburg Formation-----	59
Figure 46. Stratigraphic variations in sandstone composition and texture in the Doswell Formation along Stagg Creek-----	60
Figure 47. Hand specimen of the Newfound Member of the Doswell Formation-----	61
Figure 48. Photomicrographs of thin-sections of the Doswell Formation-----	61
Figure 49. Thin-section of sandstone porosity evaluated by image analysis-----	62
Figure 50. Photomicrographs of secondary porosity-----	63
Figure 51. Photomicrographs of porosity from feldspar dissolution-----	64
Figure 52. Photomicrographs of pore-filling cements-----	64
Figure 53. Heterogeneity within Poolesville and New Oxford sandstones-----	65
Figure 54. Heterogeneity within sandstones of the Doswell Formation-----	66
Figure 55. Trends in porosity and permeability and their relationship to lithofacies association in the Ellis Well-----	68
Figure 56. Generalized distribution of CO <sub>2</sub> point sources in the Mid-Atlantic Region and their distribution to exposed and buried Triassic basins-----	69
Figure 57. Potential CO <sub>2</sub> reservoir and seal intervals in the Gettysburg, Culpeper and Taylorsville Basins-----	71
Figure 58. Fracture within igneous bodies of the Gettysburg and Culpeper Basins-----	73
Figure 59. Distribution of exposed and buried igneous bodies of the Gettysburg and Culpeper Basins-----	74
Figure 60. Generalized relationship between igneous bodies and lacustrine sediments-----	75

### TABLE CAPTIONS

Table 1. Lithologic coding for illustrations-----	8
Table 2. Lithofacies and environments from Smoot (1991)-----	19
Table 3. Lithofacies associations of the Culpeper and Gettysburg Basins-----	20
Table 4. Differences of estimates of primary porosity based on analytical methods-----	50
Table 5. Average framework grain composition-----	55
Table 6. Average percent porosity within individual lithofacies associations-----	62
Table 7. Average framework grain composition for each depositional basin-----	67

## ABSTRACT

Stratigraphic architecture of the lithofacies associations was studied within the exposed strata of the Culpeper and Gettysburg basins of Pennsylvania, Maryland, and Virginia, as a basis for understanding the buried rock succession of the Taylorsville Basin, Maryland and Virginia. Based upon the study of outcrops in the Culpeper and Gettysburg basins, recurring associations of lithologic facies were identified and deemed the fundamental constructs of basin infilling. These groups of facies, herein termed lithofacies associations, represent genetically related lithologic packages formed by broad depositional systems. These exposed deposits provide insight into the vertical and lateral succession of strata within infilling East Coast rifts. Alluvial fan deposition on both the faulted and overlapping margins of the basin represent the initial depositional episode. These deposits are replaced upsection and basinward by coarse-grained fluvial successions formed initially by braided and then subsequently by meandering fluvial river systems. The fluvial deposits are in turn replaced upward and basinward by fine-grained lacustrine deposits. Along the steep-sided, faulted margins of the basins alluvial fan facies continued to prograde basinward and interfinger with lacustrine deposits to create upward-coarsening and laterally fining successions that fine toward the basin center.

To evaluate the reproducibility of the exposed basin lithofacies model, their facies associations were compared with those known from the Taylorsville Basin, which is buried beneath the Atlantic Coastal Plain. This basin preserves over 8,000 feet of Triassic rocks near its center, but is concealed beneath more than 2,000 feet of Cretaceous and Tertiary Coastal Plain sediments. These younger concealing sediments thin to the west and southwest, where the Taylorsville Basin is partially exposed. The composition and stratigraphic architecture of strata in the Taylorsville Basin are comparable to those exposed in the Culpeper and Gettysburg basins. The infilling of these basins was the result of vertical aggradation and lateral progradation from coarse-grained to fine-grained facies both vertically and laterally towards the basin center.

Triassic rift basins of the eastern United States may provide an opportunity for long-term carbon dioxide (CO<sub>2</sub>) sequestration since their internal stratigraphy presents a number of lithologies that can serve as reservoirs. Both exposed and buried basins are located near large point-source CO<sub>2</sub> producers. Based on thin section analysis of samples from exposed basin strata, porosity values are higher in alluvial fan and braided fluvial lithofacies. Porosity is highest in shallowly buried samples that show less compaction, as well as in high-energy deposits with lower percentages of ductile lithic fragments. Data from the Taylorsville Basin indicate that porosity and permeability values in basin marginal fluvial strata are high, but diminish near the basin center owing to the fine-grained character of the lacustrine deposits.

Several East Coast Triassic basins also contain thick intervals of concordant extrusive and intrusive mafic igneous rocks. These igneous bodies may serve as potential CO<sub>2</sub> reservoirs for several reasons. Firstly, extrusive lava flows provide potential storage in primary porosity formed at the upper surface of the flows. Secondly, both lava flows and subsurface igneous sills exhibit extensive fracture porosity produced by the rapid cooling of the flows and intrusions. Thirdly, these igneous rocks are mafic in composition, and studies have shown that iron- and magnesium-rich mafic rocks provide sequestration opportunities through carbonate remineralization. Lastly, extrusive and intrusive igneous rocks are invariably preserved within fine-grained lake deposits that may serve as confining layers that encase the igneous rocks both above and below.

The findings presented here contradict long-held views of East Coast Triassic rift basin geometry and internal character. This study suggests that rift basin strata are not formed in layer cake geometries as commonly portrayed. Rather, these basins contain a complex internal architecture generated by the intergrading of alluvial, fluvial, and lacustrine processes. These facies appear to provide many suitable sequestration intervals based both on internal character as well as the enveloping succession of strata. Further study can provide refined facies attribution as well as key storage characterizations such as porosity, permeability, lateral distribution, and thickness.

## INTRODUCTION

This report describes and discusses studies carried out by the Maryland Geological Survey (MGS) with the objective of identifying the distribution and genesis of exposed strata of the Culpeper and Gettysburg Triassic rift basins of Maryland, Virginia, and Pennsylvania. This effort and the insight gleaned from it serve as a proxy for understanding the stratigraphic architecture of similar structures buried beneath the Atlantic Coastal Plain. It was an a priori assumption that the stratigraphic and sedimentologic signatures of exposed and buried basins were similar. This premise is based on the belief that because exposed and buried basins were formed at approximately the same time and by the same structural and tectonic forces, their infilling sediments should be comparable. To test the stratigraphic findings from the exposed basins, one of the larger buried Triassic rift basins, the Taylorsville Basin, also was evaluated. The Taylorsville Basin is a mostly buried structure with exposed stratigraphy only within a small inlier near its southwestern corner. Thus, the Taylorsville Basin provides a transition in understanding between those basins known from exposed strata and those that are completely buried.

This effort was initiated and partially funded by the Battelle Memorial Institute as part of its Midwest Region Carbon Sequestration Program (MRCSP) consortium funded by the U.S. Department of Energy that was tasked with identifying potentially suitable geologic areas for long-term storage of carbon dioxide (CO<sub>2</sub>). The remainder of the study was funded by the US Geological Survey EarthMRI and Statemap programs and by the Maryland Geological Survey.

Triassic basins occur near population centers within the Mid-Atlantic region. Furthermore, because these high population areas contain numerous point-source carbon emitters, such as power generators, cement-plants, and oil refineries, there is a need for the identification of potential long-term carbon storage locations within this area. Therefore, the proximity of large-scale carbon producers and Triassic rift basins represents a juxtaposition that may be fortuitous if potential

storage intervals are identified within those basins. While exposed Triassic basins may have diminished utility for this purpose, the greatest potential for long-term CO<sub>2</sub> storage lies with the basins that are buried beneath the eastward-thickening Coastal Plain sediments. These rift basins conceal early Mesozoic strata beneath more than 2,500 feet of Cretaceous and Tertiary sediments. These potential storage sites, however, have been evaluated only cursorily as carbon reservoirs (Craddock et al., 2012).

Along the East Coast of North America numerous Triassic rift basins occur stretching from Atlantic Canada to Georgia (Figure 1A). Known as the Central Atlantic Margin (CAM) rift system, these structures consist, in the Mid-Atlantic region, of both exposed and buried basin (Figure 1B). In this area, extensive exposed basins extend along the eastern margin of the Blue Ridge and western edge of the Piedmont physiographic provinces (Figure 2). Furthermore, numerous analogous structures are inferred to exist beneath the Atlantic Coastal Plain sediments (Benson, 1992). The Atlantic Coastal Plain physiographic province comprises a body of late Mesozoic and Tertiary strata that are gently inclined eastward from the Fall Line (Figure 2). These sediments cover crystalline rocks of the Piedmont Province that were metamorphosed during numerous orogenic events during the Paleozoic. Within these concealed crystalline basement rocks are subsurface features including fault-bound basins (Benson, 1992).

### Triassic Basin Studies

Triassic basins of the eastern North Atlantic continental margin (NAM) have been extensively studied. Recounting those investigations is beyond the scope of the present study; however, the reader is directed to Olsen (1997) for a summary of previous understanding and the references therein. The preponderance of the NAM basin studies have concentrated on their structural origins (Schlische, 1992, 1993; Withjack et al., 1998, 2002, 2012, 2013 and references therein), chronostratigraphy (Cornet, 1977; Cornet and Olsen, 1990; Olsen et

al., 1996; Olsen et al., 1989; Olsen and Kent, 1999), or vertebrate paleontology (Olsen et al., 1989 and references therein). In contrast, the few works of Van Houten (1963) and Smoot (1999, 2010, 2016) are genetic stratigraphic studies that looked at depositional aspects of Triassic basins. In general, there has been a dearth of subsurface or exploratory drilling data. Because of the paucity of drilling data, the internal sedimentary geometries of East Coast rift basins have generally been char-

racterized as simplified tilted faulted basins in which the sedimentary formations are represented as nothing more complex than inclined layers with minor up-ramp thinning (Schlische, 1993, fig. 7; LeTourneau, 2003). For that reason, substantial questions still surround the lithofacies architecture within Mid-Atlantic Triassic rift basins and their prospects as hydrocarbon source and reservoir strata.

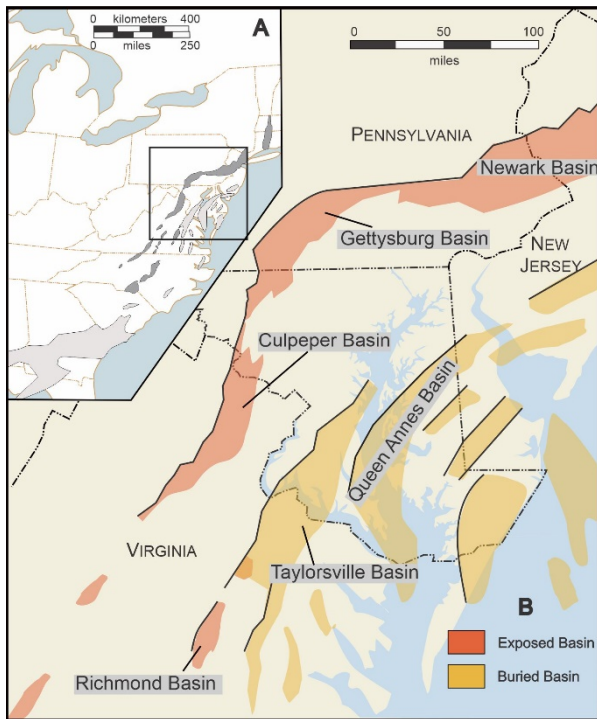


**Figure 1. A, CAM (central Atlantic margin) Triassic rift basins of the United States (modified from Olsen, 1997). B, Rift basins of the Mid-Atlantic region and distribution of exposed and buried Triassic rift basins (from Benson, 1992).**

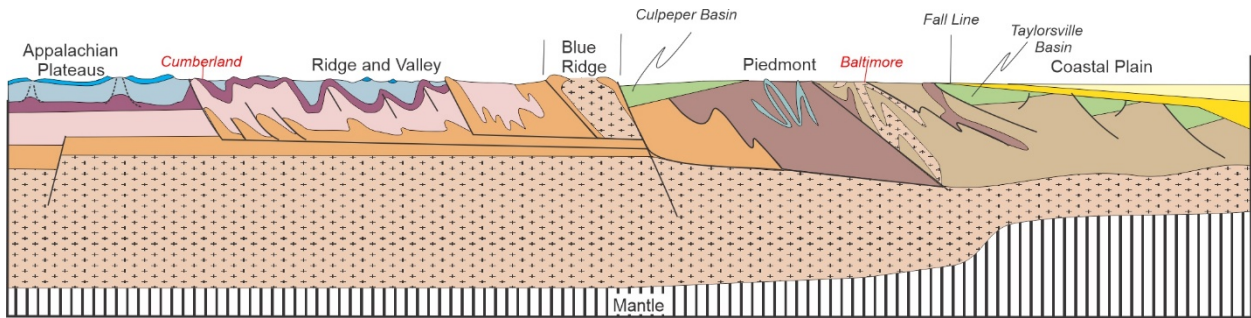


**Figure 2. Idealized geologic and tectonic cross-section of Maryland from the Appalachian Plateaus to Ocean City. Continental crustal thicknesses idealized and modified for Maryland from Olsen et al. (2018, fig. 1.2).**

### **Origin of Triassic Basins**

Extensional tectonics during the Late Triassic (237-201 Mya) produced a series of isolated to semi-isolated fault-bound basins, or half grabens, along the eastern margin of North America. The growth of these basins by subarcuate normal faulting that is listric at depth, attenuated the continental crust and resulted in the fragmentation of the supercontinent Pangea (Figure 2). Many of these faults formed along zones of structural weakness created by Appalachian compressional events of the Late Paleozoic (Schlische, 1993). These grabens became filled by thick successions of Late Triassic terrestrial sediments formed by fluvial, lacustrine, and alluvial fan processes (Olsen, 1997). While exposed and eroded remnants of several of these basinal structures are preserved from North Carolina to the Bay of Fundy in Nova Scotia, Canada, an unknown number are buried, by early Cretaceous sediments, beneath the Atlantic Coastal Plain. Weems et al. (2016) suggested that several of these exposed, now isolated, basins may have originally been connected and that their similar stratigraphy is a product of this congenetic linking.

While study of the exposed basins has been thorough, examination of identical basins buried beneath the Atlantic Coastal Plain and continental shelf has been sparse (Figure 1) (Benson, 1992; LeTourneau, 2003). In these areas similar features known to be buried beneath Cretaceous and Tertiary sediments of the Atlantic Coastal Plain are recognized mainly from seismic and magnetic data (Hansen, 1988; Benson, 1992). These poorly known and inadequately understood features extend from Georgia to the Grand Banks, and provide exploration targets for petroleum exploration as well as long-term carbon storage potential.

## **LITHOSTRATIGRAPHY**

### **Newark Supergroup Stratigraphy**

The Newark Supergroup is the name applied to an aggregate of Late Triassic and Early Jurassic rock formations deposited within the isolated to semi-isolated rift basins along the eastern edge of North America (Luttrell, 1989) (Figure 3). The

term "Newark Supergroup" as introduced by Van Houten (1977) encompasses the formal nomenclatural assemblage of units that are recognized within each of the exposed depositional basins. For this study, stratigraphy of the Culpeper and Gettysburg basins were examined.

### **Culpeper Basin Strata**

The Culpeper Basin extends for 83 miles from Frederick County, Maryland, southward into Madison County, Virginia. The stratigraphic nomenclature employed within this report follows that outlined by Smoot (2016) and is illustrated in Figure 4A. The Culpeper Basin strata are as much as 27,000 feet thick (Olsen et al., 1989), and overlie metasediments of the western Piedmont in Virginia and Montgomery County, Maryland, and Cambrian and Ordovician carbonates of the Frederick Valley Synclinorium in Frederick County, Maryland. Along its western border, the basin abuts the eastern limb of the Blue Ridge Anticlinorium along the Bull Run Mountains in Virginia and Catoctin Mountain in Maryland. The basin fill comprises a succession of continental siliciclastics and carbonates deposited in alluvial, fluvial, and lacustrine environments (Smoot, 2016).

### **Sub-Triassic Contact**

Brezinski (2004) described numerous locations in the northern Culpeper Basin where there is discernable angular discordance between Triassic strata and the underlying Piedmont crystalline rocks. In each case, the coarse clastics of the Manassas Formation are gently inclined westward and overlap the highly folded, and steeply dipping, carbonate rocks of the Frederick Valley or chloritic phyllites of the Urbana and Ijamsville formations in Maryland and the Potomac Terrane in northern Virginia (Southworth et al., 2006).

### **Manassas Formation**

The Manassas Formation (Manassas Sandstone of Roberts, 1928) is present at the base of the Newark Supergroup in the northern Culpeper Basin. Lee (1977) and Lee and Froelich (1989) subdivided this formation into four members, the

Tuscarora Creek, Rapidan, Reston, and Poolesville.

**Basal Conglomeratic Members:** The base of this formation is characterized by thin, discontinuous conglomerates. In Frederick County, Maryland, the conglomerate is termed the Tuscarora Creek Member. At its type section the Tuscarora Creek Member consists of light gray-weathering, mud- and clast-supported carbonate conglomerate with

clasts ranging in size from 0.5 inch to 4.0 inches in diameter. In Montgomery County, Maryland, and Loudoun County, Virginia this basal conglomerate interval consists of loosely cemented quartz pebbles that Lee (1977) termed the Reston Member. Near the southern end of the basin a coeval basal conglomerate, consisting of greenstone clasts, is termed the Rapidan Member.

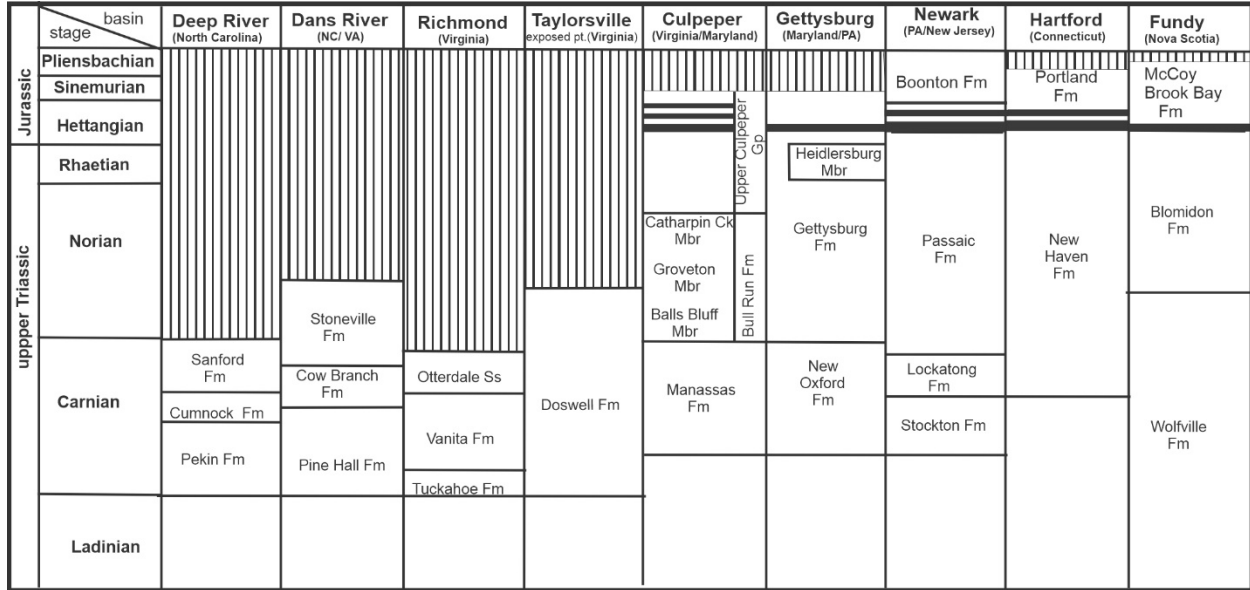


**Figure 3. Generalized stratigraphic nomenclature of Newark Supergroup within individual depositional basins of the Central Atlantic Margin (CAM) (Modified from Luttrell, 1989, pl. 1). Additional stratigraphic references for each basin include: Deep River (Reinemund, 1955), Dan River (Thayer, 1970), Richmond (Ressetar and Taylor, 1988), Taylorsville (Weems, 1980), Culpeper (Smoot, 2016), Gettysburg (Smoot, 1999), Newark (Olsen, 1980), Harford and Deerfield (Hubert et al., 1992), and Fundy (Wade et al., 1996).**

**Poolesville Member:** Above the basal conglomerates, the Manassas Formation consists of alternating intervals of pinkish gray, coarse-grained, pebbly sandstone and red siltstone to mudstone. Lee (1977) and Lee and Froelich (1989) named this part of the formation the Poolesville Member. Lee (1977) estimated the maximum thickness of the Poolesville Member to be 3,270 feet. The lower part of the Poolesville Member is dominated by coarse- to very coarse-grained, gray to pink, trough cross-bedded, pebbly arkosic to subarkosic sandstone. These coarse-grained

sandstones are interbedded with thin intervals of red-brown, massive, deformed, or rooted mudstone containing abundant pedogenic carbonate (Figure 5). This part of the Poolesville Member is as much as 1,500 feet thick in Frederick County, Maryland (Brezinski, 2004), and 3,000 feet thick in Loudoun County, Virginia (Southworth et al., 2006), but feathers out towards the southern end of the basin.

Upsection the sandstone intervals of the Poolesville Member become increasingly finer grained and are pervasively red to reddish brown in color. Typically, sandstones in this part of the

member exhibit convex-down bases with shale-pebble conglomerates, and fine both upward and laterally into fine-grained, platy micaceous, silty sandstone to sandy siltstone. Interbedded with

these sandstone intervals are massive to rooted, red-brown to variegated mudstone containing root casts and carbonate nodules (Figure 6).

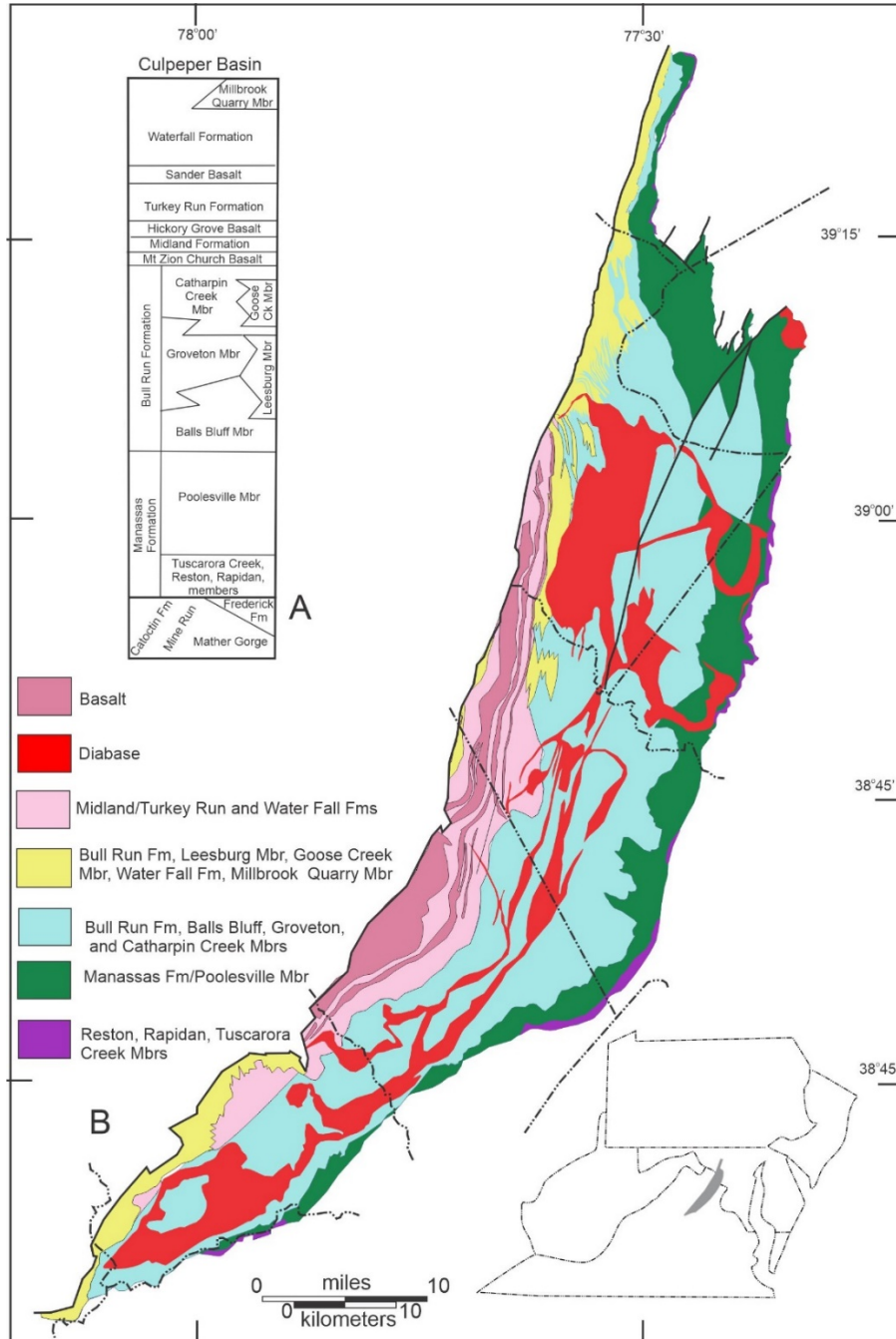


**Figure 4. General geology and stratigraphy of the Culpeper Basin. A. Stratigraphic nomenclature of the Culpeper Basin (Smoot, 2016). B. Generalized geologic map of the Culpeper Basin. Areal distribution of map units based on Leavy et al. (1983), Brezinski (2004), Southworth et al. (2006).**

Near the top of the formation the Poolesville Member contains sandstone units that are fine- to medium-grained, silty, and exhibit gradational bases with reddish brown sandy siltstone that tends to coarsen upwards upsection into massive, red-brown, fine-grained sandstone. These sandstone intervals are interbedded with laminated and mudcracked siltstone, and planar-bedded fine-grained sandstone. This interval of upward coarsening sandstone gradually grades into the overlying massive siltstones of the Bull Run Formation (Figure 7).

### Bull Run Formation

The Manassas Formation gradually transitions upsection into interbedded reddish brown, fine-grained sandstone, laminated sandy siltstone, and massive siltstone originally termed the Balls Bluff Siltstone (Lee, 1977; Lee and Froelich, 1989), but later was assigned member status as part of the Bull Run Formation (Weems and Olsen, 1997; Smoot, 2016). Although Lee (1977) portrayed the Balls

Bluff as primarily a siltstone, many intervals, especially in the lower part, contain fine-grained sandstone and interbedded siltstone and mudstone. Nonetheless, this interval of fine-grained clastics is gradational over several hundred feet with the sandy strata of the upper Poolesville Member of the Manassas Formation (Lee and Froelich, 1989; Weems and Olsen, 1997; Smoot 2016) (Figure 7). Balls Bluff Member: The lower part of the Balls Bluff Member consists of intervals of massive red siltstone and thin-bedded, reddish brown, fine- to medium-grained sandstone that becomes progressively finer grained upsection. These sandy strata have been mapped as a separate unit within the Balls Bluff Member (Southworth et al., 2006). Above the basal sandy strata, the Balls Bluff Member tends to display a more clay-rich character and exhibits vertical (cyclic?) alternations of reddish brown to brownish red, thin- to medium-bedded, locally massive, argillaceous, sandy siltstone to rooted, silty mudstone. Mudcracks, root traces, and irregularly shaped carbonate nodules are common within the mudstone intervals (Figure 8).

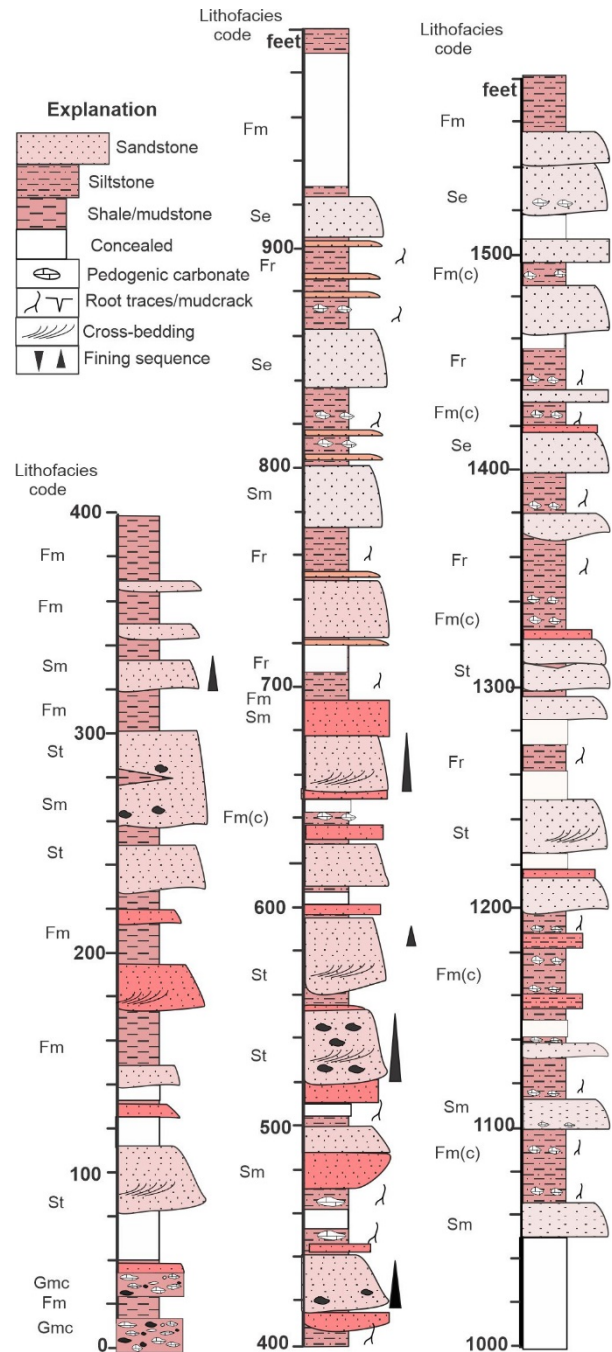


**Figure 5. Composite measured section of the Tuscarora Creek and lower Poolesville members of the Manassas Formation near Nolands Ferry, Frederick County, Maryland. See Table 1 for explanation of lithofacies codes**

From the Potomac River northward into Frederick County, Maryland, the Balls Bluff outcrop belt is very narrow, suggesting that the member is very thin (Figure 4B). However, in Montgomery County, Maryland, and Loudoun County, Virginia broad belts of these siltstone strata indicate thicker preserved intervals of this member in that area. Along the Potomac River in eastern Loudoun County, Virginia, the sandy siltstone strata of the lower Balls Bluff Member are interbedded with thin (<3 feet) distinctive beds of carbonate conglomerate. The interbedding is well displayed within the Balls Bluff County Park (Figure 8). Composite measured section of the Tuscarora Creek and lower Poolesville members of the Manassas Formation near Noland's Ferry, Frederick County, Maryland and National Cemetery in Loudoun County, Virginia (Figure 9). These carbonate conglomerate strata have been shown to thicken to the west where they replace the siltstone strata of the Balls Bluff Member (Southworth et al., 2006). In that area the Balls Bluff Member wedges-out against these carbonate conglomerate beds (Southworth et al., 2006).

Lithofacies Code	Lithology
Gmc	Gravel-cobbles, massive, clast supported
Gmm	Gravel-cobbles, massive to weakly bedded, mud supported
Gg	Gravel-cobbles, graded, normal or inverse
Gt	Gravel-cobbles trough cross-bedded
Gh	Gravel-cobbles, planar stratified
Sm	Sandstone, massive
Sm (s)	Sandstone, massive, abundant scour surfaces
Sm (g)	Sandstone, massive, normal to inverse graded
St	Sandstone, trough cross-bedded
Sp	Sandstone, planar cross-bedded
Se	Sandstone, epsilon cross-stratified
Sh	Sandstone horizontal to planar-bedded
Sr	Sandstone, rippled
Fm	Siltstone/mudstone, massive
Fm (c)	Siltstone/mudstone, massive, carbonate nodules
Fm (e)	Siltstone/mudstone, massive, evaporite casts
Fm (d)	Siltstone/mudstone, massive, deformed
Fl	Siltstone/mudstone, laminated
Fr	Siltstone/mudstone, rooted

**Table 1. Lithology coding in illustrations. Codes modified from Miall (1977).**

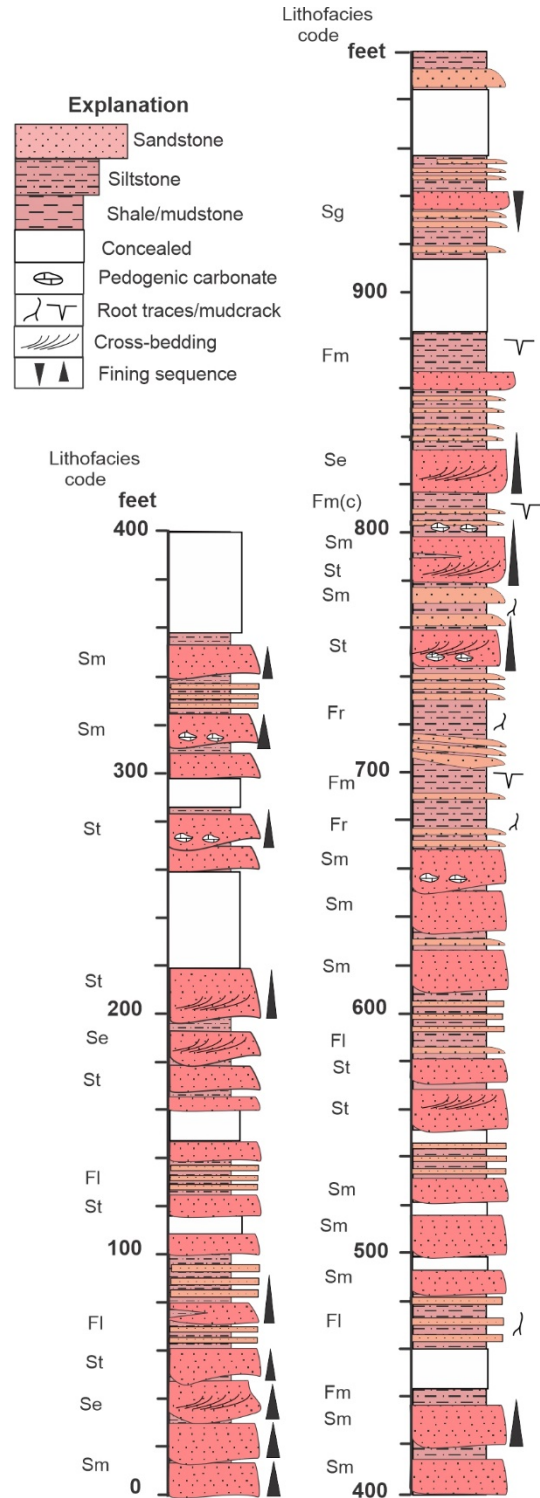


**Figure 6. Measured section of the upper Poolesville Member of the Manassas Formation near Seneca, Montgomery County, Maryland. See Table 1 for explanation of lithofacies codes.**

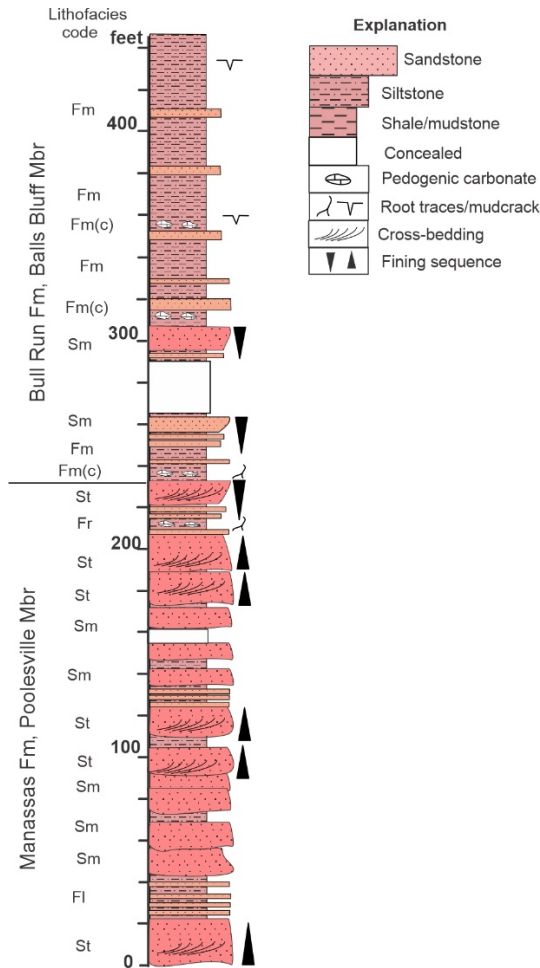


**Figure 7. Measured section of the upper Poolesville Member of the Manassas Formation and lower Balls Bluff Member of the Bull Run Formation along C&O Canal National Historic Park at Marble Quarry, Montgomery County, Maryland. See Table 1 for explanation of lithofacies codes**

**Leesburg Member:** Lee (1977) termed the limestone conglomerates that replace the Balls Bluff Siltstone, especially around the town of Leesburg, Loudoun County, Virginia, the Leesburg Conglomerate. Lee and Froelich (1989) considered this conglomerate to be a member of the Balls Bluff Siltstone; however, Weems and Olson (1997) considered it to be a separate member of the Bull Run Formation. Lee (1977) estimated that the thickness of the Leesburg Member ranges from 630 feet to 3,500 feet.

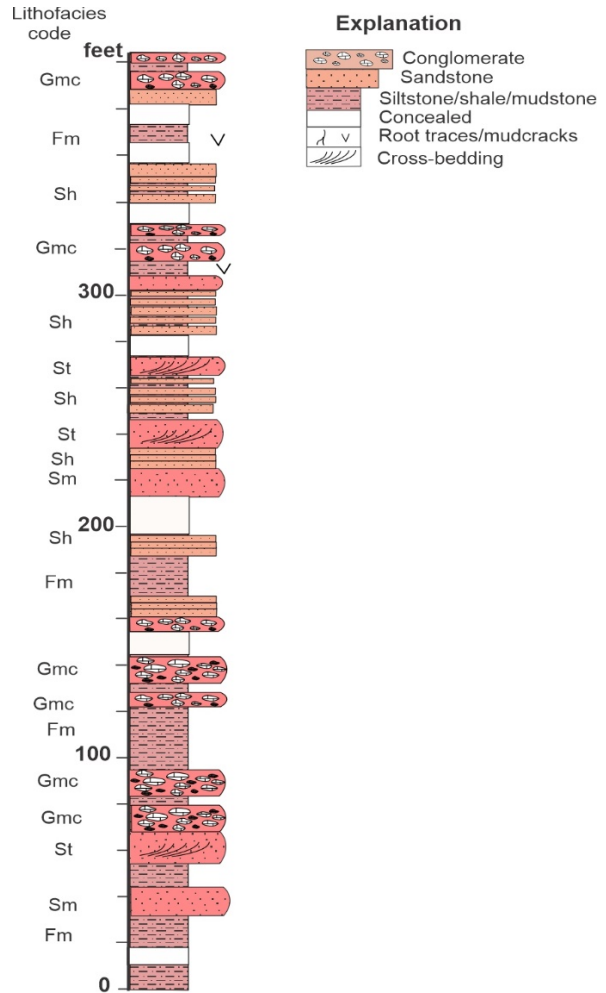


**Figure 8. Measured section through the lower Balls Bluff Member at Balls Bluff National Cemetery, Loudoun County, Virginia. See Table 1 for explanation of lithofacies codes.**

The Leesburg Member is characterized by a light reddish gray, cobble to boulder, limestone and dolomite conglomerate, containing localized thin parting layers of reddish brown, sandy siltstone. Clasts vary in composition from light gray, lime mudstone to tan dolomite, and less commonly reddish brown, sandy siltstone. These clasts are rounded to subangular and range from pebbles less than 0.5 inch in diameter to cobbles more than 1 foot. Stratification consists of thick-bedded, clast- and mud-supported conglomerate intervals that are normal to inversely graded, and generally poorly sorted (Brezinski, 2004, fig. 20 A-D). Clast-



fine- to coarse-grained sandstone, and argillaceous siltstone to mudstone. It can be distinguished from the Groveton Member because it contains a greater percentage of sandstone (Smoot, 2016). The Catharpin Creek Member was estimated to be more than 1,600 feet thick by Lee and Froelich (1989), and more than 3,000 feet thick by Southworth et al. (2006).

**Goose Creek Member:** Along the western margin of its outcrop belt, the Catharpin Creek Member becomes interstratified with lenses and beds of gray-green and reddish brown, pebble to cobble conglomerate. Farther to the west this conglomerate replaces the Catharpin Creek Member (Southworth et al., 2006). Lee and Froelich (1989) named these strata the Goose Creek Member of the Catharpin Creek Formation, but Smoot (2016) considered it a member of the Bull Run Formation (Figure 4A). The Goose Creek Member is an upward coarsening interval that contains interbeds of sandstone near its base and is dominantly conglomeratic upsection and to the west. These conglomerates pinch out to the north and south and are as much as 2,500 feet thick (Southworth et al., 2006).

### Upper Culpeper Group

Sharply overlying the Catharpin Creek Member of the Bull Run Formation is an interval of intercalated basaltic lava flows, reddish sandstone, and red-brown, greenish gray, gray to black shales and conglomerate. Originally named the Buckland Formation (Lindholm, 1979), subsequent authors (Lee and Froelich, 1989; Weems and Olsen, 1997; Smoot, 2016) subdivided each basalt and clastic interval into separate formations. The basal unit, the Mount Zion Church Basalt (Lee, 1977), consists of medium to dark gray, fine to medium crystalline, porphyritic vesicular basalt. The Mount Zion Church Basalt extends for more than 30 miles along the strike of the basin, and pinches out near Haymarket in the northeast, and along the border fault to the southwest. It ranges in thickness from nearly 280 feet in the north to 10 feet thick in southern Fauquier County, Virginia. The formation is composed of several individual lava flows

separated by intervening intervals of gray to dusky-red, micaceous sandstone and siltstone.

Overlying the Mount Zion Church Basalt is a succession of interbedded, dark reddish brown, cross-bedded, medium-grained sandstone, reddish brown siltstone, and greenish gray to dark gray, calcareous shale, with thin argillaceous limestone termed the Midland Formation (Lee and Froelich, 1989). Locally, conglomeratic and coarse-grained, reddish brown, sandstone lenses are present within this unit (Southworth et al., 2006). These coarser layers are interspersed with shaly layers that exhibit abundant mudcracks. The Midland Formation ranges from 500 feet in thickness to the south to more than 980 feet to the north (Lee and Froelich, 1989).

Above the Midland Formation is a second succession of basaltic lava flows named the Hickory Grove Basalt (Lee and Froelich, 1989). This unit occurs as two separate flows, and consists of medium to dark gray, coarsely crystalline basalt flows separated by an interval of reddish sandstone and siltstone up to 160 feet thick. Vesicular intervals are present along the upper surface of each flow. The Hickory Grove Basalt ranges in thickness from 260 to 700 feet.

Overlying the Hickory Grove Basalt is an interval of interbedded sandstone, siltstone, shale, and conglomerate that Lee and Froelich (1989) named the Turkey Run Formation. The Turkey Run Formation consists of cyclic-bedded, red to grayish green, micaceous, ripple-laminated, cross-bedded, thick-bedded to massive, coarse-grained sandstone and reddish-brown siltstone and silty shale and local conglomerate (Southworth et al., 2006). The Turkey Run Formation ranges in thickness from 500 to 700 feet (Southworth et al., 2006).

Above the Turkey Run Formation is a third lava flow that is known as the Sander Basalt (Lee and Froelich, 1989). The Sander Basalt is medium to dark gray, and microcrystalline. The upper part of this flow exhibits vesicles. The Sander Basalt is composed of three or more different lava flows that are separated by intervals of sandstone and siltstone. These clastic intervals are reddish gray, micaceous, coarse-grained and pebbly. The Sander Basalt ranges from 500 to 800 feet in thickness.

Overlying the Sander Basalt is another interval of interbedded reddish sandstone, greenish gray siltstone, mudstone, conglomerate, and limestone termed the Waterfall Formation (Lindholm, 1979). The Waterfall Formation is the stratigraphically highest formation of the Culpeper Group. Hentz (1985) showed that this formation locally consisted of polymictic conglomerates that intertongue with cyclic, fluvial sandstone and mudstone, gray lacustrine mudstone, argillaceous limestone, and calcareous sandstone. Its maximum thickness is 4,500 feet (Hentz, 1985).

The top of the Waterfall Formation is marked by the Millbrook Quarry Member (Lee and Froelich, 1989). This wedge-shaped unit consists of thick-bedded to massive, polymictic, cobble conglomerate. Lee and Froelich (1989) estimated the thickness of this conglomerate at nearly 1,500 feet.

### **Gettysburg Basin Strata**

The Gettysburg Basin is a composite rift basin containing Late Triassic clastic and Jurassic igneous rocks (Figure 10A). For the purpose of this report the Gettysburg Basin extends from the western limits of Frederick City in Frederick County, Maryland, to the Susquehanna River in Pennsylvania where the narrow neck of Triassic sediments connects it with the Newark Basin (Figure 10B). Although these strata are continuous with those of the Newark Basin of eastern Pennsylvania and New Jersey, these strata have traditionally supported their own stratigraphic nomenclature.

### **Sub-Triassic Basement**

Triassic strata of the Gettysburg Basin overlap a variety of Cambrian carbonate strata of the Frederick Valley Synclinorium, the western Conestoga Valley, and early Paleozoic phyllites and schists of the Westminster Terrane along its eastern margin (Stose and Bascom, 1929; Stose and Jonas, 1939; Brezinski, 2004) (Figure 10). Along its western margin, composite ramping of the border fault gives the Gettysburg Basin its arcuate appearance as it abuts the metasediments and metavolcanics of the northern Blue Ridge

(Schlische, 1993). The basin is filled by a succession of continental siliciclastics and carbonates deposited in alluvial, fluvial and lacustrine environments as well as Early Jurassic igneous rocks.

### **New Oxford Formation**

The lowest stratigraphic unit in the Gettysburg Basin is the New Oxford Formation (Stose and Bascom, 1929). This unit is correlative, both in composition and stratigraphic position, to the Manassas Formation of the Culpeper Basin and the Stockton Formation of the Newark Basin (Weems and Olsen, 1997).

**Irishtown Member:** The lowest strata of the New Oxford Formation consist of interbedded reddish to red-brown, and locally gray shale, red mudstone, fine-grained sandstone, and polymictic and quartz-rich conglomerates (Brezinski, 2004, fig. 22A, B). Weems et al. (2016) termed this interval the Irishtown Member. Although its name was confined to areas of southern Pennsylvania, its usage is herein extended into Maryland. While conglomerates are a minor component of the Irishtown Member in its type section, locally they are the dominant lithologic component of the member. Weems et al. (2016) stated that the Irishtown Member is about 30 feet thick near its type section, however Brezinski (2004) found that a correlative conglomeratic interval in Maryland was as much as 150 feet thick (Figure 11).

**Post-Irishtown New Oxford Formation:** Above the Irishtown Member, the New Oxford Formation consists of pinkish gray, very coarse-grained, pebbly, trough cross-bedded, arkosic sandstones that are interbedded with reddish, rooted siltstone and massive mudstone. These coarse-grained, gray sandstones are widespread in northern Frederick and Carroll counties in Maryland, but wedge out northward into Pennsylvania. They are replaced upward by dusky red to red-brown, lenticular, medium- to thick-bedded, fine- to medium-grained, argillaceous sandstone. These lenticular sandstones exhibit sharp basal contacts, and basal lag conglomerates, range in thickness from 15 to 45

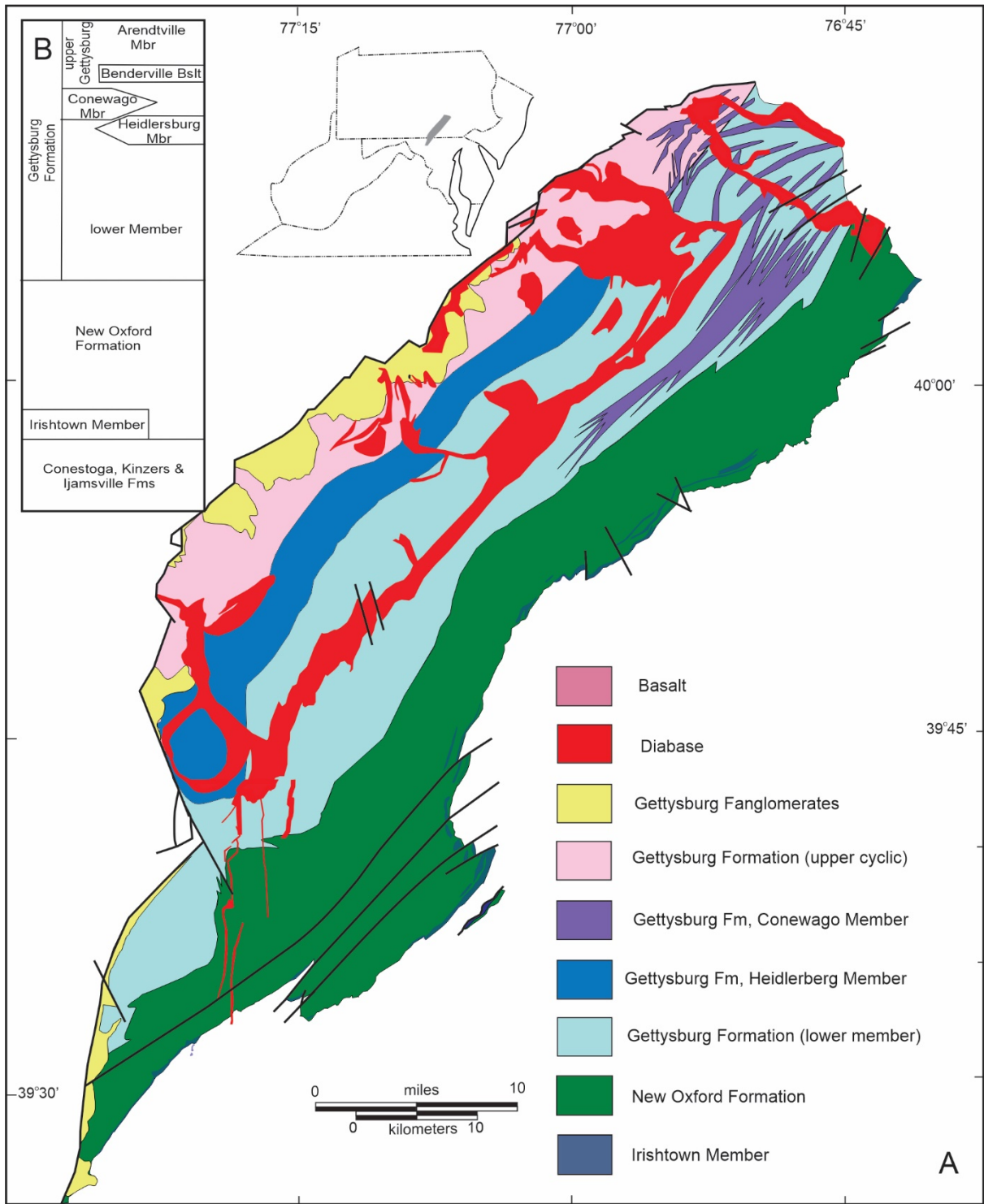


**Figure 10. General geology and stratigraphy of the Gettysburg Basin. A, Stratigraphic unit distribution modified from Stose (1932), Stose and Jonas (1939), Berg et al. (1980), and Brezinski (2004, 2021). B, Stratigraphic nomenclature of the Gettysburg Basin modified from Smoot (1999).**

feet, and locally display large-scale, epsilon cross-stratification. Interbedded with these sandstone units are intervals of red-brown, sandy siltstone and red, rooted mudstone. The tops of these sandstone units typically grade into thin-bedded to platy, micaceous, sandy siltstone to silty, fine-grained sandstone intervals and then into the rooted mudstone layers. The mudstone intervals contain abundant root-casts and locally display buff weathering to light gray caliche nodules (Figure 12) (Brezinski, 2004, fig. 21D). Locally, these lenticular sandstones can exceed 50 feet in thickness.

The uppermost several hundred feet of the New Oxford Formation consist of red-brown, fine-grained, argillaceous, medium-bedded to massive sandstone, interbedded with laminated siltstone and shale and massive, rooted mudstone. The fine-grained sandstone intervals often exhibit an upward-coarsening character from platy, laminated, silty sandstone, to medium-bedded, fine- to medium-grained sandstone to massive, medium-grained sandstone. The thickness of the New Oxford Formation has been estimated at between 6,800 (Smoot, 1999) and 8,000 feet (Root, 1988).

The contact between the New Oxford Formation and overlying Gettysburg Formation is gradational (Smoot, 1999). The top of the New Oxford Formation is recognized by the reduced prominence of fine-grained sandstones and increased percentages of laminated, mudcracked siltstone and massive, rooted mudstone (Figure 13). This transition is similar to that identified for the Poolesville Member of the Manassas Formation and the base of the Bull Run Formation (i.e., Balls Bluff Member) in the Culpeper Basin.

### **Gettysburg Formation**

Originally named the Gettysburg Shale (Stose and Bascom, 1929), the interval of red, fine-grained clastics that overlies the New Oxford Formation is now termed the Gettysburg Formation (Berg et al., 1980; Smoot, 1999). This formation has been correlated to the Bull Run through Turkey Run Formation of the Culpeper Basin (Weems and Olsen, 1997). In Maryland and Pennsylvania three

broad subdivisions of the formation can be recognized (Figure 10). This tripartite subdivision consists of a thick unnamed lower member, a middle interval composed of the Heidlersburg and partially equivalent Conewago member, and a thin, upper conglomeratic member. The Susquehanna, the lower strata of the Gettysburg Formation consist of alternating intervals of sandy siltstone and mudstone. The apparent cyclicity consists of reddish brown, cross-laminated, fine-grained sandstone and platy, mudcracked, micaceous siltstone alternating with layers of massive, red-brown, rooted, silty mudstones, locally containing calcareous nodules and evaporite casts (Figure 14). The siltstone intervals are typically 2 to 9 feet in thickness and grading upsection to gray to greenish gray shale and siltstone. These alternating mudstone intervals are massive, red, rooted, and contain calcareous nodules and evaporite casts (Smoot, 1999). The upper part of this interval consists of interbedded red and greenish gray shale and siltstone.

**Unnamed lower member:** Stretching from the southern end of the basin near Frederick, Maryland, northward to the Susquehanna River, the lower strata of the Gettysburg Formation consist of alternating intervals of sandy siltstone and mudstone. The apparent cyclicity consists of reddish brown, cross-laminated, fine-grained sandstone and platy, mudcracked, micaceous siltstone alternating with layers of massive, red-brown, rooted, silty mudstones, locally containing calcareous nodules and evaporite casts (Figure 14). The siltstone intervals are typically 2 to 9 feet in thickness and grading upsection gray to greenish gray shale and siltstone. These alternating mudstone intervals are massive, red, rooted, and contain calcareous nodules and evaporite casts (Smoot, 1999). The upper part of this interval consists of interbedded red and greenish gray shale and siltstone.

**Heidlersburg Member:** In Adams and York counties, Pennsylvania, the cyclic lower Gettysburg is replaced upward by interbedded gray to black shale, greenish gray to dusky red siltstone, and gray limestone (Figure 15). Named the Heidlersburg Member (Stose and Bascom, 1929),

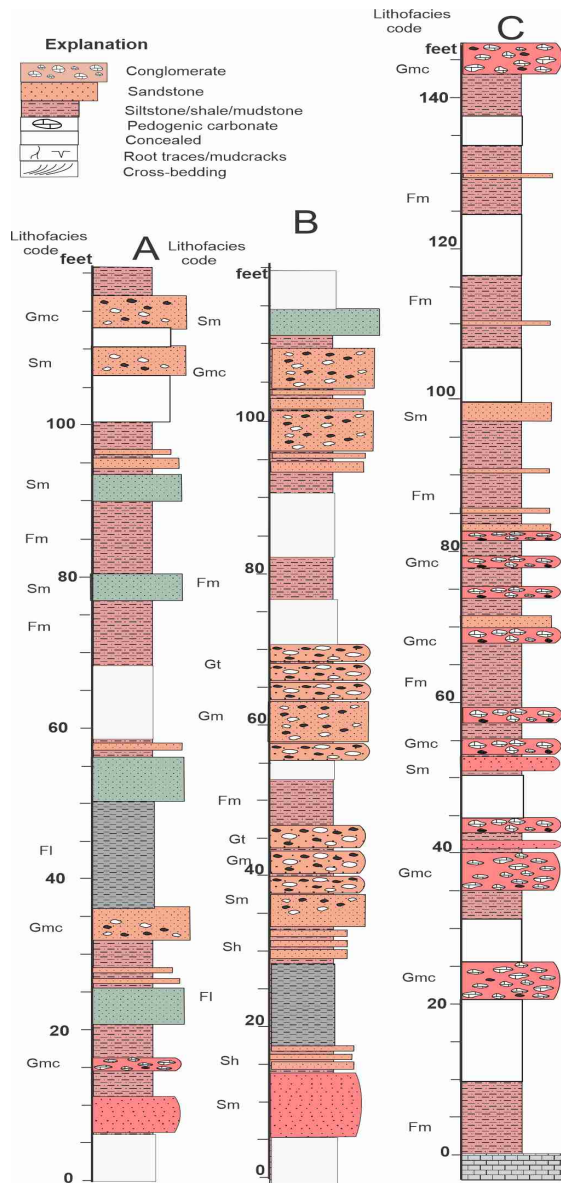


**Figure 11. Measured sections of the Irishtown Member of the New Oxford Formation. A, Type section near Irishtown, Pennsylvania, re-measured from Stose and Bascom (1929). B, Section of basal New Oxford Formation along the Monocacy River at the boundary between the Frederick Valley and Gettysburg Basin (modified from Brezinski, 2004). C, Lithologic variability of the Irishtown Member of the New Oxford Formation along Fishing Creek, Frederick County, Maryland. See Table 1 for explanation of lithofacies codes.**

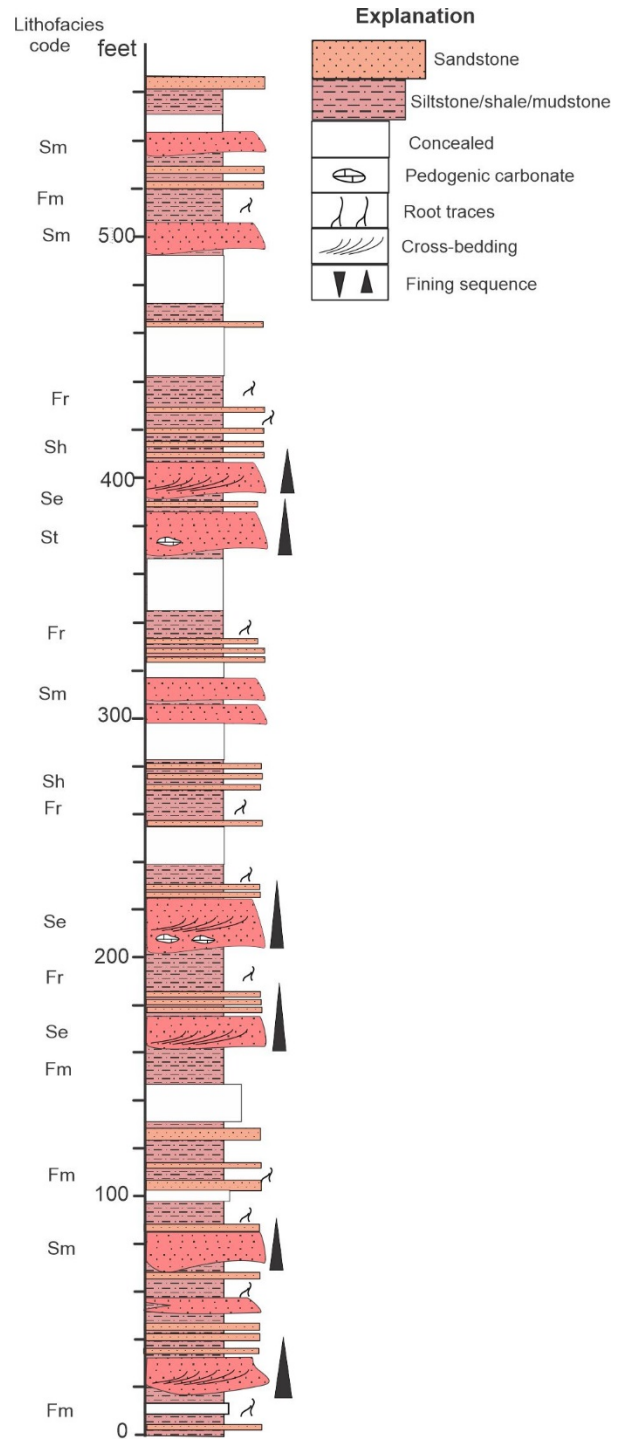


**Figure 12. Measured section of strata of the upper New Oxford Formation along railroad tracks on the northern bank of Big Pipe Creek at Detour, Carroll County, Maryland. See Table 1 for explanation of lithofacies codes.**

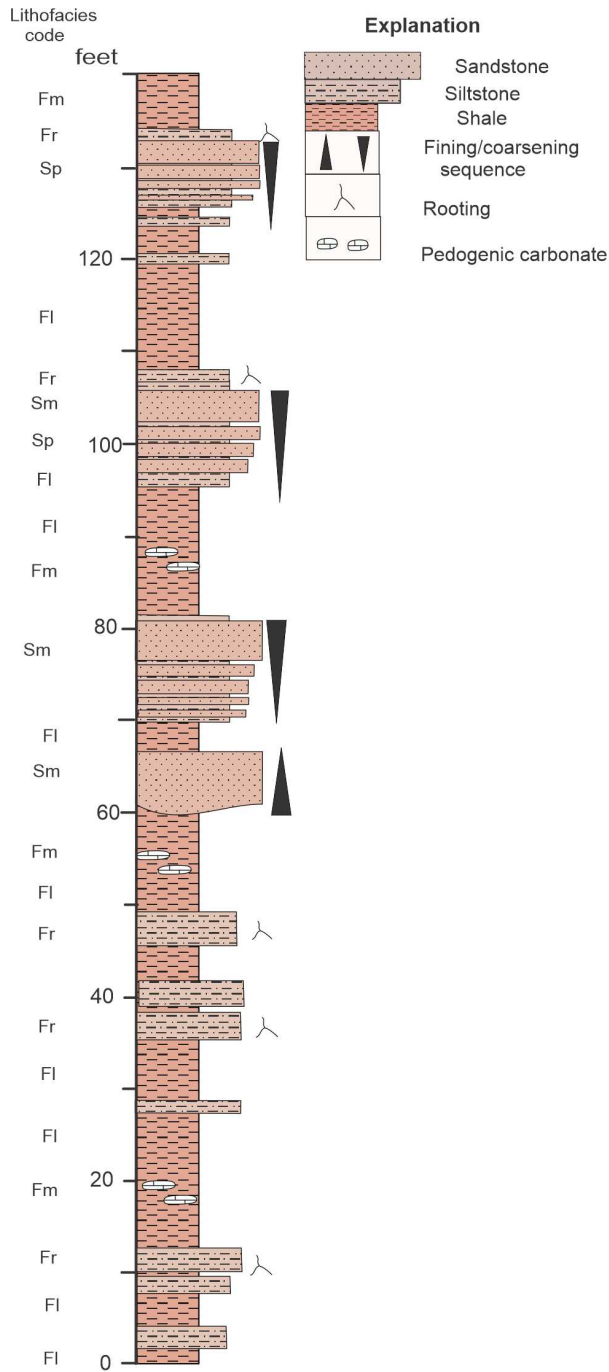


**Figure 13. Measured section of the transitional strata between the New Oxford and Gettysburg formations along Maryland Midland tracks near Rocky Ridge, Frederick County, Maryland. See Table 1 for explanation of lithofacies codes.**

the outcrop belt of these strikingly gray strata terminates near the Pennsylvania-Maryland State boundary line to the south; the strata interfinger with conglomerates and pebbly coarse-grained sandstone of the Conewago Member to the north (Figure 10A). The gray shales and mudcracked limestone that characterize the Heidlersburg Member contrast markedly with the dominantly red sandy and mudstone strata that typify the Triassic strata in the remainder of the basin. The Heidlersburg Member has been estimated at 4,800 feet thick by Stose and Bascom (1929), but may be significantly less than that.

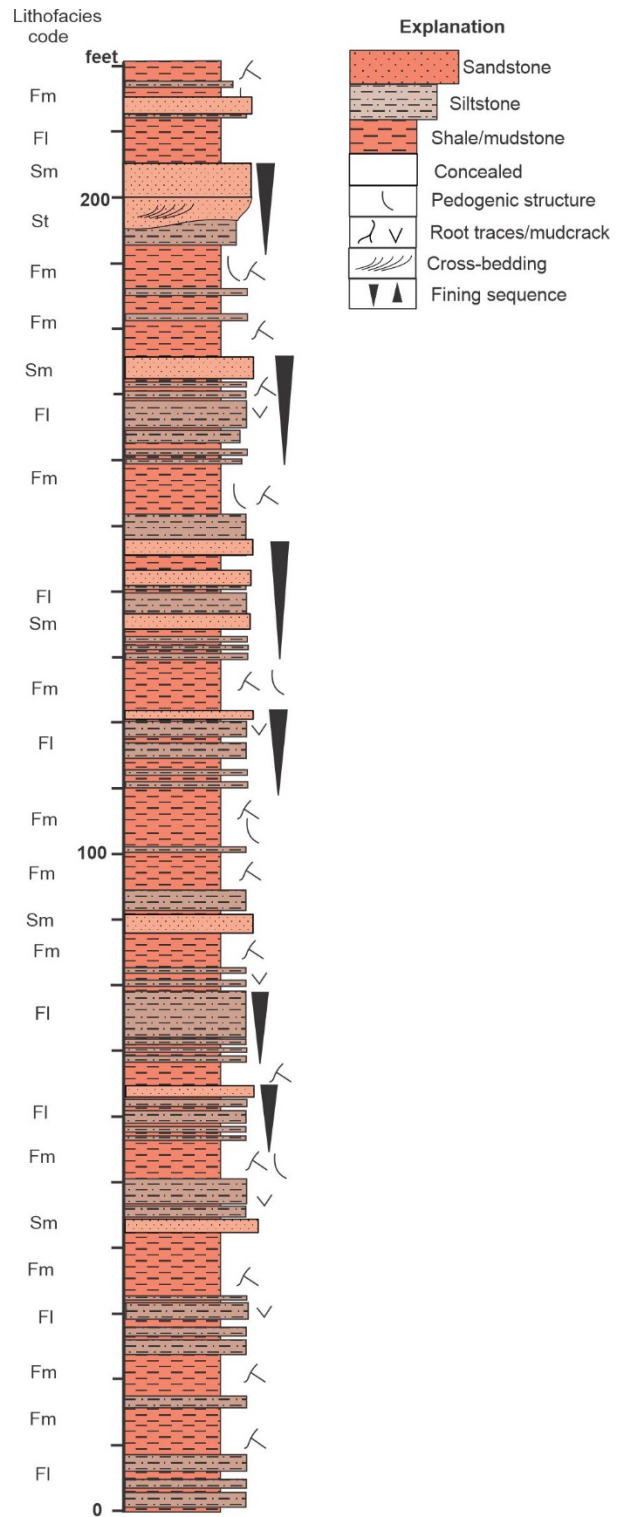
**Conewago Member:** Along the northeastern edge of the Gettysburg Basin, near the Susquehanna River, the gray Heidlersburg strata appear to interfinger with/or are replaced by a succession of interbedded conglomerates, pebbly, coarse-grained sandstones, and fine-grained red siltstones and mudstone. Stose and Jonas (1939) termed this wedge of coarse-grained clastics, that is up to 7,300 feet thick, the Conewago Conglomerate. However, much of this unit consists of fine-grained laminated siltstone and shale and thus will be considered the Conewago Member here (= Conewago Conglomerate of Berg et al., 1983). Along the eastern part of the unit's outcrop belt, the Conewago strata consist of interbedded cross-bedded, coarse-grained, arkosic sandstone and red silty massive and laminated mudstone (Glaeser, 1966) (Figure 16). However, westward and northwestward in the basin, and higher stratigraphically within the formation, the sandstone intervals of the Conewago Member become coarser and interstratified with matrix-supported, quartz-pebble and polymictic conglomerates.

**Unnamed upper member:** Above the Heidlersburg Member, the Gettysburg Formation becomes progressively coarser towards the top of the formation. This part of the Gettysburg Formation consists of alternating strata of greenish gray to reddish brown, laminated, rippled to wavy-bedded sandstone, and dusky red-brown and green-gray siltstone and laminated shale (Smoot, 1999). Higher in this part of the formation, thin polymictic conglomerate strata also are commonly

interbedded with the cyclic sandstone and shaly strata. Several basalt flows punctuate the sedimentary succession as well (Weems and Olsen, 1997).

Near the western border fault, and near the top of the Gettysburg Formation's stratigraphic succession, conglomerates become a dominant lithologic component of the upper Gettysburg Formation. In this area, the polymictic conglomerates, both mud- or grain-supported, are interbedded with thin-bedded to massive, coarse-grained sandstone. Stose and Bascom (1929) termed this conglomeratic interval the Arendtville fanglomerate lentil. Weems and Olsen (1997) assigned much of this upper succession to their Bendersville Formation, but because of priority the Arendtville Member terminology will be utilized herein. This upper part of the Gettysburg Basin succession has been correlated to the Midland Formation of the Culpeper Basin (Weems and Olsen, 1997). Also present in this part of the basin are thin, basaltic lava flows, the most prominent of which is the Aspers Basalt. This basalt flow may be as much as 200 feet thick (Weems and Olsen, 1997; Smoot, 1999). The overall thickness of the Gettysburg Formation has been estimated at between 8,000 feet in Maryland (Brezinski, 2004) and 22,000 feet in Pennsylvania (Root, 1988).

**Figure 14. Measured section of fine-grained cyclic strata of the lower Gettysburg Formation along Maryland Midland railroad tracks west of Rocky Ridge, Frederick County, Maryland. See Table 1 for explanation of lithofacies codes.**



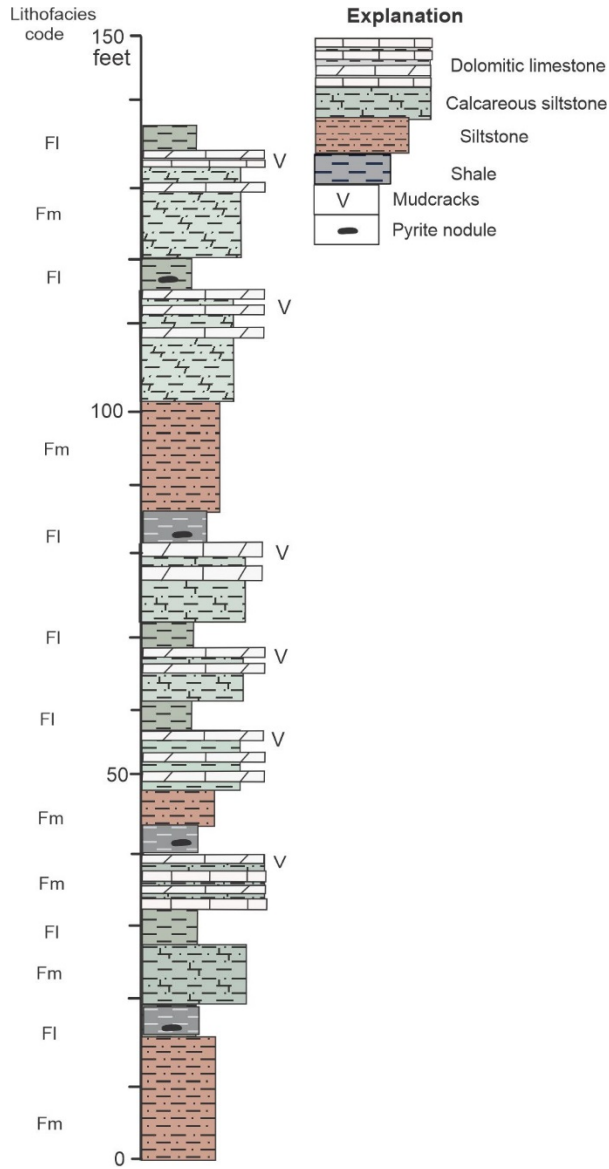


Figure 15. Measured section of cycles in the Heidlersburg Member of the Gettysburg Formation along Pennsylvania Route 116, Adams County, Pennsylvania. See Table 1 for explanation of lithofacies codes.

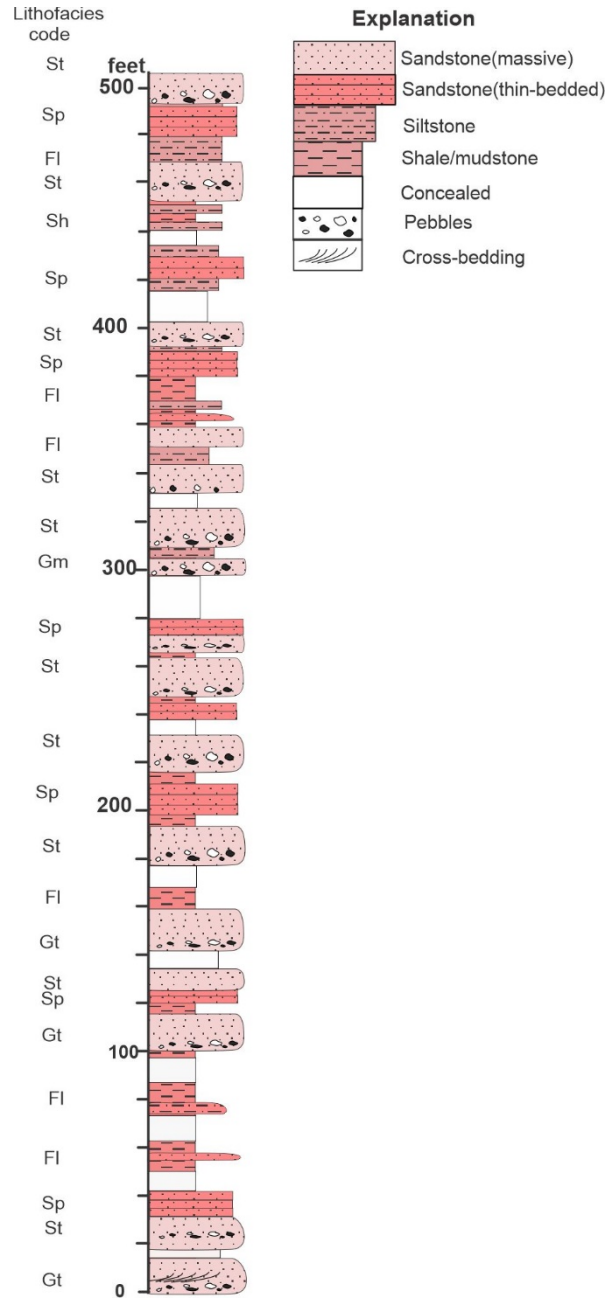


Figure 16. Measured section of the Conewago Member of the Gettysburg Formation, on Lewisbury Road at Conewago Creek, York County, Pennsylvania. Interpreted alluvial/lacustrine cycles inferred based on interbedding of conglomeratic sandstones and laminated mudstone. See Table 1 for explanation of lithofacies codes.

## Lithofacies Associations of the Culpeper and Gettysburg basins

Because rift basin formation tends to produce diagnostic depositional patterns, one should expect to encounter similarly arranged vertical and lateral lithofacies when comparing geographically distinct basins (Burggraf and Vondra, 1982). As discussed above, the Culpeper and Gettysburg basins display differing nomenclatural identities, but similar vertical and lateral trends in the character and distribution of the enclosed lithofacies. These similarities reflect shared tectonic origins as well as parallel depositional events.

Smoot (1991) described twenty-one lithofacies that he believed to be contained within the rift basin rocks of the Newark Supergroup. He also presented interpreted depositional environments for each (Table 2). Smoot (1991, p. 373) asserted that individual lithologies could not be mapped

because of their thinness, paucity of outcrop, and fineness of intercalation. In contrast, a study of African rift basins suggests that six recurrent lithofacies could be identified between geographically separate rift valleys (Burggraf and Vondra, 1982). While both Smoot (1991) and Burggraf and Vondra (1982) termed their individual lithologic entities "lithofacies", each study was actually discussing different levels of lithologic characterization. Smoot's (1991) lithofacies were comparable to individual uniform bodies of rock, or lithosomes. Each of these lithosomes can be considered to be a product of depositional events or environments within a broader depositional system. In contrast, the term "lithofacies" as employed by Burggraf and Vondra (1982) represented recurring aggregates of lithosomes that had lateral continuity, and likely were the product of several depositional environments within a particular depositional

Lithology Code	Lithofacies	Lithologic Character
AF1	Alluvial Fan	Matrix-supported conglomerate
AF 2	Alluvia Fan	Clast-supported conglomerate
AF 3	Alluvial Fan	Imbricated to cross-bedded conglomerate and sandstone
AF 4	Alluvial Fan	Pebbly muddy sandstone
F1	Braided Fluvial	Poorly sorted sandstone and imbricate conglomerate
F2	Braided Fluvial	Poorly sorted, cross-bedded sandstone
F3	Braided Fluvial	Moderately sorted sandstone to conglomerate
F4	Meandering Fluvial	Rhythmic sandstone/siltstone/mudstone
F5	Meandering Fluvial	Epsilon cross-bedded sandstone w/ scoured base
F6	Overbank Fluvial	Fine-grained sandstone, rooted mudstone, and pedogenic carbonate
F7	Braided? Fluvial	Matrix-supported conglomerate and pebbly sandstone
L1	Lacustrine	Laminated organic shale
L2	Lacustrine	Thin-bedded to massive mudstone
L3	Lacustrine	Thin-bedded, mudcracked mudstone
L4	Lacustrine	Massive, mudcracked mudstone
L5	Lacustrine	Sandy mudstone with evaporite casts
L6	Lacustrine	Massive mudstone and siltstone with root-casts and pedogenic carbonate
LM1	Lake margin	Lenticular sandstone beds
LM2	Lake margin	Inclined sandstone beds
LM3	Lake margin	Wedge-shaped sandstone
LM4	Lake margin	Conglomeratic sandstone
LM5	Lake margin	Sheet to wedge sandstone

**Table 2. Lithofacies exhibited by Triassic rocks of the Newark Supergroup and their proposed depositional environments. Summarized and modified from Smoot (1991, table 2). Abbreviations of lithofacies codes: AF=alluvial fan, F=fluvial, L=lacustrine lake, LM=lake margin.**

system. The six broad “lithofacies” outlined by Burggraf and Vondra (1982) included interbedded conglomerate and pebbly mudstone; lenticular conglomerate and sandstone facies; interbedded sandstone, siltstone, and claystone; lenticular fine-grained sandstone and lenticular-bedded siltstone; arenaceous bioclastic carbonate facies; and laminated siltstone facies. These groups of lithofacies represent depositional manifestations of alluvial fan to fluvial to deltaic and lacustrine depositional systems.

Aspects of the lithofacies groups described by Burggraf and Vondra (1982) were identified within the Culpeper and Gettysburg basins, as were individual lithologic entities as described by Smoot (1991). The heterolithic nature, intergrading character, and paucity of exposure made recognition and tracing of individual lithofacies (*sensu* Smoot, 1991) within the Culpeper and Gettysburg basins impossible. Therefore, it was deemed necessary to group recurring associations of lithologies into distinct groups. These lithosome groups, herein termed “lithofacies associations”

(abbreviated herein LA, see Table 3), are roughly equivalent to the “lithofacies” outlined by Burggraf and Vondra, (1982) for the East African rift valleys. Each of the five lithofacies associations is comprised of assemblages of characteristic or overlapping lithologies interpreted as having been produced within the same depositional system. Four of these five depositional systems are equivalent to “lithofacies” delineated by Smoot (1991). However, because many of these lithologies can form in multiple environmental settings, the lithofacies associations presented here constitute intergrading environmental products. As an example, mud-supported conglomerates can occur in alluvial fans as debris-flow deposits, and in lacustrine systems as either shoreline or fan-delta deposits. Therefore, the lithofacies associations, as well as their inferred stratigraphic context, represent a methodology that can be employed in delineating and mapping the geographic and vertical extent of respective depositional systems.

<b>Lithofacies Association (LA)</b>	<b>Salient Lithology</b>	<b>Depositional Environments</b>	<b>Ancillary Lithology (Smoot (1991) Lithofacies Equivalence)</b>
LA A	Polymictic conglomerate, pebbly, thin- to planar-bedded sandstone, laminated siltstone, shale.	Debris flow, sheet flood, marginal lake alluvial fan to fan-delta deposits.	Mud-supported conglomerate; laminated sandstone; ripple-laminated siltstone (AF 1-4; F1; LM 3, 4).
LA B	Pink to gray, trough cross-bedded, pebbly, very coarse-grained sandstone, conglomerate, and red, root-mottled mudstone.	Braided fluvial-channel, bar and abandoned channel, and extra-channel mudstone.	Trough cross-bedded, coarse-grained quartzose and arkosic sandstone; granule conglomerate; reddish, rooted mudstone; caliche nodules and horizons (AF 3, 4; F 1-3, 6,7).
LA C	Lenticular, red brown, cross-bedded, argillaceous sandstone, upward-coarsening, planar-bedded sandstone, rooted mudstone.	Meandering channel and overbank. Upward-coarsening deltaic and subaerial overbank.	Lenticular, reddish, upward- and laterally fining sandstone; large-scale cross-beds; shale-pebble lag conglomerate; rooted, reddish siltstone and mudstone; caliche nodules (F 4-6; LM 1-3).
LA D	Planar-bedded sandstone, interbedded, red, mudcracked siltstone and rooted mudstone.	Deltaic to proximal seasonally-exposed, lacustrine mudflat.	Fine-grained laminated, rippled to bioturbated sandstone; red, rooted mudstone; red-brown, mudcracked, laminated siltstone and rooted red mudstone, rare limestone. (L 3-6; LM 4).
LA E	Interbedded, gray, laminated sandstone, carbonaceous shale, and gray limestone.	Distal, perennially wet, subaqueous lake.	Dark gray to gray green siltstone, shale; gray to dark gray, fine-grained, thin-bedded sandstone; coal to coaly shale (L1,2; LM 4,5).

**Table 3. Lithofacies associations (LA) of the Culpeper and Gettysburg basins, and their salient and ancillary lithologic characteristics, interpreted depositional environments, and equivalence to Smoot’s (1991) lithofacies.**



**Figure 17. Lithologies of Lithofacies Association A. A, Grain-supported, massive conglomerate (Gm) of the Leesburg Formation, Frederick County, Maryland. B, Stratified gravel (Gms) of the Manassas Formation. B, Interbedded massive conglomerate (Gm) and laminated shale (Fl), Loudoun County, Virginia. D, Massive, mud-supported conglomerate (Gmm) of the Gettysburg Formation, York County, Pennsylvania. E, Stratified mud- (Gmm) and clast-supported (Gmc) conglomerates of the Conewago Member of the Gettysburg Formation.**

Perhaps the most dramatic and recognizable lithofacies present within the Triassic rift basins of eastern North America is the package of clast- and mud-supported polymictic conglomerates. This eye-catching, coarse-grained lithofacies commonly is interbedded with pebbly sandstone, laminated and graded, intraclastic sandstone, greenish gray

and reddish brown mudcracked siltstone, and laminated mudstone (Smoot, 1991; Weems et al., 2016) (Figure 17 A-C). The aggregate of these individual lithofacies is herein assigned to Lithofacies Association A. The polymictic conglomerates have been shown to grade laterally into fine-grained sandstone, laminated greenish

gray mudstone, and argillaceous limestone (Smoot, 1985, fig. 2.3; Hentz, 1985). This assemblage of lithologies characterizes the border areas on both the eastern and western sides of the basins. Even though these strata are characteristic of both the lowest part of the successions (Reston, Tuscarora Creek, and Irishtown members) and highest (Millbrook Quarry Member, Arendtville Member), they are interpreted as representing similar depositional regimes.

Smoot (1991) attributed such conglomeratic lithofacies to alluvial fan depositional environments. Hentz (1985) interpreted this amalgamation of lithologies as having been deposited within marginal and deeper lake environments. Based on his interpretation, the conglomerates and sandstone intervals represent current-reworked debris flows while the laminated mudstone and limestone are more distal lacustrine deposits. Contradicting this environmental scenario is the mud-supported character of some of the polymictic conglomerates. Nemeč and Steel (1984) proposed that nearshore conglomerates typically are clast-supported, contain little to no mud admixture, and are relatively well-sorted. Moreover, Larsen and Steel (1978, fig. 16) and Nemeč and Steel (1984, fig 11) have shown that in alluvial fan systems, subaerial, mud supported, debris flow conglomerates commonly interfinger with thin-bedded, bioturbated and graded sandstones that represent sheet flood deposits coeval to upslope debris flows. These coarser deposits have been shown to intergrade with subaqueous fine-grained, laminated muds and limestones of lake environments (Hentz, 1985, fig. 5). Thus, Lithofacies Association A consists primarily of Smoot's (1991) lithofacies AF1-AF4, but also may contain minor components of lithofacies F1, F2, L1, LM4, and LM5.

The broadly diverse lithologies comprising Lithofacies Association A are interpreted as representing both subaerial and subaqueous components of alluvial fans. The conglomerate lithologies are interpreted as representing mainly debris flow deposits that locally extended to lake shoreline environments as well as into subaqueous settings. This depositional scenario is consistent

with local reworking of coarse-grained deposits at the shoreline by wave activity. The thin-bedded, laminated, and intraclastic sandstone intervals are proposed to represent both sheet-flood, reworked shoreline, and, locally, turbidity current deposits of the proximal and more distal reaches of intrabasinal lakes.

Another assemblage dominated by coarse-grained lithologies is grouped into Lithofacies Association B. This association consists of thickly interbedded pebbly sandstone and red mudstone. Sandstone intervals within this lithofacies association are typically coarse-grained to pebbly, granule conglomerate and vary in color from pink and purple and gray (Figure 18).

They are pervasively massive and trough cross-bedded. Unlike the conglomerates of Lithofacies Association A, those present within this association are characteristically grain-supported, better sorted, granule-size, contain isolated pebbles or lenses of pebbles, and are cross-bedded. Individual sandstone units range between 15 and 30 feet in thickness, but can be up 40 feet thick. These coarse-grained sandstone intervals are interstratified with thick intervals of massive, deformed, reddish brown mudstone containing pedogenic carbonate, root rhizomes, and rooted bioturbation (Figure 18C).

Lithofacies Association B characterizes the lower part of the Poolesville Member of the Manassas Formation, the New Oxford Formation above the Irishtown Member, and the Conewago Member of the Gettysburg Formation. Although there is little discernible fining within individual sandstone units, there is a general trend towards fining upsection through the lower half of the formation where this lithofacies is found (Figure 18F). The pebbly sandstones and well-sorted conglomerates of Lithofacies Association B are equivalent to lithofacies AF4, F1-F3, and F6 of Smoot (1991). This combined group of lithologies is interpreted as having been formed by braided streams, both within the stream channels and subaerial overbank area. The presence of pedogenic carbonate within the interbedded mudstones reflects a high rate of evaporation associated with a climate consistent with the form-



**Figure 18. Lithologies of Lithofacies Association B. A, Light gray, trough cross-bedded, gravelly braided stream channel deposit (Sm) interbedded with rooted, caliche-bearing paleosols (Fm(c)). B, Close-up of trough cross-bedded, pebbly, coarse-grained sandstone. C, Deformed reddish brown, rooted paleosol separating sandstone units. Note resistant caliche interval below hammer. D, Massive (Gm) and cross-stratified gravels (Gt) within the Irishtown Member of the New Oxford Formation. E, Massive, pink sandstone with gravel lag conglomerate within the Manassas Formation. F, Interbedded red, trough cross-bedded sandstone (Sm, St), and thinly bedded red shales (Fl) of the Conewago Member of the Gettysburg Formation.**

ation of caliche soils (Retallack, 2001). The characteristic cyclic alternations of sandstone and mudstone are similar to other sandy braided stream deposits. Miall (1977) noted this type of cyclicity within the South Saskatchewan River where the thicker sandstone intervals represent deposition within major channels, while thinner sandstones form in compound bars and the fine-grained

deposits formed within interbar overbank areas (Walker and Cant, 1978). Although the fine-grained intervals within Lithofacies Association B are considerably thicker than those illustrated by Miall (1977), the overall character of the sandy parts of the succession are identical to those models (Walker and Cant, 1978).



**Figure 19. Lithologies of Lithofacies Association C. A, Alternating trough cross-bedded (St), massive (Sm), and epsilon foresets (Se) within the upper Manassas Formation at Seneca, Maryland. B, Fluvial cycles consisting of alternations of massive (Sm) and epsilon-bedded (Se) sandstone with laminated siltstone (Fl). C, Alternating horizontal to wedge-shaped (Sh) argillaceous sandstone units and laminated and rooted red mudstone (Fl) within the upper New Oxford Formation. D, Upward-coarsening deltaic sandstone within the uppermost New Oxford Formation, Rocky Ridge, Maryland.**

A second fluvial association, herein termed Lithofacies Association C, also is present within the Manassas Formation and equivalent New Oxford Formation (Glaeser, 1966; Smoot, 1999). This association of lithologies consists of lenticular, cross-bedded, red brown, sandstone, laminated siltstone, and rooted, red mudstone. The sandstone intervals are characteristically upward-fining, exhibit a sharp base with a basal shale-pebble lag conglomerate, range from fine- to coarse-grained, and commonly possess large, epsilon cross-bedding (Figure 19A, B). These sandstone lenses grade, both laterally and vertically, into thin-bedded, fine-grained sandstone, red siltstone, and red, rooted mudstone that commonly contains carbonate nodules and blebs. One of the best exposures that exemplifies this association are in the northern Culpeper Basin, along the Chesapeake and Ohio National Historical Park at Seneca, Maryland, where the sandstones were quarried and cut for building stone (stratigraphy in Figure 6).

Near the top of this lithofacies association, sandstone intervals become thinner, finer grained, and more wedge-shaped (Figure 19C). Furthermore, many of the sandstone layers in this part of the formation tend to exhibit an upward-coarsening character (Figure 19D). This lithologic change is discernible in both the Culpeper and Gettysburg basins and appears to coincide with the stratigraphic transition into the overlying Bull Run and Gettysburg formations, respectively. Detailed mapping of this interval in the Gettysburg Basin discloses dramatic orientation changes between these stacked sandstones interval (Figure 20). This mapping portrays the rapidly changing strike of these sandstone units from northwest to due east. The arcuate bend that the sandstone and contact creates is interpreted to represent the limits of a fluvial-dominated delta that formed during the latter stages of New Oxford deposition. This feature, herein termed the Emmitsburg delta, suggests that the New Oxford fluvial lithofacies were deposited contemporaneously with lake deposits of the coeval lower Gettysburg Formation. Moreover, this feature suggests that the Gettysburg lake, which extended throughout Adams and York

Counties, Pennsylvania, may have been reduced to nothing more than a small inlet in northern Frederick County, Maryland.

Lithofacies Association C is composed of Smoot's (1991, table 2) lithofacies F4- F6 and LM 1- LM 3. The salient lithologic features that identify this lithofacies association are consistent with those that are characteristic of fine-grained fluvial cycles in a meandering stream system. The lenticular geometry of the sandstone units, which are commonly finer grained than those in Lithofacies Association B, contain the sharp erosional base, shale-pebble channel-lag conglomerates, and upward fining. These characteristics are consistent with channel-phase deposits in a meandering river system (Walker and Cant, 1979). Furthermore, the large epsilon cross-stratification indicates lateral accretion surfaces of a meandering channel point bar (Smoot, 1991). Also, included within this association are numerous wedge-shaped or upward-coarsening sandstone bodies. These sandstone intervals are interpreted as lake margin fluvial deposits, including those produced by deltas. The lateral and vertical gradation of these sandstones into thin-bedded, fine-grained sandstone and rooted mudstone containing carbonate nodules also is consistent with a meandering channel and overbank scenario. These fine-grained intervals are interpreted as representing pedogenically deformed mudstone and thin-bedded levee deposits that formed on floodplains adjacent to the river channel.

Lithofacies Association D contains a wide array of primarily fine-grained lithosomes that appear to represent a transitional succession between the coarse-grained, fluvial deposits, characteristic of Lithofacies Association C, and the finer sediments typical of Lithofacies Association E. This lithofacies association is comprised of lithologies present primarily in the Balls Bluff and Groveton members of the Bull Run Formation, and the lower member of the Gettysburg Formation. Typically, these strata consist of interbedded thin-bedded to platy, reddish brown, very fine-grained sandstone, laminated, mudcracked siltstone, and massive mudstone exhibiting a significant level of

pedogenic overprinting (Figure 21 A-C). Near the base of this association, lenses and tongues of dusky red, fine-grained, laminated, argillaceous sandstone are present (Smoot, 1999) (Figure 14). In the northern Culpeper Basin, this part of the succession was termed the fluvial-deltaic sandstone by Southworth et al. (2006). Above the basal sandy strata this lithofacies association consists of red, laminated, mudcracked siltstone

interbedded with red-brown, rooted, bioturbated, and disturbed mudstone containing carbonate nodules and evaporite casts. These cyclic reddish lithologies grade upsection into cyclic intervals of laminated, bioturbated, greenish gray shale and red and reddish brown mudstone (Southworth et al., 2006).

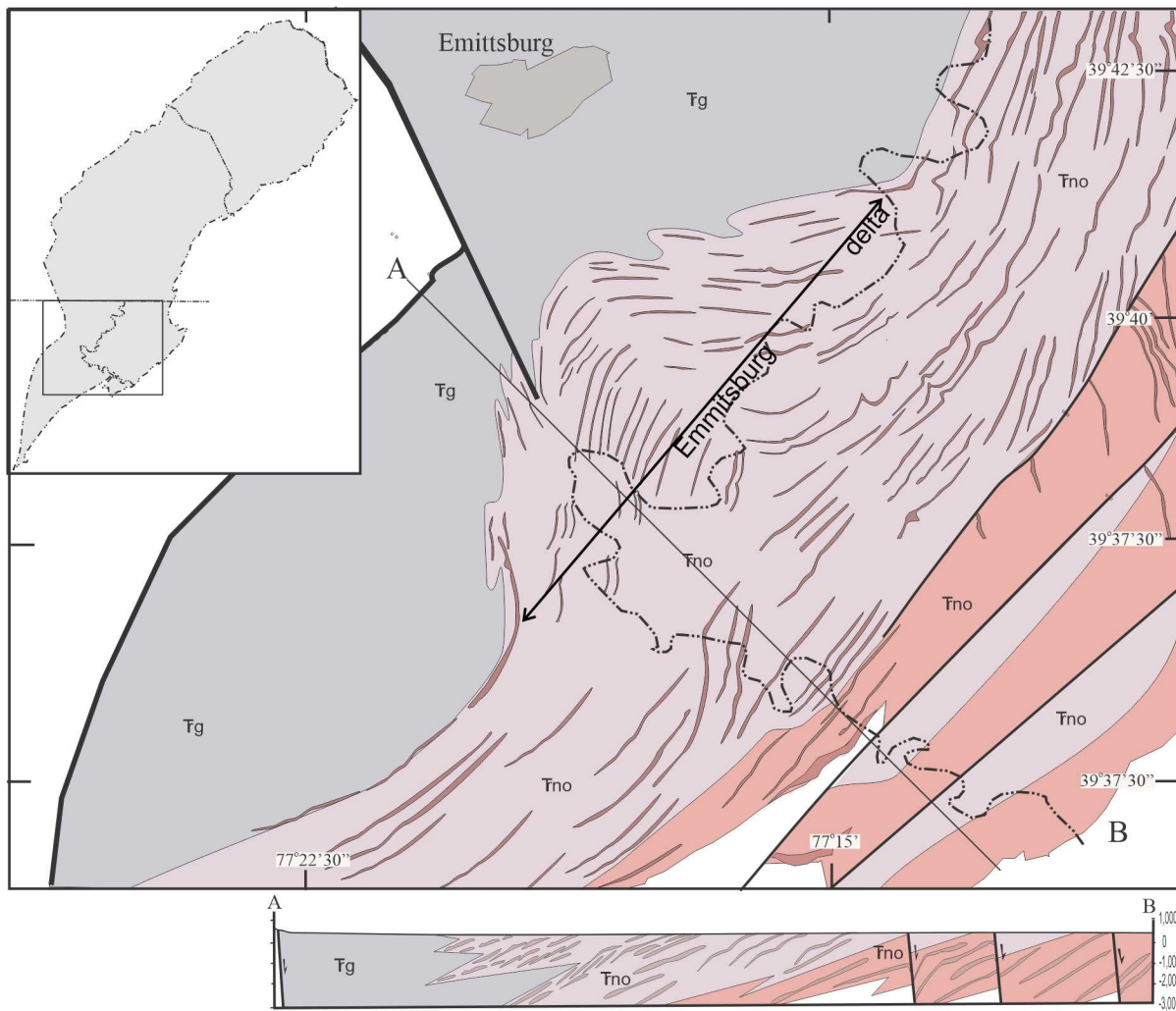


**Figure 20. Geologic map illustrating the transition between the New Oxford and Gettysburg formations in the southern Gettysburg Basin. The irregular change in strike of sandstone bodies is interpreted as representing a deltaic lobe at the contact between the upper New Oxford Formation and lower Gettysburg Formation (Brezinski, 2021).**

Near the northern end of both the Culpeper and Gettysburg basins, the cyclic fine-grained strata of the Bull Run and Gettysburg formations interfinger with red argillaceous conglomerates and coarse-grained sandstones of the Leesburg and Conewago members, respectively. These coarse-grained facies stand in stark contrast to the typically finer grained lithologies of this lithofacies association that occur elsewhere. In these areas the fine-grained lithologies of Lithofacies Association D are intimately interbedded with sandstone and conglomerate deposits that are considered part of Lithofacies Association A.

The various fine-grained clastic strata of Lithofacies Association D are considered comparable to Smoot's lithofacies L3-L6 and LM4, LM5. This assemblage of lithologic components is interpreted as representing seasonally exposed mudflats that formed along the edges of rift basin lakes. Many features that characterize this association, such as desiccation cracks, root casts, stromatolites, and evaporite casts, are suggestive of shallow water, nearshore lake deposits that were frequently subaerial (Gore, 1988). The cyclic nature of these proximal lake deposits is manifested by alternations of very fine-grained sandstone intervals that grade into reddish brown and locally greenish gray, laminated and mudcracked siltstone. These strata invariably alternate with irregularly thick intervals of rooted mudstone that commonly contain evaporite casts (Gore, 1988). Collinson (1978) has shown that cyclic lacustrine lithologies are a reflection of alternating wet and dry climate periods. During the wet part of these cycles laminated sandstone and siltstone are interpreted to have been deposited. These strata are the result of increased turbidity from high sediment input. These wet periods alternate with the dry part of the cycle which is the result of high evaporation, pedogenesis, and desiccation.

The presence of greenish gray strata near the top of Lithofacies Association D appears to signal the initiation of deposition of a wetter depositional

episode. Within the Gettysburg Basin the overlying association, Lithofacies Association E, consists of cyclic intervals of gray shale and laminated and mudcracked limestone of the Heidlersberg Member (Figure 22). Within the Culpeper Basin this facies association is best developed in the Midland through Waterfall formations (Hentz, 1985; Lee and Froelich, 1989).

The repetitive nature of the lithologies of Facies Association E is manifested by the alternation of gray to black shale, red siltstone, and mudcracked limestone. These lithologies suggest that they were deposited in perennially wet environments distally located from clastic input (Van Houten, 1962; Turner-Peterson and Smoot, 1985). This association is interpreted to be identical to lithofacies L1 and L2 delineated by Smoot (1991). Similar repetitions of mudstone and carbonate elsewhere have been shown to represent lacustrine climate cycles (Collinson, 1978; Picard and High, 1981; Dunagan and Turner, 2004). These authors have interpreted lacustrine cycles elsewhere as consisting of a lower siliciclastic half cycle produced during wet climate conditions and concomitant high turbidity. The wet part of these cycles are succeeded, in the upper half, by dry periods when sediment supply and turbidity were low and evaporation produced chemical deposition out of solution (Collinson, 1978).

#### **Areal and temporal distribution of Culpeper and Gettysburg lithofacies associations**

The broadly defined lithofacies associations employed herein provide the prospect for mapping the migration of lithosomes through time and space. These varying facies exhibit a recurrent lithologic distribution that is related to the stacking and migration of depositional systems both laterally and vertically. If separate rift basins exhibit similar lithologic patterns, a dynamic depositional model may be developed that can be employed for future environmental study and exploration.



**Figure 21. Lithologies of Lithofacies Association D. A, Cyclic alternation of massive, rooted mudstone and laminated siltstone within the lower Gettysburg Formation, Rocky Ridge, Maryland. B, Laminated siltstone underlain and overlain by massive mudstone from the same location. C, Massive rooted mudstone of Lithofacies Association D. D, Layer of reworked caliche clasts at base of laminated siltstone interval. E, Mudcracks and burrowed laminated, sandy siltstone. F, Upward-coarsening, fine-grained, deltaic sandstone. Same location as A.**



**Figure 22. Lithologies of Lithofacies Association E. A, Grayish green shale of the Heidlersburg Member of the Gettysburg Formation. B, Alternating light and medium gray lake lithologies within the Balls Bluff Member of the Bull Run Formation. Lithologies have been altered by contact metamorphism. C, Single lacustrine cycle composed of black shale (FI) alternating with limestone. D, Thin-bedded limestone representing the dry phase of lacustrine climate cycle. E, Mudcrack from the top of medium-bedded limestone. F, Lakes cycles within the Groveton Member of the Bull Run Formation. Cycles consist of alternations of gray shale and tan limestone. Manassas National Battlefield Park.**

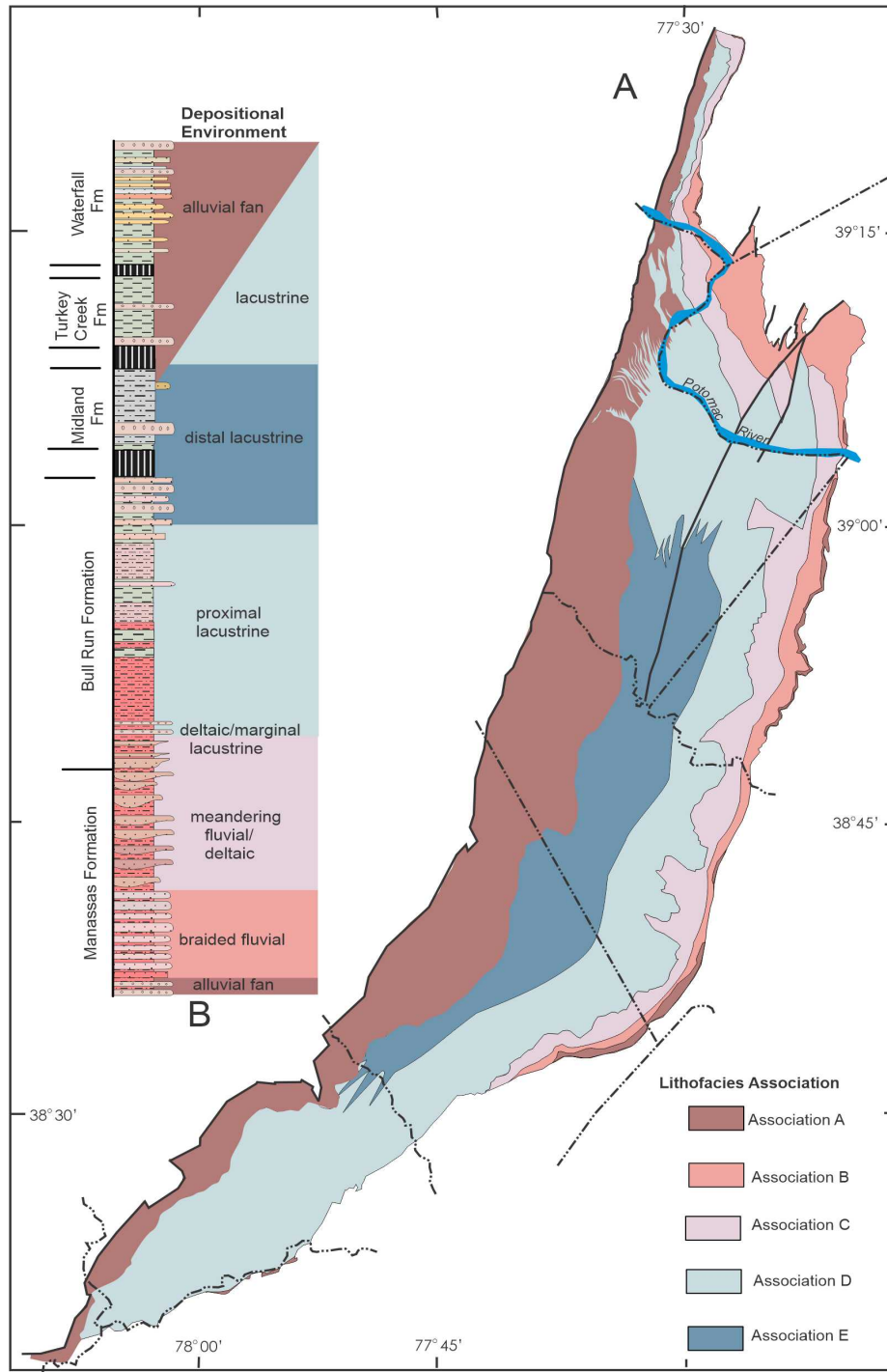


**Figure 23. A, Distribution and lateral relationship of Triassic lithofacies associations within the Culpeper Basin. B, Vertical arrangement of lithofacies associations through the Culpeper Basin stratigraphic succession showing upward fining and then coarsening megasequences.**

Lithofacies associations within the Culpeper Basin display a distribution that is somewhat similar to that of the basins geologic formations (Figures 4, 23). However, the geographic distribution of lithofacies associations indicates that depositional patterns were not symmetric. Figure 23A illustrates that fluvial lithofacies associations (LAs B, C) are concentrated in the northern part of the basin, while lacustrine lithofacies (LAs D, E) are dominant in the southern part. This distribution appears to reflect a southward-prograding fluvial system that was widespread along what is now the Potomac River and that gave way to a broad mudflat and lake to the south. Alluvial fan deposits (LA A) such as the Leesburg, Goose Creek, and Millbrook Quarry members are prevalent along the western border faults. Similar, but thinner lithofacies associations are found at the base of the overlapping edge to the east (Reston, Tuscarora Creek members). The southward pinchout of fluvial lithofacies associations and replacement by lacustrine lithofacies appears to contradict the traditional simplified stratigraphic framework commonly portrayed for the Culpeper Basin (Schlische, 1993, fig. 7J; Southworth et al., 2006). Based on the currently defined lithofacies associations, it would seem that either a wedge-on-wedge or interfingering facies pattern might better represent the environmental relationship.

Geographic distribution of lithofacies associations in the Gettysburg Basin subparallels that of the named stratigraphic units. Lateral changes in lithologies within LAs B and C can be traced to local thickening within the Taneytown sub-basin where sandstones of LA B are well-developed (Figure 24A). Younger units also display disparate changes in thickness and distribution. Outcrop patterns of LAs D and E reflect narrowing and thinning, especially with regards to LA E, near both the northeastern and southwestern margins of the basin. The basin center area of gray shale and limestone appears to coincide with an absence of deltaic deposits (LAs A, C). This change in outcrop pattern is interpreted as representing a central deep basin area coincident with the thalweg (Figure 24A). No deep borehole

data are available to verify the depositional structure of these basins, but map patterns of lithofacies associations seem to suggest substantial facies changes along the basin edges that is equivalent to its shallowing (Smoot, 1999, fig. 12A-17C). Therefore, the conventional view that these deposits are distributed within the subsurface simply as tilted continuous layers is called into question (Root, 1988; Schlische, 1993).

The vertical arrangement of lithofacies associations within both basins defines an upward-fining succession of environments from braided fluvial to meandering fluvial (LAs A-C) and then proximal to distal lacustrine (Figures 21A, 22B). This upward fining is supplanted above the Heidlersburg Member as the succession coarsens with alluvial fan progradation (LAs E-A). These vertical relationships are identical to those exhibited in the Culpeper Basin with upward fining (LAs A-E) during Manassas and Bull Run deposition, and upward coarsening reflected by deposition of the Midland through Waterfall formations (LAs E-A) (Figure 23A).

The interpreted megasequence successions identified by the upward-fining and -coarsening successions are similar to those preserved within the Deep River (Reinemund, 1955), Dan River (Thayer, 1970; Olsen et al., 2015), Richmond (Ressetar and Taylor, 1988), Newark (Olsen, 1980), and Fundy basins (Wade et al., 1996). Although the proportional thicknesses of component parts of each sequence differ between the basins, these patterns appear to be consistent within the closed-basin rift models (Lambiase, 1990; Smoot, 1985). This tripartite stratigraphy begins with basin-wide fluvial deposits, overlain by sharp deepening into a lacustrine succession, followed by gradual shallowing and progradation of a fan delta into a marginal lacustrine and fluvial succession (Nemec and Steel, 1988; Lambiase, 1990; Schlische and Olsen, 1990; Fig. 3.3.1.6). Similar upward-fining then -coarsening megasequences are discussed by Blair (1987) for

Cretaceous rift basins that predate the formation of the Gulf of Mexico. Blair found that tectonic subsidence and hydrologic controls created a

number of upward-fining and upward-coarsening megasequences that were evidenced by the stacking of sedimentologic entities.

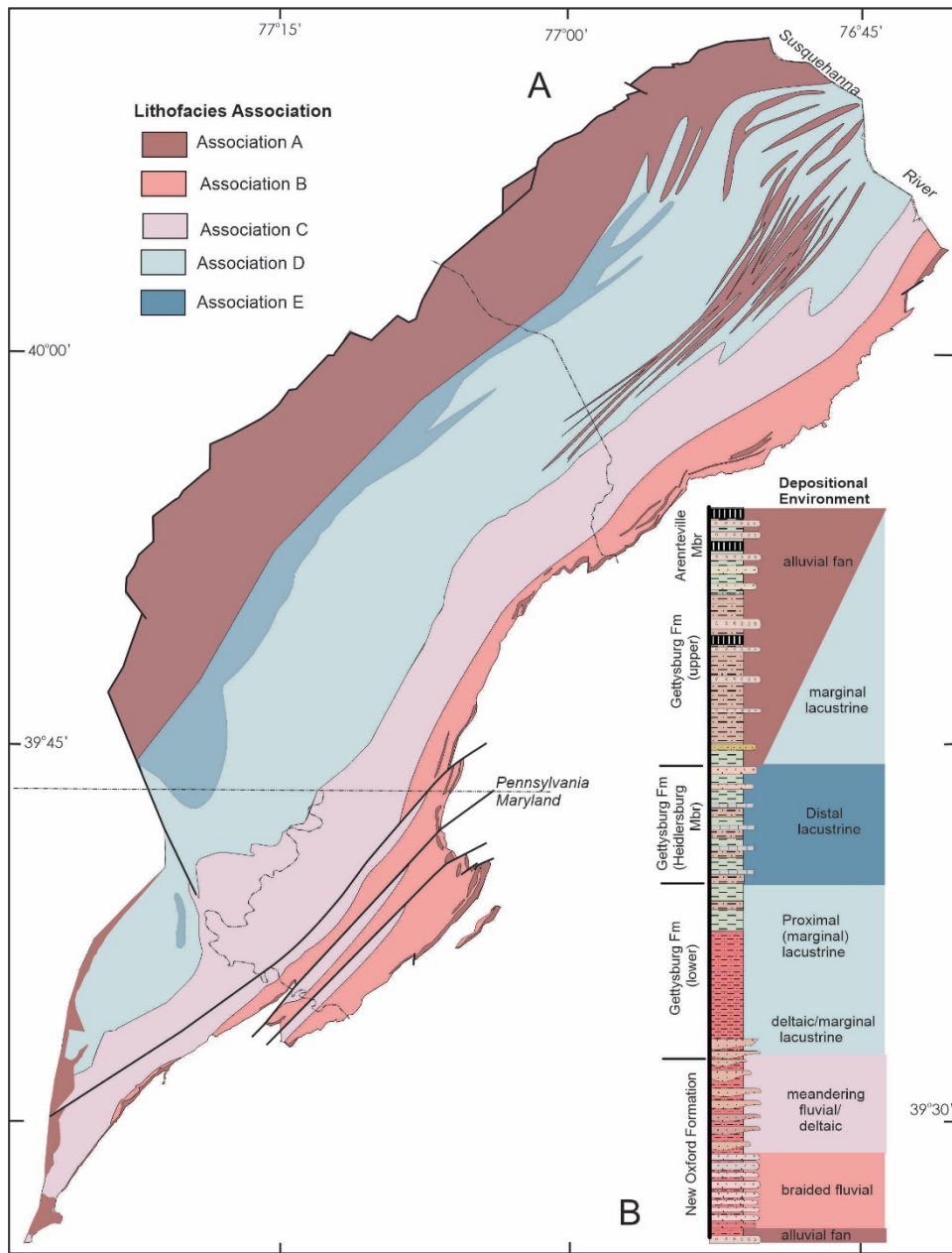


Figure 24. A, Distribution and lateral relationship of Triassic lithofacies associations within the Gettysburg Basin. B Vertical arrangement of lithofacies associations through the Gettysburg Basin stratigraphic succession showing upward-fining and then -coarsening megasequences.

### **Taylorsville Basin Stratigraphy**

The occurrence of Triassic rift basins buried beneath the Mid-Atlantic Coastal Plain have long been understood (Hansen and Edwards, 1986; Hansen, 1988; Benson, 1992; Olsen, 1997) (Figure 1B). Although researchers are not quite certain as to their number and precise distribution, the presence of some of these basins is known from deeper drilled wells and seismic data. One of the largest buried basins currently identified is a half-graben structure that extends from Prince George County, Virginia, to Anne Arundel County, Maryland (Figure 25). This structure underlies approximately 1,970 square miles of the Maryland and Virginia Coastal Plain, and has been termed the Taylorsville Basin (Weems, 1980). The nadir of this structure lies at a point roughly beneath the Potomac River in southern Charles County, Maryland (Figure 26). Near this point the basin is estimated to preserve more than 8,000 feet of Triassic rocks (LeTourneau, 2003), even though as much as 7,800 feet of rock may have been eroded prior to deposition of the overlying Cretaceous Coastal Plain strata (Malinconico, 2003). The main border fault creating the Taylorsville Basin is present along its western margin, and has generally been interpreted to be a reactivated shear surface within the Hylas shear zone of the Virginia Piedmont (Bobyarchick and Glover, 1979; Milici et al., 1991).

This buried basin was chosen to test the applicability of methodologies developed for the deciphering of the stratigraphy within the Gettysburg and Culpeper basins for two reasons. Firstly, seismic surveys and drilling of several deep exploratory wells in the Virginia portion of the basin were completed in the 1980s (LeTourneau, 2003) and provide subsurface data for comparison with outcrop data from the Culpeper and Gettysburg basins. Secondly, strata near the southwestern margin of this basin are exposed as an inlier that is created by fluvial incision along upper tributaries of the Pamunkey River (Weems, 1980). Thus, study of the Taylorsville Basin presents transitional data for environmental reconstruction between exposed to buried basins.

### **Taylorsville Basin Cover Succession Thickness and Character**

The Taylorsville Basin is largely concealed beneath the western part of the Atlantic Coastal Plain of Virginia and Maryland. The Coastal Plain is an eastward-thickening wedge of largely unconsolidated Cretaceous and Tertiary sediments that is as thick as 8,000 feet near Ocean City, Maryland. The sediments thin to a feather edge at the Fall Line (Hansen and Edwards, 1986; Vroblesky and Fleck, 1991; Meng and Harsh, 1991; McFarland and Bruce, 2006) (Figure 26). Because the Taylorsville Basin lies near the western edge of the Coastal Plain, it appears to be buried beneath no more than 2,500 feet of these sediments. However, progressive westward thinning of this cover succession exposes a small portion of the basin near its southwestern margin in the vicinity of the town of Doswell, Hanover County, Virginia (Weems, 1980, fig. 3) (Figure 25).

In Virginia, the Coastal Plain sediments consist of alternating intervals of porous and permeable aquifers and impermeable confining layers. Eight aquifers and eight confining intervals have been identified in the Virginia Coastal Plain (Meng and Harsh, 1991; McFarland and Bruce, 2006). However, only four of these aquifers and their corresponding confining units are present in the Coastal Plain succession covering the Taylorsville Basin in Virginia (Meng and Harsh, 1991, figs. 10-22).

The Maryland Coastal Plain succession consists of sixteen sandy aquifers separated by eleven confining units (Andreasen et al., 2013). Six of the sixteen aquifers are confined layers that overlie the Maryland part of the Taylorsville Basin. The remaining two aquifers are unconfined. The maximum thickness of confining layers for this part of the Taylorsville Basin is 400 feet.

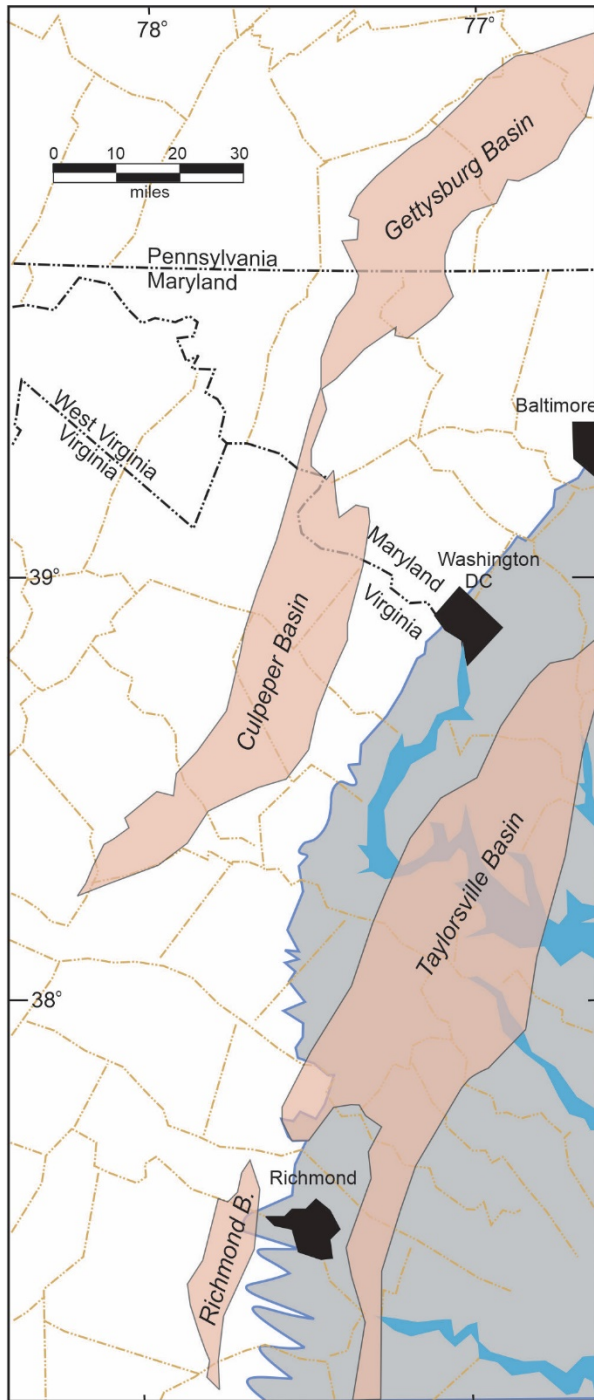


**Figure 25. Distribution of the known extent of the Taylorsville Basin and its relationship to the Culpeper and Gettysburg basins. Generalized overlap of Coastal Plain cover succession (gray) modified from Hansen and Edwards (1986), Vroblesky and Fleck (1991), and Meng and Harsh (1991).**

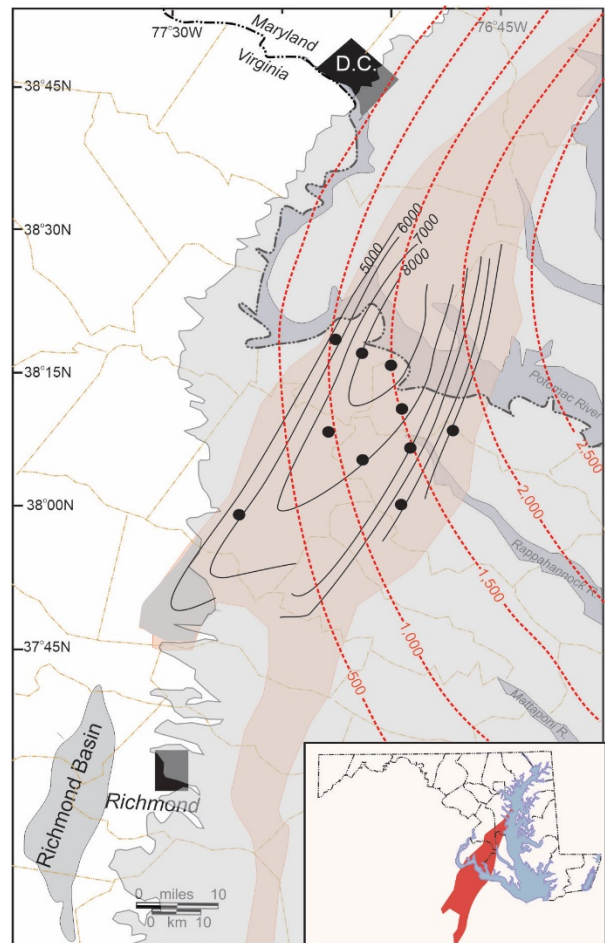


**Figure 26. Thickness of Coastal Plain strata covering the Taylorsville Basin, and generalized thickness of the basin fill determined from well logs.**

### **Taylorsville Basin Succession**

Based on well logs presented by LeTourneau (2003), more than 8,000 feet of Triassic rocks are buried within the central portion of the Taylorsville rift basin (Figure 26). This wedge of Late Triassic strata is thickest near the basin center and thins to the north and south, so that near the southwestern margin of the basin, as little as 5,000 feet of strata are preserved (Weems, 1980). In this area, the Triassic strata are assigned to the Doswell Formation (Weems, 1980). The rocks are partially exposed by fluvial incisions in what is herein termed the Doswell inlier (Figure 27). Within this inlier Triassic strata can be shown demonstrably to overlie the Late Paleozoic Petersburg Granite. The

stratigraphic succession of the Doswell Formation within the inlier consists, in ascending order, of the Stagg Creek, Falling Creek, and Newfound members. The character and distribution of these exposed strata have been discussed by numerous authors (Weems, 1980, 1981, 1986; Cornet and Olsen, 1990; LeTourneau, 2003). As part of this study, strata exposed along Stagg Creek in the southwestern margin of the basin were examined and sampled for petrographic analysis.

correlations with similar lithologies of the Newark Basin. Furthermore, interpretations presented herein suggests that both of these units are basinward facies of the Vinita and Newfound members of the Doswell inlier. Thus, we are in agreement with Weems et al. (2016) that the terms Port Royal and Leedstown formations should be discarded.

### Doswell Formation

**Stagg Creek Member:** The basal unit of the Doswell Formation, the Stagg Creek Member, rests unconformably upon the Late Paleozoic Petersburg Granite (Weems, 1980; Cornet and Olsen, 1990) and consists of more than 750 feet of tan-weathering, massive to cross-bedded, pebbly, coarse-grained sandstone with intervals of granule and pebble conglomerate. This member is named for exposures along Stagg Creek located south of Virginia State Highway 54 in Hanover County, Virginia (Figures 27, 28).

At its type section, the base of the Stagg Creek Member consists of weathered, subangular quartz and feldspar crystals comprising conglomeratic layers that demarcate the unconformity between the Triassic and older granitic substrate. Individual sandstone intervals within the Stagg Creek Member exhibit sharp bases, are between 20 and 40 feet in thickness, and tend to fine upsection into medium-bedded, coarse-grained sandstones at their tops (Figure 28A). The top of the Stagg Creek Member is not exposed at the type section, but the poorly exposed strata that overlie it suggest that the member is less resistant to erosion and is finer grained.

**Vinita Member:** Weems (1980) assigned the interbedded gray to dark gray sandstone and shales overlying the Stagg Creek Member to the Falling Creek Member. LeTourneau (2003) recommended abandoning this name and replacing it with the Deer Creek and Poor Farm Members. However, Weems et al. (2016) demonstrated the utility of the original stratigraphic arrangement and recommended replacing the Deer Creek, Poor Farm, and Falling Creek names with the Vinita Member, a name with priority, similar stratigraphic

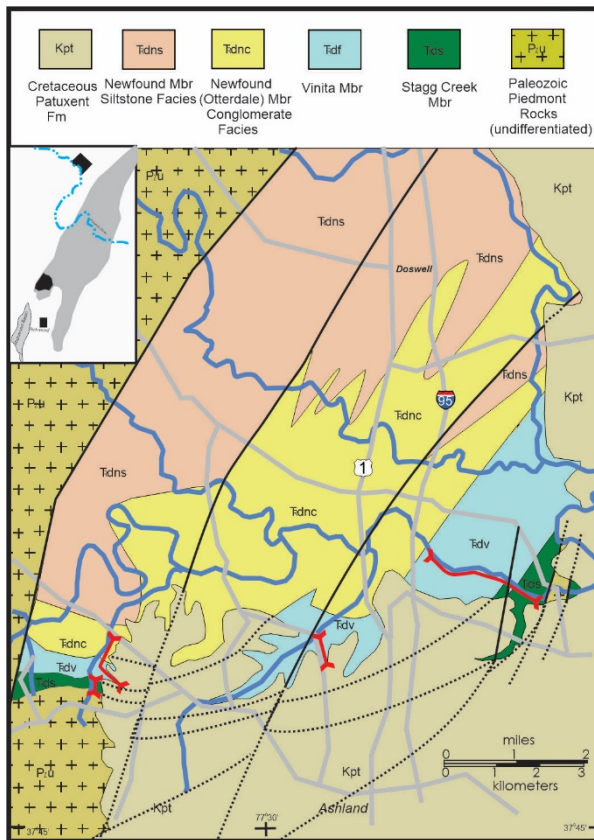


**Figure 27. Geologic map of the Doswell inlier in the southwestern part of the Taylorsville Basin, modified from Weems (1980, 1981, 1986). Stagg Creek section demarcated in southwestern corner of the map by black line.**

Within the central part of the Taylorsville Basin, LeTourneau (2003) named the Port Royal and Leedstown formations for more than 3,000 feet of subsurface strata overlying the Doswell Formation. Weems et al. (2016) recommended these terms be abandoned based on interpreted

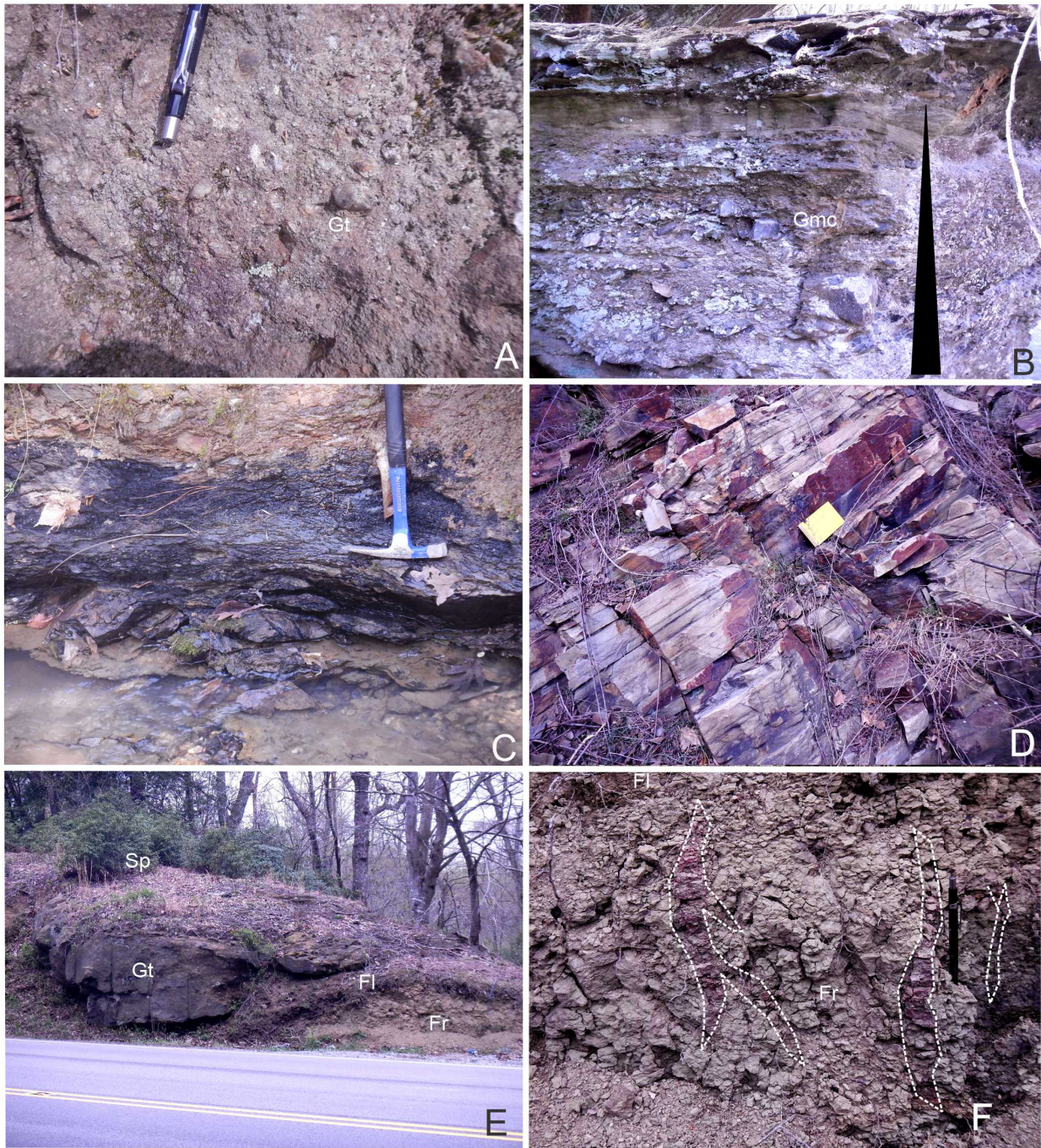


**Figure 28. Lithologic character of the Doswell Formation along Stag Creek. A, Cross-bedded conglomerate in the lower Stag Creek Member of the Doswell Formation. B, Fining upward, clast-supported debris flow conglomerate, Stag Creek Member. Pencil at top of outcrop for scale. C, Coaly shale of the lower Vinita Member. D, Flaggy, planar-bedded, medium-grained, upward-fining sandstone of the upper Vinita Member. E, Channel forms massive conglomerate (Gt) and adjacent rooted, laminated mudstone (Fl) of the Newfound Member. F, Close up of rooting within mudstone shown in E.**

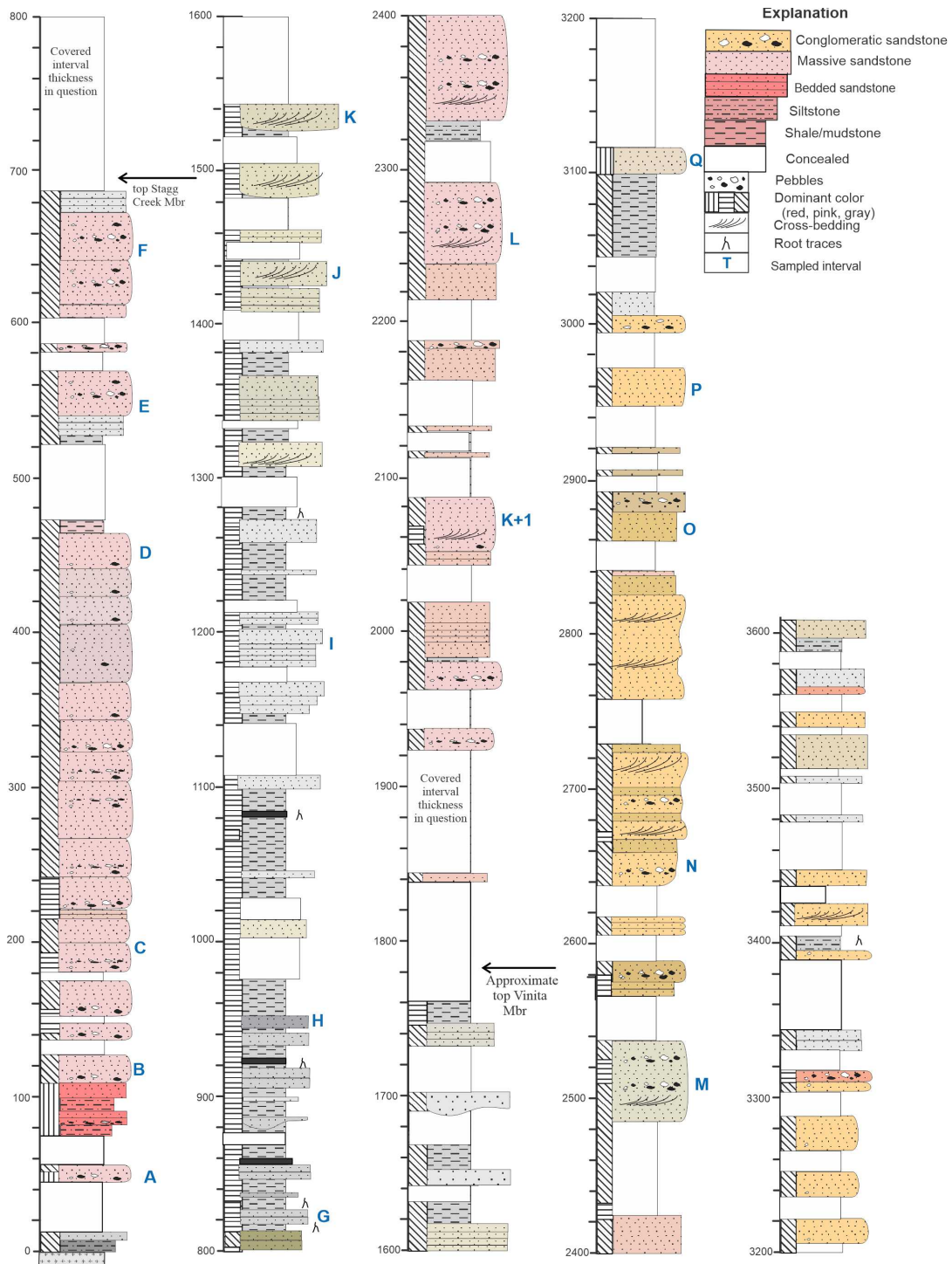


Figure 29. Graphic measured section of the Doswell Formation exposed along Staggs Creek, Hanover County, Virginia (based on descriptions of Weems, 1980). Letters represent sampled sandstone intervals. Vertical scale in feet.

position, and identical lithologic attributes in the adjacent Richmond Basin.

Weems (1980) placed the basal contact of this member between the lowest limestone, coal, or black shale above coarse-grained sandstone beds of the Stagg Creek Member. At the measured section along a tributary of Stagg Creek, the lower Vinita Member consists of interbedded gray to dark gray, laminated to flaggy, medium- to fine-grained, calcareous sandstone, dark gray claystone to shale, thin argillaceous coals, and thin argillaceous limestone (Figure 28D).

Above the gray shaly and coal-bearing lower half of the member, the unit consists of interbedded tan, medium-grained, upward-coarsening sandstones and greenish gray to drab, laminated and bioturbated siltstone and shale (Figure 28C). Within this upper half of the member the sandstone intervals tend to progressively increase in thickness and coarseness upsection (Figure 29). They also exhibit some conglomeratic interbeds and lenses, especially near the top of the member.

The thickness of the Vinita Member along Stagg Creek is approximately 1,100 feet. In the nearby Richmond Basin, Ressetar and Taylor (1988) suggested that the Vinita Member may be as much as 4,000 feet thick. Weems (1980) placed the top of the Vinita Member in the Taylorsville Basin above the highest claystone, siltstone, or laminated sandstone, and below the first massive, coarse-grained, cross-bedded conglomeratic sandstone of the overlying Newfound Member.

**Newfound Member:** The upsection coarsening represented by the upper Vinita Member continues into the overlying interval named the Newfound Member (Weems, 1980). This part of the Doswell Formation consists of interbedded, tan to light gray, massive and cross-bedded conglomerates, pebbly, coarse-grained sandstone, and greenish gray, rooted, silty shale and siltstone. Approximately 1,800 feet of this member are discontinuously exposed, but Weems (1980) postulated that as much as 3,000 feet may be present. Ressetar and Taylor (1988) proposed that the Newfound Member was equivalent to the Otterdale Sandstone of the Richmond Basin.

Correlations provided herein suggest that this is only partially correct. Therefore, the Newfound Member name is retained for this study.

Along Stagg Creek, the lower part of the Newfound Member consists of interbedded, tan-weathering, light gray, massive, cross-bedded conglomerates, pebbly, coarse-grained sandstone, and greenish gray, rooted, silty shale and siltstone. Weems (1980) termed this part of the member the conglomerate facies. For this part of the unit, conglomerate makes up about 35% of the member, while sandstone constitutes about 63%. Above the lower coarse-grained part of the member the unit exhibits a tendency toward upward-fining, whereby the conglomerate interval is replaced by intervals of interbedded sandstone and siltstone. This upper, finer part of the member consists of interbedded, light brown, upward fining sandstone and dusky red siltstone. In this upper part of the Newfound Member, conglomerate makes up only about 5% of the member while sandstone comprises 65% and siltstone 30% (Weems, 1980). Approximately 1,800 feet of this member are discontinuously exposed along Stagg Creek. Based on geologic map distribution, the Newfound Member appears to exhibit a wedge-shaped geometry that thins away from the western border fault towards the southeast (Weems, 1980, fig. 5). In total, the Newfound Member is approximately 3,000 feet thick (Weems, 1981).

#### **Stagg Creek Lithofacies Associations**

Although the lithofacies associations developed from strata in the Culpeper and Gettysburg basins are evident within the Stagg Creek section, the vertical array of lithofacies associations differs substantially (Figure 30). At the Stagg Creek measured section, LA A was not clearly identified. Components of LA B preserved in the Stagg Creek Member are replaced upsection directly by Lithofacies Associations E near the bottom of the Vinita Member. There are no intervening proximal lake deposits of Lithofacies D, and thus the succession reflects a sharp

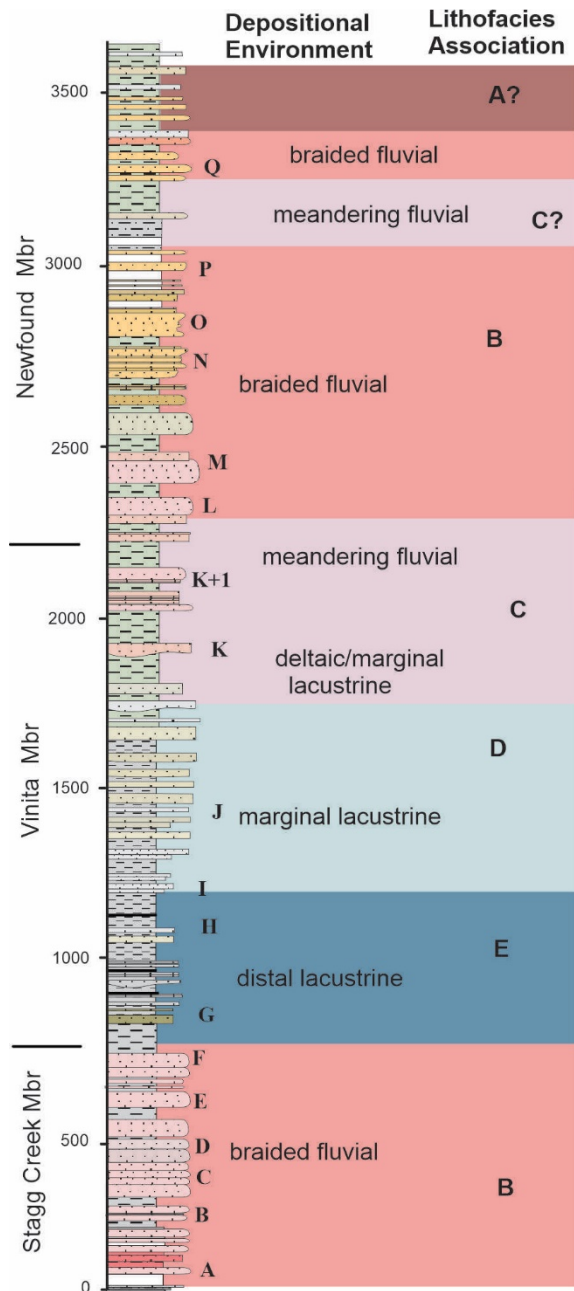


**Figure 30. Interpreted vertical arrangement of lithofacies associations within the Stagg Creek measured section.**

transition from fluvial to distal lacustrine (LA B to LA E). The distal lacustrine strata are then succeeded upsection by margin lacustrine and fluvial strata of Lithofacies Associations D and C at the top of the Vinita Member. At the top of the Stagg Creek succession, the Newfound Member marks the transition to braided fluvial deposition.

Massive, cross-bedded conglomerates of braided stream origin appear to represent prograding alluvial fan deposits along the border fault.

The rather sharp replacement of LA B by dark gray shales of LA E at the Stagg Creek-Vinita contact is dissimilar to the gradual transition of braided to meandering fluvial sediments followed by proximal lacustrine deposits observed in the Culpeper and Gettysburg basins. The difference may reflect the paleogeographic proximal position of the Stagg Creek section relative to the border fault. However, it should not be overlooked that this sharp environmental transition is comparable to that in the Newark Basin where the Stockton Formation sharply transitions into the Lockatong Formation (Olsen et al., 2016, fig. 4)

### Taylorville Basin Lithofacies Associations

The lithofacies associations identified within the exposed strata of the Culpeper and Gettysburg basins are comparable to those observed within the Doswell Formation along Stagg Creek. Furthermore, this consistency in lithologic character between exposed basin strata suggests that comparable lithofacies also should be expected to occur within the buried strata of the Taylorville Basin. Assessing these buried basin lithologies is substantially more difficult and their study requires evaluation of incomplete geophysical and descriptive logs provided to MGS by LDEO (Lamont Doherty Earth Observatory). Information supplied by LDEO includes descriptive and interpretive logs of the coreholes (Payne, Bowie, Butler, Ellis, Roberts wells), interpretive well cuttings logs (Thorn Hill and Wilkens wells), and grain-size logs from LeTourneau (2003) (Thorn Hill and Campbell boreholes).

To help develop a level of equivalence between exposed and subsurface stratigraphic successions, an effort was made to determine if the five lithofacies associations within exposed strata could be established through buried basin logs. In an effort to make this interpretive leap, several assumptions regarding lithology were necessary. The first of these presumptions was that thick intervals of massive, red siltstone and mudstone likely represent proximal lake deposits (LA D).

Secondly, gray to dark gray shaly intervals were interpreted to represent perennially wet areas of distal lake environments (LA E). Polymictic conglomerates and intraclastic sandstones with interbeds of black shaly facies represent distal parts of alluvial fan deposits (LA A). Massive, cross-bedded, quartzose or arkosic conglomerates and interbedded, rooted or pedogenically altered mudstone were interpreted to represent braided stream channel and overbank deposits of LA B, respectively. Lastly, reddish intervals containing thick upward-fining or upward-coarsening, medium to coarse-grained sandstone interbedded with red mudstone were interpreted as representing meandering stream or marginal lake deltaic sand bodies (LA C).

These interpretive presumptions regarding the buried succession of lithologies necessitate the a priori depositional insight gathered from evaluating exposed strata. Figure 31 provides examples of this interpretative translation. Each example of the lithofacies associations was extended from borehole evaluations that were published or acquired from LDEO. Specifically, Figure 31A is extracted from examination of the core from the Campbell well. This sequence consists of interbedded clast- and mud-supported polymictic conglomerates and black shale. The paleogeographic setting of this well near the western border fault along with the intrinsic lithologic character suggest that it was formed by debris flows along a lake margin (LA A). The example portrayed in Figure 31B consists of pebbly, cross-bedded sandstone interbedded with rooted, caliche-rich paleosols of a fluvial braidplain (LA B). Figure 31C reflects the more pronounced fining succession suggestive of meandering fluvial environments (LA C), while Figures 31D and E reflect successions characteristic of lacustrine deposits. Figure 31D contains few caliche horizons while 31E has numerous limestone interbeds. These examples are interpreted as representing the succession consistent with lithologies assigned to Lithofacies Associations D and E, respectively, within the Culpeper and Gettysburg basins.

To ascertain the vertical and lateral relationships of lithofacies associations and their presumed depositional environments, generalized cross-sections were constructed utilizing the geophysical, descriptive, and interpretive logs obtained from LDEO and gleaned from LeTourneau (2003, figs. 3.4, 3.5). One of these interpretive sections was oriented parallel to the strike of the basin (Figure 32) and the second was oriented normal to strike (Figure 33).

The strike-parallel section was extended into the Richmond Basin by including extrapolated data from the Bailey well and the interpreted depositional facies that exemplified it (Ressetar and Taylor, 1988, fig. 17.4). Furthermore, gross lithologic attributes based upon outcrop data from the Stagg Creek outcrops (Weems, 1980) (Figure 30) were incorporated as a correlative section. The arrangement of lithofacies associations depicts a vertical succession of basin infilling that fines upsection from a thin, but pronounced, basal fluvial package (LA B), that is equivalent to the Stagg Creek Member in outcrop and appears to fine and interfinger with finer grained lithologies towards the basin center. Dark gray, distal lacustrine deposits (LA E), equivalent to the lower Vinita Member, thicken into the deepest part of the basin. At Stagg Creek, marginal lacustrine facies (LA D) are thin, but dramatically thicken into the basin along strike. The prograding alluvial fan deposits similar to the Otterdale Sandstone and Newfound Member in the southern part of the cross-section appear to grade into lacustrine deposits near the basin center.

The overall depositional trends observed in this cross-section suggest depositional sequences that expectedly fine from the basin margin to basin center. These trends are complemented by an overall up-section shoaling from distal lacustrine near the basin center to more proximal lacustrine, and even fluvial deposits, near the top of the succession.

The interpretive cross-section that is oriented normal to depositional strike presents patterns of lateral and vertical changes across the basin that are consistent with other studied basins (Figure 33). Debris flow conglomerates of Lithofacies

Association A are present along the western margin of the basin. This lithologic association is preserved within the Campbell well (Figure 31A) as well as in interfingering conglomerates and distal black shales in the Thorn Hill and Wilkens descriptive logs. The basin center deposits are primarily black shale and gray siltstone and sandstone suggestive of Lithofacies Association E. Eastward in the basin, thick intervals of red mudstone and siltstone suggest proximal lake deposits (LA D) that are punctuated by debris flow conglomerates. Along the eastern margin these reddish, proximal lake mudstones are punctuated by intervals of fluvial-derived sandstone and conglomerates within the Gouldman and Ellis wells.

The two stratigraphic profiles appear to suggest that basin infilling of the Taylorsville Basin was accomplished both by alluvial and fluvial progradation and by upward fining and shallowing. The lithofacies approach applied here does not display a high level of congruence with the depositional patterns presented by LeTourneau (2003, fig. 3.8C). The reason for this incongruity is not clear. It may be the result of differing approaches to depositional analysis, or perhaps the incomplete dataset available for this study produced the divergent interpretations.

Milici et al. (1991, plate 1) presented an interpretation for the Teledyne 11A seismic line that transects the basin near its widest point. This interpretation points to several groups of reflectors whose presence may assist in confirming depositional reconstruction interpretations. One such grouping of inclined reflectors is present near the eastern margin of the basin. These reflectors were proposed to represent coarser strata that intersect the generally flat-lying strata of the basin center at oblique angles (Figure 34A), and were interpreted to be a coarse-grained, progradational succession (Milici et al., 1991). When compared to the arrangement of lithofacies associations (Figure 33), the interpreted progradational stratigraphic package shows parallel coarsening lithologies near the western margin of the basin. This coarsening is interpreted to represent tongues of fluvial deposits that punctuate the largely

lacustrine deposits between the Bowie and Ellis wells. This coincidence tends to verify the interpretations presented herein.

Although there is direct evidence within the subsurface logs and seismic cross-section for the progradational package of coarse-grained strata near the top of the rift basin succession, there is also indirect evidence for an alluvial fan sequence along the faulted western margin. This presumed wedge of alluvial fan deposits has not been definitively identified in any of the subsurface cores or cuttings; however, its presence can be inferred based upon lithologic components within well logs from drill holes nearest to the western border fault (Figure 31A). Within wells located nearer the Taylorsville Basin's western border fault (Campbell and Thorn Hill wells), distal lacustrine lithofacies (Association E) appear to be interbedded with thin sandstone and conglomeratic strata (Figure 31A). This type of textural incongruence is compatible with debris flow deposits on a distal alluvial fan (Larsen and Steel, 1978; Nemeč and Steel, 1984). The presence of these coarse-grained sandstone and conglomerate strata within black shaly intervals is interpreted to be identical to lithofacies documented in the western Culpeper Basin by Hentz (1985) and the upper Gettysburg Basin (Arendtsville Member). The occurrence of identical lithologies within deep-water lacustrine deposits of the western Taylorsville Basin suggests that these areas may have been located near the distal end of a basin margin alluvial fan or set of coalescing fans (Nemeč and Steel, 1984; Horton and Schmitt, 1996).

### **Stratigraphic Architecture of Triassic Basins**

Fail (2008) suggested that the Culpeper, Gettysburg, and Newark basins were symmetrical structures that were faulted and deformed after deposition. The outcrop-based study of the Culpeper and Gettysburg basins provides a reason to question the integrity of the traditional, structurally-based, symmetrical sedimentation models where formations are interpreted to be tilted post-depositionally. Schlische and Olsen (1990) has shown the most CAM basins preserve a

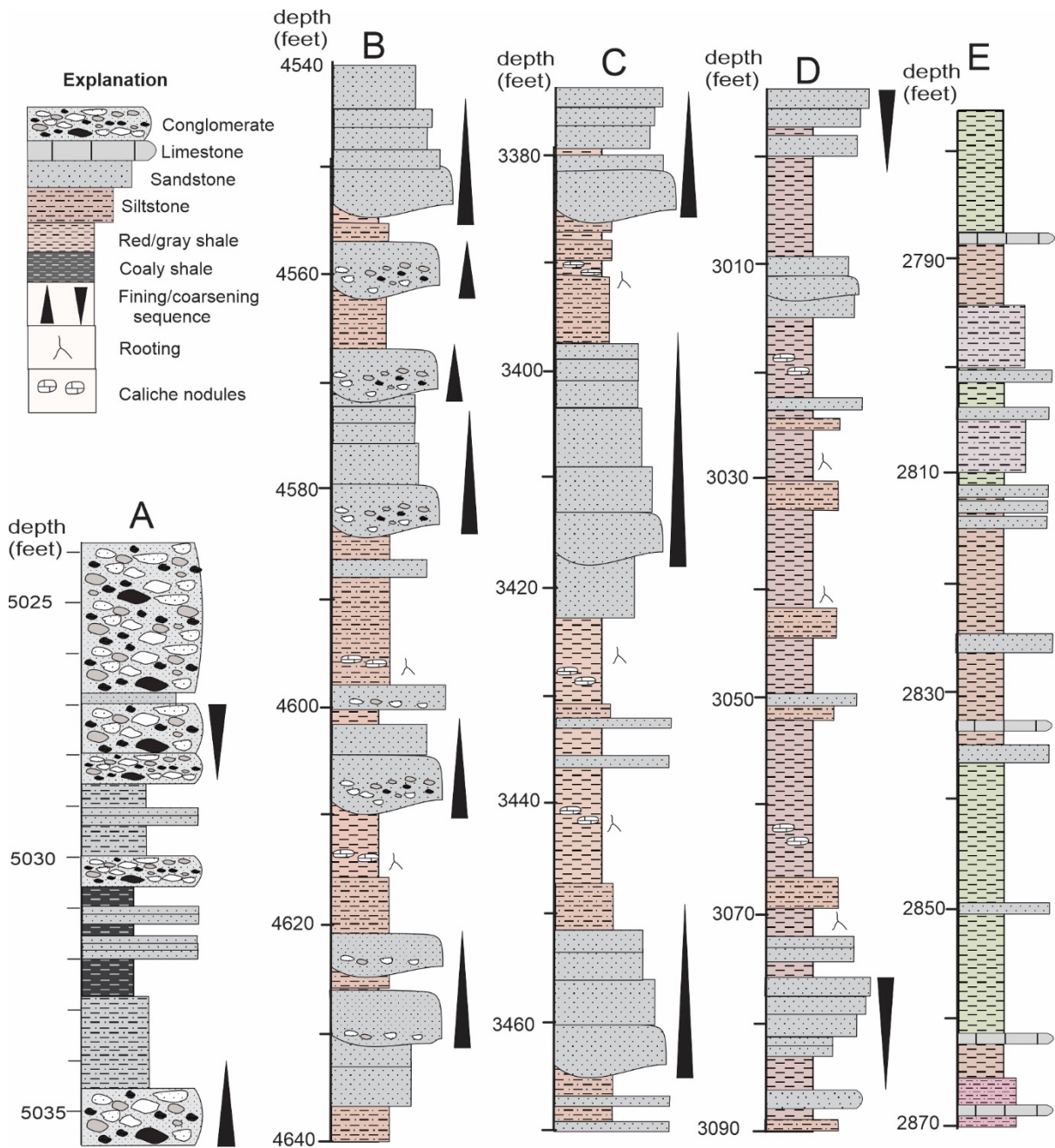


**Figure 31. Interpreted facies associations based on geophysical and interpretive logs within Taylorsville Basin wells. A, Graphic log of a section of the Campbell well showing interbedded conglomerates and black shale that illustrate Lithofacies Association A. B, Succession of sandstone and mudstone within the Ellis well core suggesting deposits of Lithofacies B. C, Interval of lenticular, fining-upward sandstones within the Ellis core that indicate Lithofacies Associations C. D, Sequence of interbedded mudstone and siltstone within the Butler well core that are interpreted as reflecting Lithofacies Association D. E, Interbedded greenish gray shale, limestone, and siltstone within the Thompson well (Milici et al., 1991) that are suggestive of deposition within Lithofacies Association E.**

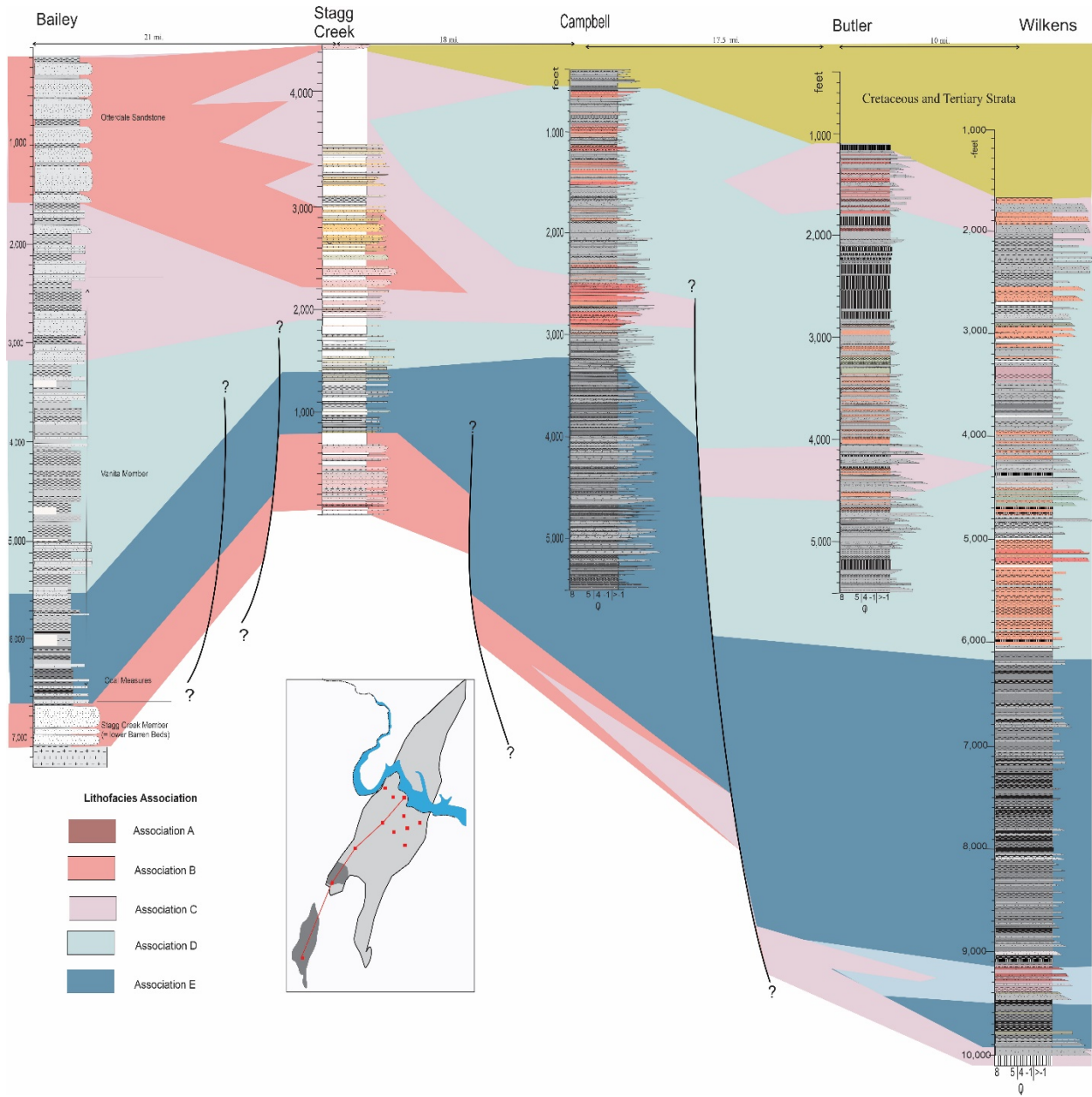


**Figure 32. Strike-oriented stratigraphic section of Triassic lithofacies associations in the Richmond and Taylorsville basins. Sections include interpreted facies within the Bailey well from Ressetar and Taylor (1988, fig. 17.4) and outcrop data from the Stagg Creek section (see Figure 30).**

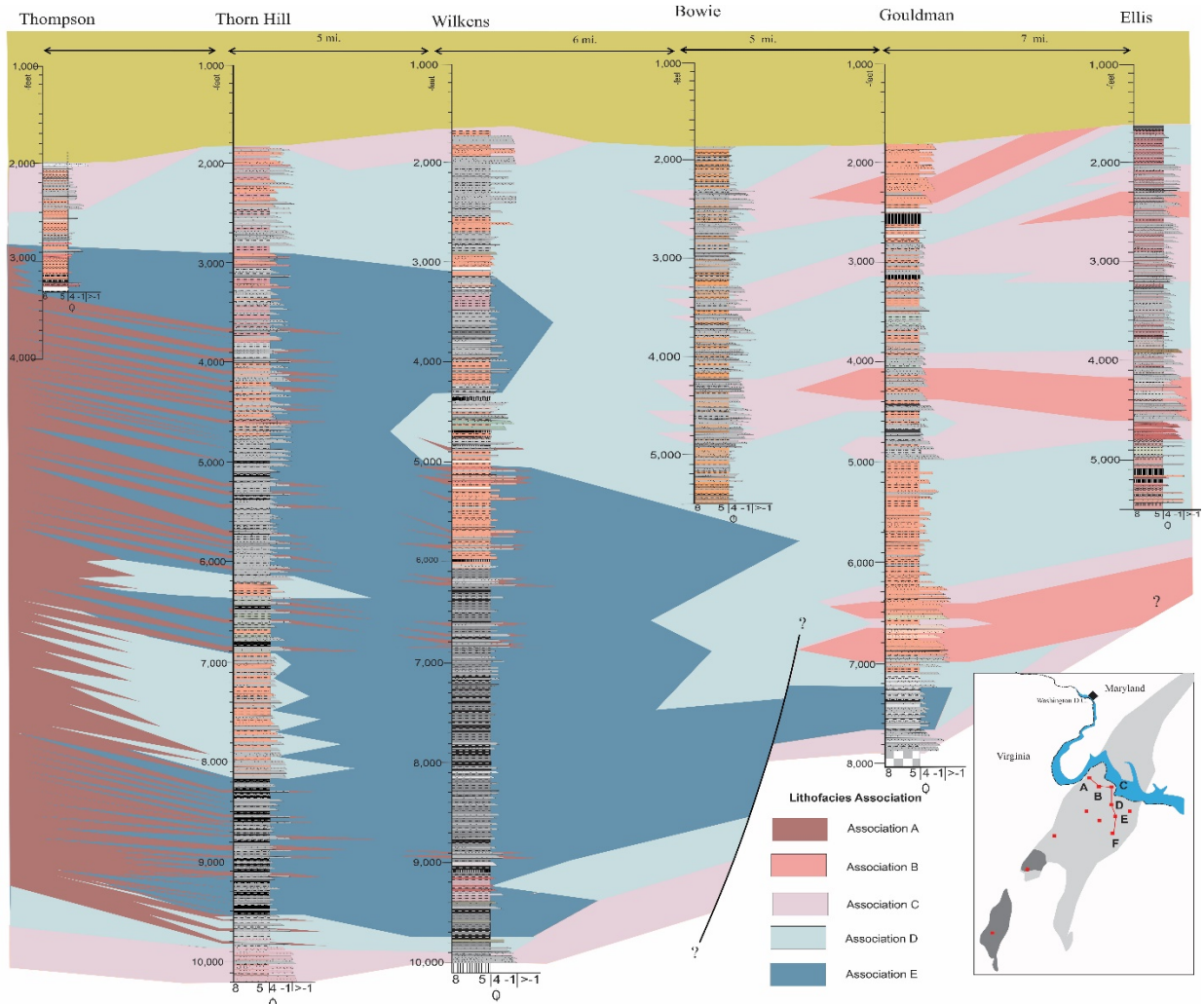


**Figure 33. Interpretive strike-normal dip-oriented cross-section of lithofacies associations of the Taylorsville Basin. A=Thompson well (from descriptions in Milici et al., 1991), B=Thorn Hill well, C=Wilkens well, D=Bowie-Fogg well, E=Gouldman well, F=Ellis well.**

tripartite infilling sequence that suggests asymmetric depositional pattern. However, by comparing the arrangement of this 3-fold pattern as reflected in the Culpeper and Gettysburg basins' succession, and that of the Taylorsville Basin suggests that the stratigraphic architecture changes from on basin to other. The lithofacies association architecture of the Taylorsville Basin suggests a sharp change from fluvial to deep lake deposition, followed by shoaling into more proximal lake deposits. This differs from the Culpeper and Gettysburg basins which appear to reflect a gradual stratigraphic change from fluvial to proximal lake then to distal lake deposits. Even

with these differences, authors have consistently portrayed the depositional units of CAM rift basins as stacked sequences that overlap towards the rifts hanging wall block (Schlische, 1993; Schlische and Olsen, 1990; Withjack et al., 2013). The lithofacies association architecture of the Taylorsville Basin presents a compelling argument to re-evaluate the currently held patterns for Triassic basin infilling sequences. The vertical and lateral lithofacies variations displayed within the Taylorsville Basin are fundamentally dissimilar to the widely accepted paradigm for the infilling of North American Triassic rift basins. The Newark, Gettysburg, Culpeper, and Dan River basins have

conventionally been portrayed as consisting of continuous layers that form semi-isochronous packages that have been tilted (Root, 1988; Schlische, 1993; Schlische and Olsen, 1990; Schlische et al., 2003; Withjack et al., 2013; Olsen et al., 2015). These interpretations are based largely on formational-level units and the quantitative filling model proposed by Schlische and Olsen (1990). This structurally-derived model predicts the tripartite group of lithofacies

producing a repeatable megasequence. Although parts of such megasequences are identifiable within the three basins studied here, it fails to satisfactorily explain the arrangement of lithofacies associations presented herein. Moreover, the basin widening and depositional onlapping fails to explain the changes in lithofacies associations within the Taylorsville (Figure 33) or Gettysburg basins (Figure 22).

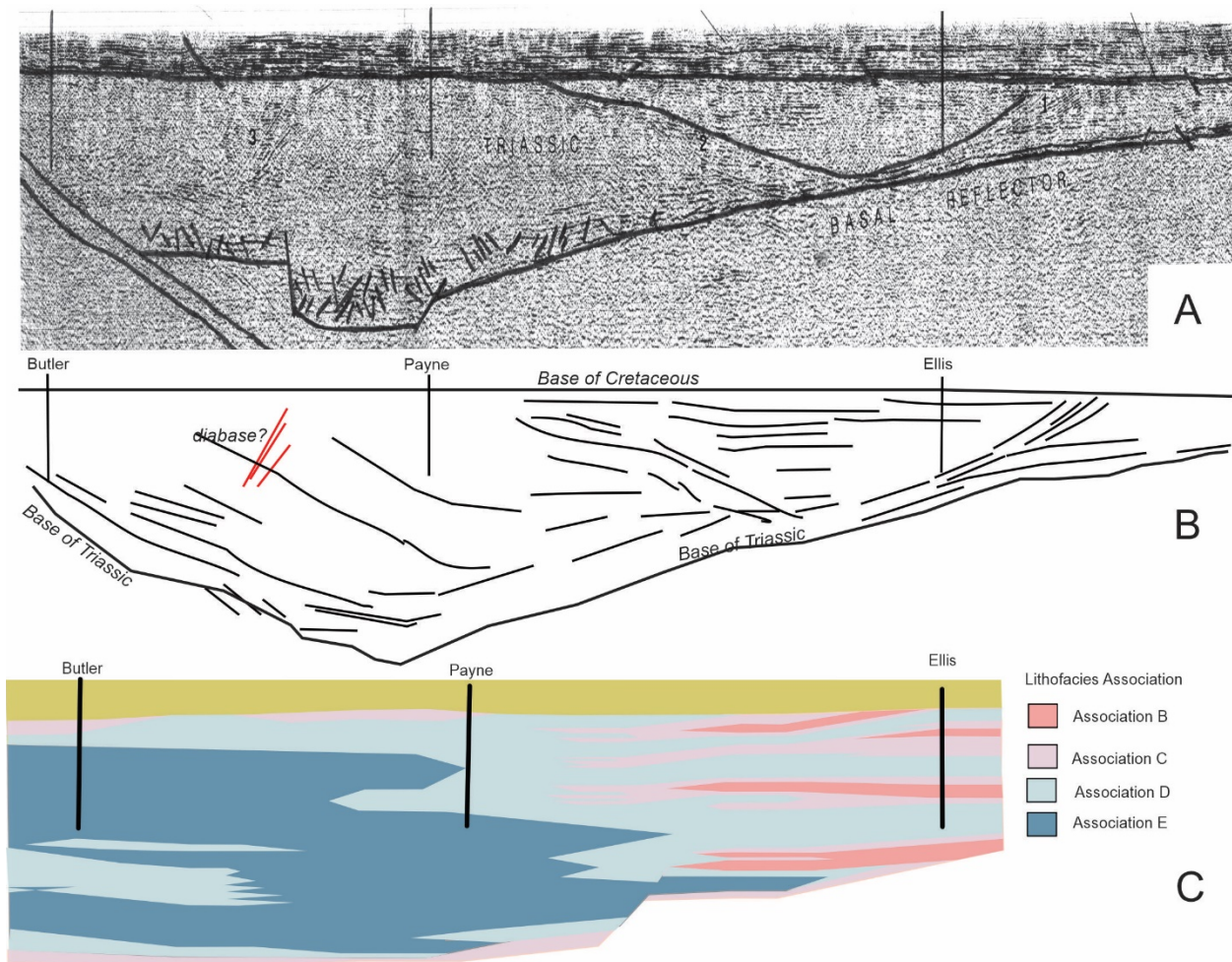


**Figure 34. Interpreted relationship between seismic cross-section and Taylorsville Basin lithofacies associations. A, Teledyne 11A seismic cross-section interpreted in Milici et al. (1991, pl. 1) exhibiting an area of presumed important reflectors. B, Distribution of identifiable reflectors within seismic cross-section. Modified from Smoot (2009, fig. 27). C, Facies associations cross-section (from Figure 26) resized to be compatible with seismic cross-section. Coincidence of inclined reflectors on eastern and western side of section with lithofacies associations is suggestive of progradational fluvial deposits.**

Smoot (2010, fig. A3) and Olsen et al. (2016, fig. 9) have shown that lithologic facies do not in fact coincide with formational designations. Thus, the arrangement of sedimentary facies, source areas, and dispersal centers depicts a much more complex pattern of deposition than simplified geologic map patterns. Based on this premise, Smoot (1991, 2010) provided a rift basin infilling and lithofacies model that is best explained by basin subsidence and climate variations. The individual facies proposed by Smoot (1991) display a predictable arrangement, but do not

appear to reflect movement of the basin border fault. The resulting model provides explanations for vagaries in local fluvial input and central lake distribution and character. This depositional model, controlled by both autogenic and allogenic processes, portrays rift infilling successions as a more complex series of depositional tongues in which younger units overlap or prograde over older (Thayer, 1970; Berg et al., 1980; Turner-Peterson, 1980; Turner-Peterson and Smoot, 1985; Smoot, 1999; Yager and Ratcliffe, 2010).

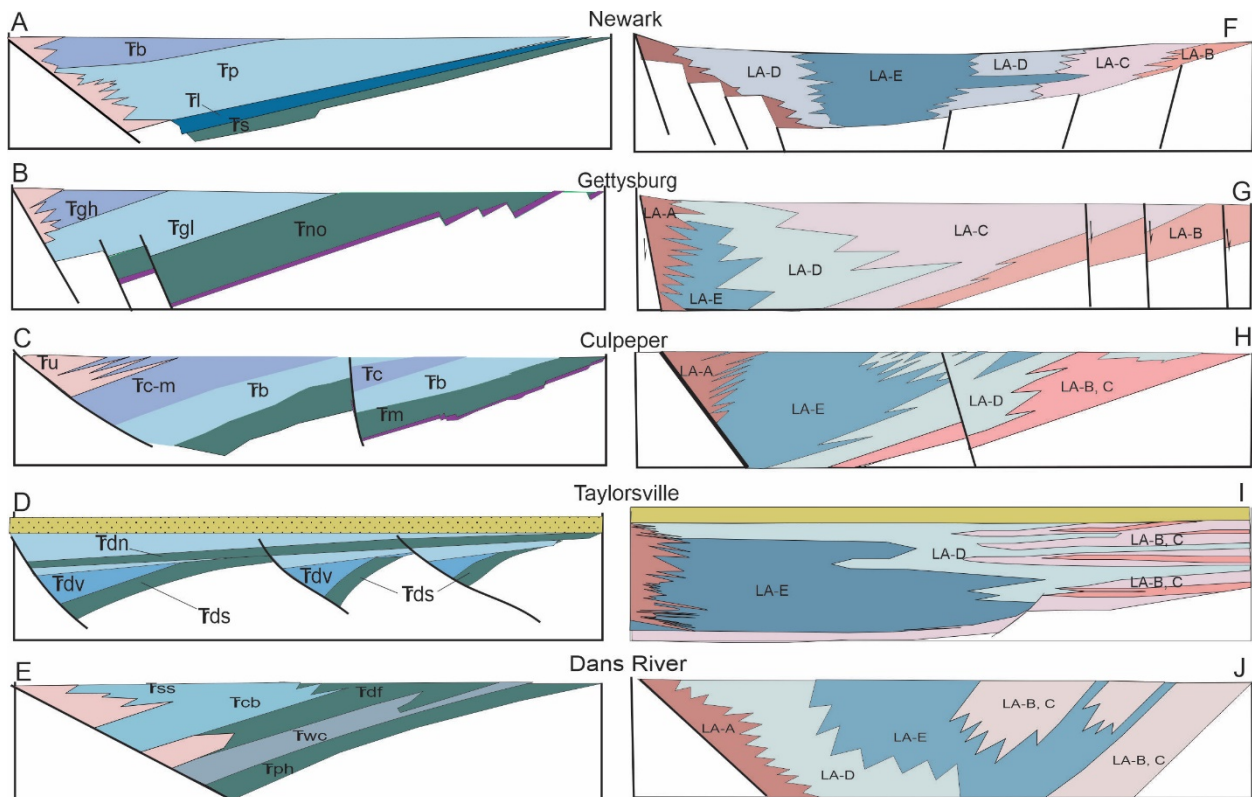


**Figure 35. Presumed differences between traditional lithostratigraphy and lithofacies associations architecture for several Triassic basins of eastern North America. A, Newark Basin (Schlische, 1993). Ts=Stockton, Tl=Lokatong, Tp=Passaic, Tb=Boonetown. B, Gettysburg Basin (Root, 1988). Tno=New Oxford, Tgl=lower Gettysburg, Tgh=Heidlersburg. C, Culpeper Basin (Southworth et al., 2006). Tm=Manassas, Tb=Bull Run, Tc-m=Catharpin Creek-Midland, Tc-u=upper formations. D, Taylorsville Basin (LeTourneau, 2003). Tds=Stagg Creek, Tv=Vanita, Tn=Newfound. E, Dan River Basin (Olsen et al., 2015). Tph=Pine Hall, Twc=Walnut Cove, Tcb=Cow Branch, Tss Stoneville. Lithofacies architectural based upon reconstruction of lithofacies associations. F, Newark Basin (Turner-Peterson, 1980). G, Gettysburg Basin (Brezinski 2021). H, Culpeper Basin. I, Taylorsville Basin (data presented herein). J, Dan River (Thayer, 1970).**

Data from the borehole data studied for the Taylorsville Basin, some penetrating the entire basin fill succession, provide a rare view into the character of an CAM rift basin sequence. This perspective goes beyond the piecemeal stratigraphic sections, disjunct incomplete well data, and seismic cross-sections that characterize other basins. The depositional complexity depicted by lithofacies associations in Figures 32 and 33 reflects a level of stratigraphic sophistication also interpreted by some authors for the Newark (Turner-Peterson, 1980; Turner-Peterson and Smoot, 1985; Smoot, 1999; Yager and Ratcliffe, 2010), Dan River (Thayer, 1970), and Richmond (Ressetar and Taylor, 1988) basins. Thus, there are discernable differences between the traditional portrayal of the unit cross sections for these basins and those proposed herein (Figure 35).

The complexity of lithofacies associations within the Taylorsville Basin reflects a level of congruence not only with other CAM rift basins (Figure 35), but rift valleys of other rift and drift sequences. Blair (1987) demonstrated the complex lithologic relationship created by variations of subsidence and hydrology within a Jurassic-Cretaceous rift valley of Mexico. This study found that while alluvial fans were constructed normal to the basin axis, fluvial deposits were formed by flow parallel to the basin axis. Moreover, lacustrine facies formed in localized depressions within the basins and their geographic extent varied in accordance with precipitation. Burggraf and Vondra (1982) demonstrated that since rift valleys tend to form in similar tectonic settings, they tend to form facies patterns that parallel one another. Cohen (1989) also found that within recent rift lakes of Turkana and Tanganyika, infilling succession were characterized by lateral progradation of marginal, coarse-grained, fluvial-derived lithofacies into and over fine-grained, lacustrine lithofacies. Such deposits were formed as laterally continuous layers. Yuretich (1979) described variations in fine-grained sediments in Lake Turkana showing distribution patterns analogous to those of ancient extensional basins. Thus, CAM rift facies patterns appear to

demonstrate a comparable complexity to extant rift deposits.

## **TRIASSIC SANDSTONE CHARACTERISTICS**

Study of Triassic sandstone characteristics is confined to exposed units only (Figure 36). Although this is not ideal for determination of porosity and permeability, the unavailability of core samples from the buried Taylorsville Basin necessitated utilization of exposed basin samples as proxies. Understanding the vertical and lateral changes in sandstone grain size, texture, and composition in units of the exposed basins, and their prospective porosity, may help focus further studies of buried Taylorsville Basin sandstones.

Almost all methods for estimating the amount of CO<sub>2</sub> storage in a geologic reservoir calculate total pore volume using porosity as a variable (Wickstrom et al., 2005). Previous studies have shown changes in percent porosity with porosity type (Kostelnik and Carter, 2009), burial depth (Medina and Rupp, 2012; Barnes and Ellet, 2014), framework grain composition (Bowen et al., 2011), and depositional features (Henares et al., 2016).

### **Methods**

Five discontinuously exposed stratigraphic sections of Triassic rift basin formations were sampled (Figure 36A). Two sections were within the Poolesville Member of the Manassas Formation in the Culpeper Basin. These sections were along the Monocacy and Potomac rivers near the boundary between Frederick and Montgomery counties, Maryland (Figure 36B), and along the bluffs of the Potomac River at Nolands Ferry in southern Frederick County, Maryland (Figure 36C). An equivalent stratigraphic interval in the New Oxford Formation was sampled in the Gettysburg Basin along the branches of Pipe Creek (Figure 36D). A section within the Conewago Member of the Gettysburg Formation was sampled along Lewisberry Road near the northern end of the Gettysburg Basin (Figure 36E). The final section was within the Doswell Formation along Stag

Creek in the southern Taylorsville Basin (Figure 36F).

At each studied section, representative hand samples were collected at regular stratigraphic intervals from sandstone units. Sampling locations were recorded with GPS as shown in Figure 36. Each hand sample was initially described for grain size, sorting, roundness, and color. Seventy-eight samples were collected and described. Samples were cut to billets the size of typical thin-sections, vacuum impregnated with blue epoxy, and cut to 30  $\mu\text{m}$  thickness (Figure 37). Fifty-nine thin sections were prepared. Because of the proximity of the Nolands Ferry's section to the Poolesville location, no thin sections were prepared from the former location.

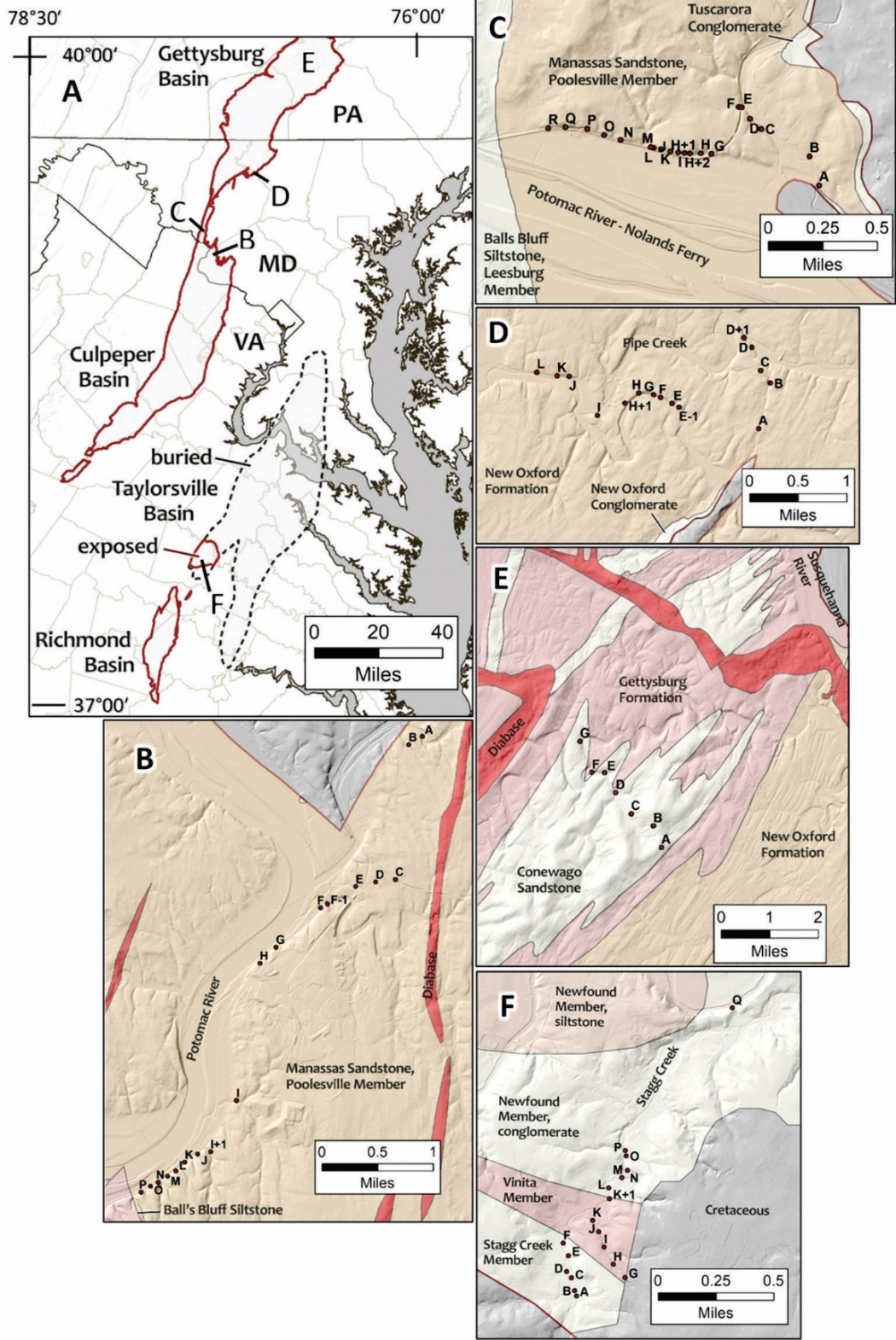
Image analysis was used to estimate percent porosity from scanned thin sections. This porosity estimation was based on any pores that had been filled with blue epoxy; therefore, it included preserved primary, secondary, and fracture porosity. High-resolution images were obtained by scanning the thin sections in plane-polarized light (PPL). Intensity hue saturation (IHS) was used to select the blue pore area in JMicrovision (Suhaimi, 2016). A rectangular area within each thin section image was selected and analyzed for percent porosity estimations (Figure 38, Appendix IA). The rectangle was drawn as large as possible (typically 1.5 x 2.5 cm) to capture most of the scanned thin section image, but the delineation was made to eliminate the edge of the sample and the surrounding blue epoxy from analysis, to avoid erroneously high porosity values.

Modal analysis was performed using the Gazzi-Dickinson method of point counting (Dickinson, 1970; Ingersoll et al., 1984) on a representative subset of thin sections under plane-

polarized light (PPL) and cross-polarized light (XPL) microscopy. Included in the point counts were framework grains (quartz/feldspar/lithics), accessory and opaque minerals, cements, and porosity types. Each sample was assigned a descriptive name (Figure 39) and provenance category (Figure 40) based on framework grain percentages, using the sandstone classification of Pettijohn et al. (1987) and Dickinson et al. (1983).

To assess diagenetic effects, original primary porosity was estimated for two samples from point count data. The two samples chosen (Conewago Member A and Poolesville Member G) represented grain size and composition of sandstones in both middle (Conewago) and lower (Poolesville) stratigraphic positions. Additionally, original primary porosity was estimated in the Poolesville G sample using analysis of scanning electron microscope (SEM) photomicrographs (Figure 41, Table 4). Only one sample was analyzed with SEM due to time and funding constraints. SEM cathodoluminescence (CL) analysis was chosen as an additional technique to find quartz overgrowths that might be missed in analysis using PPL and XPL microscopy. Diagenetic overgrowths have been shown to differ from detrital quartz in SEM CL properties (Demars et al., 1996). Overgrowths were manually selected from photomicrographs by comparison of SEM CL to PPL, XPL, and SEM secondary electron (SEM SED); percent area was then calculated in JMicrovision. In both point count and SEM analyses, any area of cement or quartz overgrowth was counted as original primary porosity. Areas of blue epoxy were not counted as original primary porosity because this present-day pore space could be secondary, due to dissolution and weathering in outcrop.

**Figure 36. Sandstone collection locations. A, Exposed (red line) and buried (black dashes) strata of the Gettysburg, Culpeper, Richmond, and Taylorsville basins. B, Detailed sampling locations in the Poolesville Member of the Manassas Formation along the Potomac River, Montgomery County, Maryland. C, Poolesville Member sampling at Nolands Ferry section, Frederick County, Maryland. D, Sample locations in the New Oxford Formation along Pipe Creek, Carroll County, Maryland. E, Sample locations in the Conewago Member of the Gettysburg Formation along Lewisbury Road, York County, Pennsylvania. F, Sampling locations for the Doswell Formation along Stag Creek, Hanover County, Virginia.** →



Sample	Primary Porosity (% cement)		Porosity (% blue epoxy)
	Point Count	SEM-CL Image Analysis	PPL Scanned Image Analysis
Conewago Member A	29	N/A	4.32
Poolesville Member G	18	15	0.02

Table 4. Estimate of primary porosity from standard microscopy point count techniques and SEM analysis compared to porosity assessed from PPL scanned thin section image analysis.

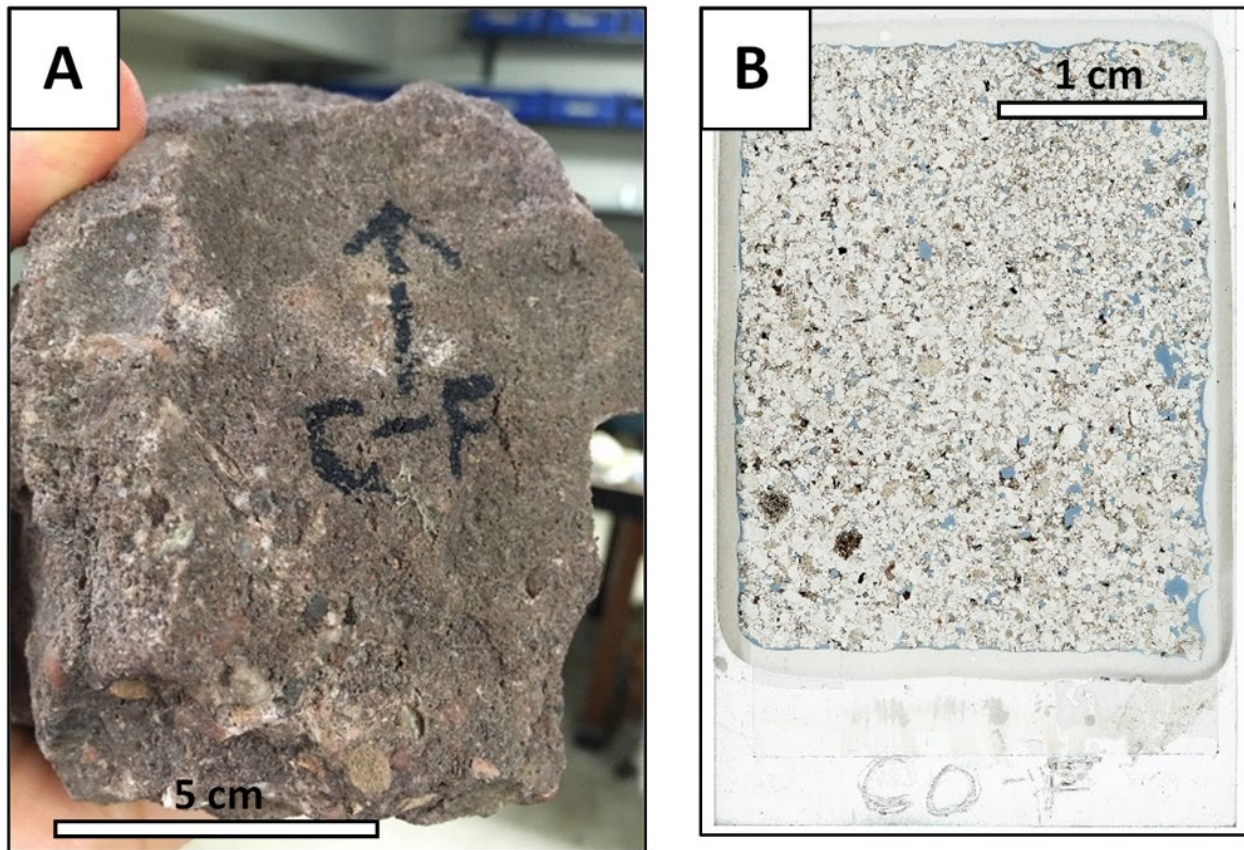
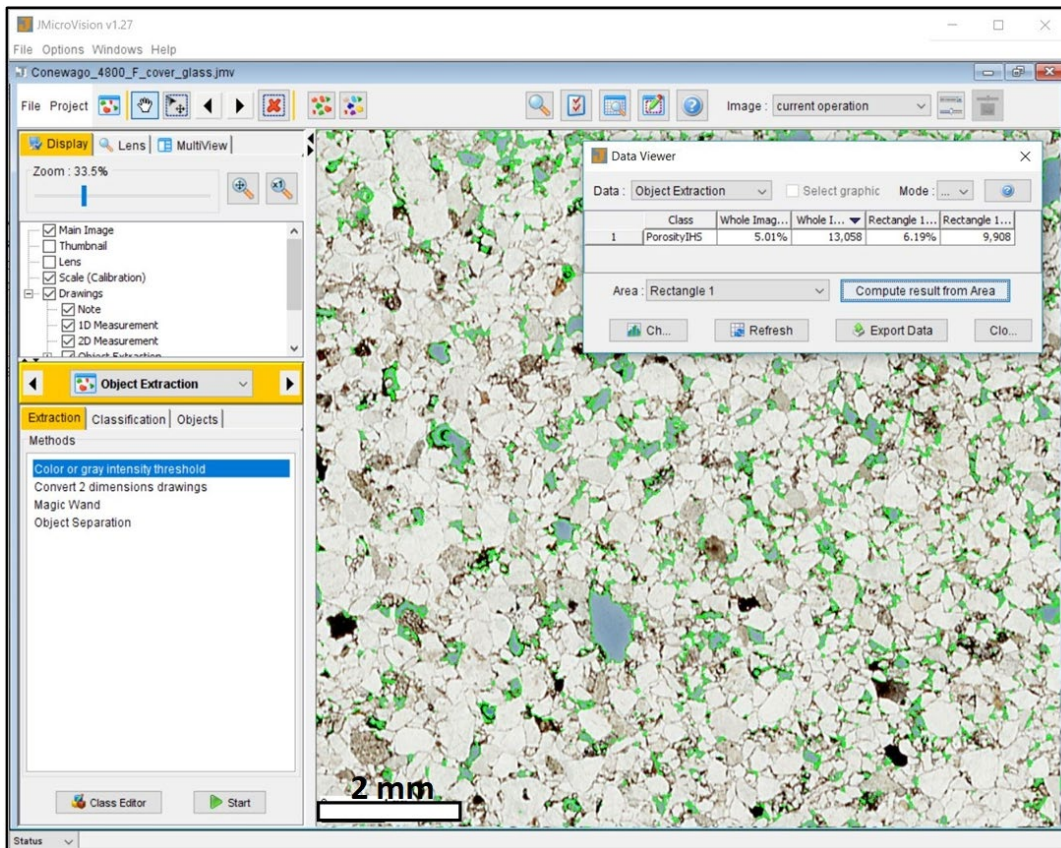


Figure 37. Sandstone sample F from the Conewago Member of the Gettysburg Formation, in hand sample (A) and thin section, vacuum impregnated with blue epoxy (B). The portion of the sample represented by thin section is often finer-grained than the sample as a whole (see larger grains at base of hand sample) due to difficulty in cutting an integral billet that contains pebble-sized grains.



**Figure 38. Image analysis of Conewago F scanned thin section. Screenshot of scanned thin section image in JMicrovision with blue pore area selected (green outline). Inset “Data Viewer” window shows percent porosity calculated for the whole image (the entire thin section) and a user-defined rectangle that eliminates the edge of the thin section.**

## Results

Thin-sections prepared from sandstone samples collected from the five stratigraphic sections in the Culpeper, Gettysburg, and Taylorsville basins were analyzed to evaluate texture, composition, and porosity.

### Sandstone Composition and Present-Day Porosity

**Culpeper Basin, Poolesville Member, and Gettysburg Basin, New Oxford Formation:** The basal sandstones of the Culpeper Basin (Poolesville Member) are subarkose and arkosic arenite (Pettijohn et al., 1987), and contain an average of 65% quartz (Figure 39, Table 5). Sandstones from the basal unit of the Gettysburg Basin (New Oxford Formation) vary more widely in composition,

ranging from sublitharenite to lithic arenite, subarkose, and arkosic arenite. On the average, they contain less quartz (56% average) and a higher proportion of lithics than the Poolesville Member samples (Table 5). Feldspar, commonly sericitized plagioclase, is more abundant in the Poolesville Member samples. In both the Poolesville Member and New Oxford Member sandstones, lithic fragments include mica, polycrystalline quartz, shale clasts, and minor zircon. Percent feldspar increases up section, from braided fluvial to meandering fluvial lithofacies, and provenance shifts from recycled orogenic to transitional continental (Figure 40) reflecting a transition from metamorphosed, orogenically uplifted highlands to rifted basement source rocks (Dickinson et al., 1983).

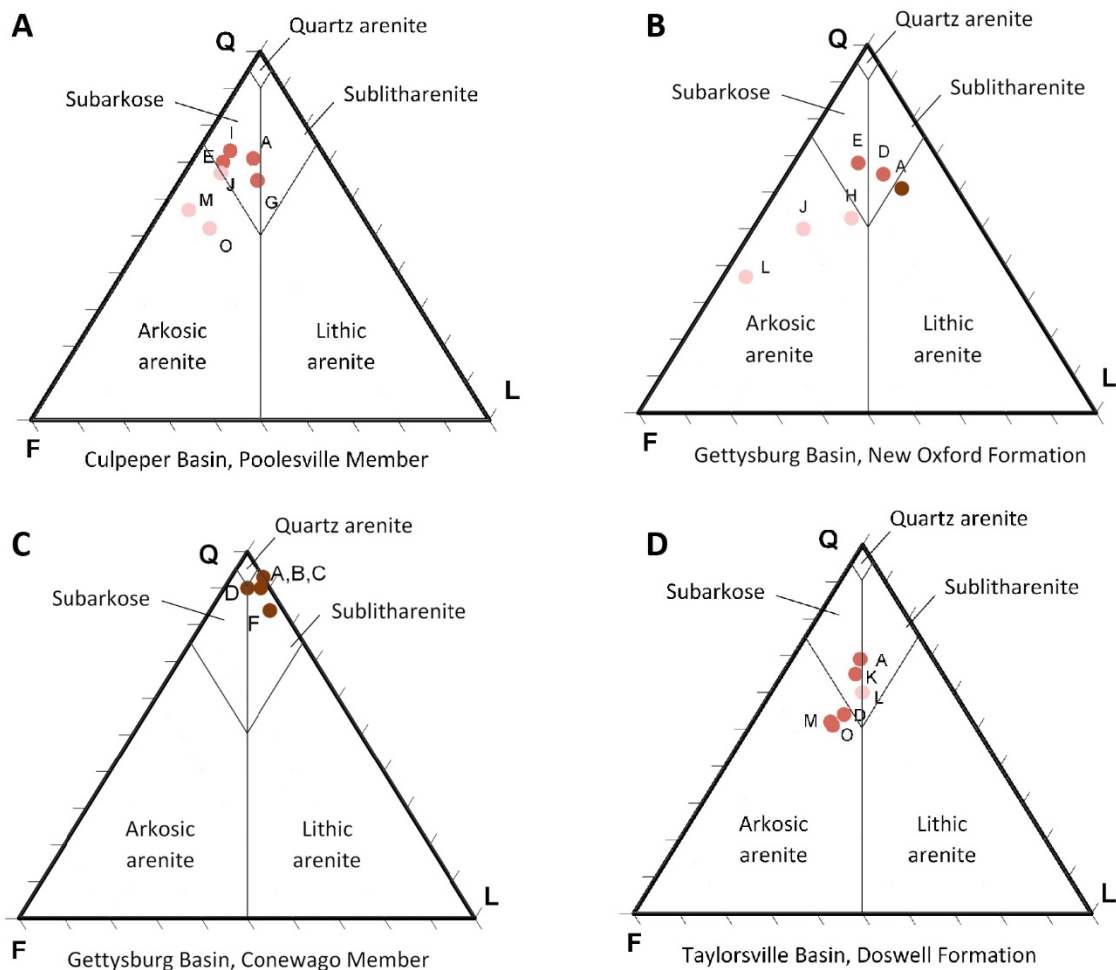


**Figure 39. Ternary quartz/feldspar/lithics diagrams illustrating compositional variations of sandstones based on modal analysis of representative thin sections, after Pettijohn et al. (1987). A, Poolesville Member sandstones. B, New Oxford Formation sandstones. C, Conewago Member sandstones of the Gettysburg Formation. D, Doswell Formation sandstones. Sample point color reflects lithofacies associations from which samples were collected.**

Grain size in the Poolesville Member and New Oxford Formation sandstones ranges from very fine to very coarse sand with pebble- and cobble-sized clasts and conglomeratic layers (Figures 42, 43, and 44). Grain size is generally finer and better sorted upsection. Sandstones of the Poolesville Member (Poolesville and Nolands Ferry sections) are coarser, and not as well sorted as sandstones in the New Oxford Formation (Pipe Creek section).

Results of image analysis for porosity show that almost all Poolesville Member and New

Oxford Formation samples have very low porosity (<1%), except for 3 samples close to the stratigraphic base (Appendix IA, Figures 42 and 43). These samples range from 2 to nearly 9% porosity. Previous work calculated effective porosity values of 1-6% for sandstones of the Poolesville Member based on neutron log analysis from 694-210 feet depth in a well in nearby Dickerson, Maryland (Nutter, 1975).

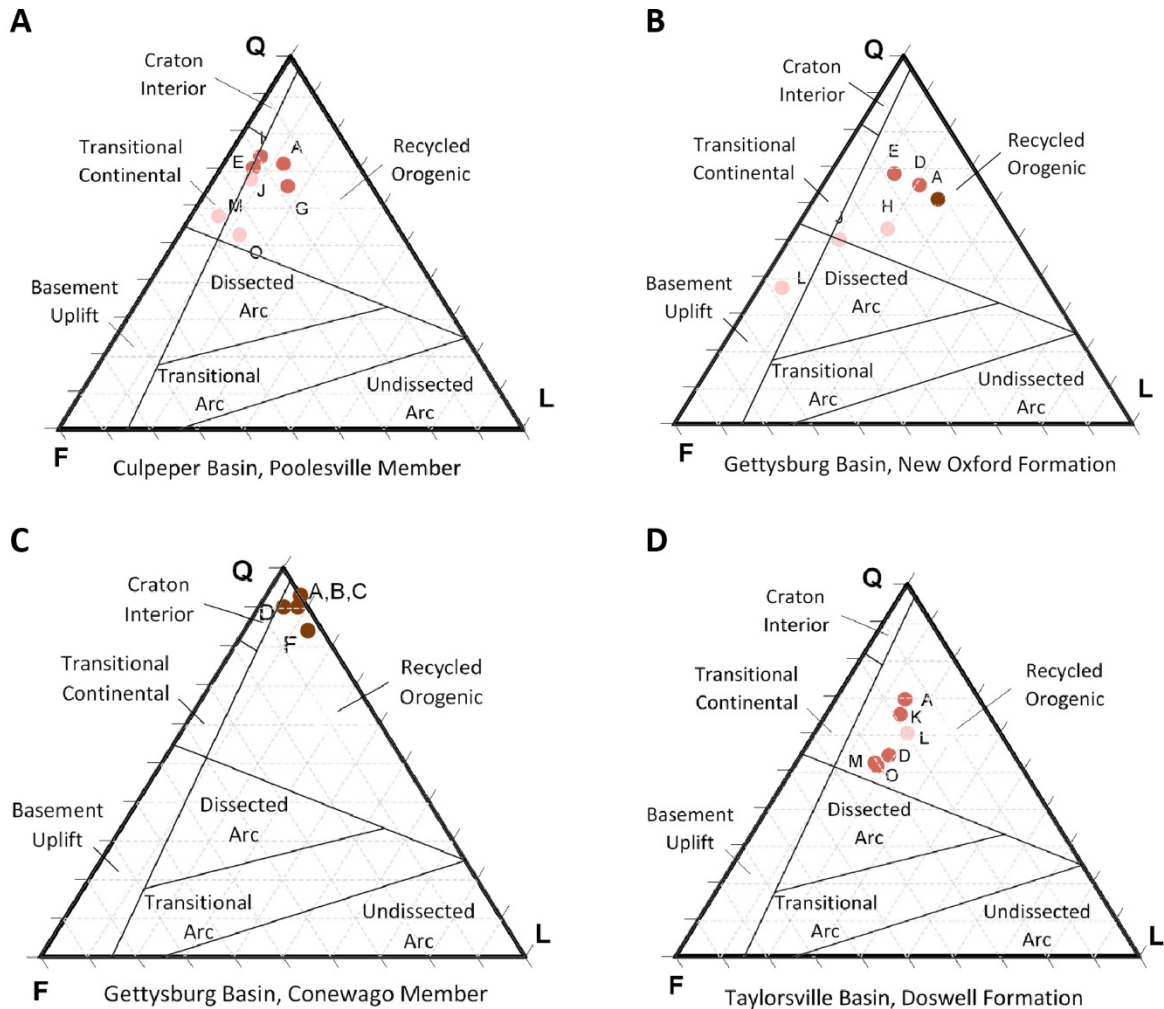


**Figure 40. Ternary quartz/feldspar/lithics diagrams illustrating provenance of sandstones based on point counts of representative thin sections, after Dickinson (1983). A, Poolesville Member sandstones. B, New Oxford Formation sandstones. C, Conewago Member sandstones. D, Doswell Formation sandstones. Sample point color reflects lithofacies associations from which samples were collected.**

**Gettysburg Basin, Gettysburg Formation, Conewago Member:** Sandstones from the Conewago Member of the Gettysburg Basin are sublitharenites, averaging 90% quartz and 2% feldspar (Figure 39, Table 5). Lithic fragments including polycrystalline quartz, shale clasts, and minor zircon also are present. The Conewago Member consists solely of alluvial fan lithofacies whose provenance plots in the top, quartz-rich third

of the recycled orogenic field (Figure 40), suggesting a shift in source area to recycled sands of the craton interior (Dickinson et al., 1983). Grain size ranges from medium to very coarse sand, with pebble conglomerate layers (Figure 45). Fine-grained sandstones are absent. Samples of this unit have the highest porosity of any outcrop samples studied, from 2-17%.

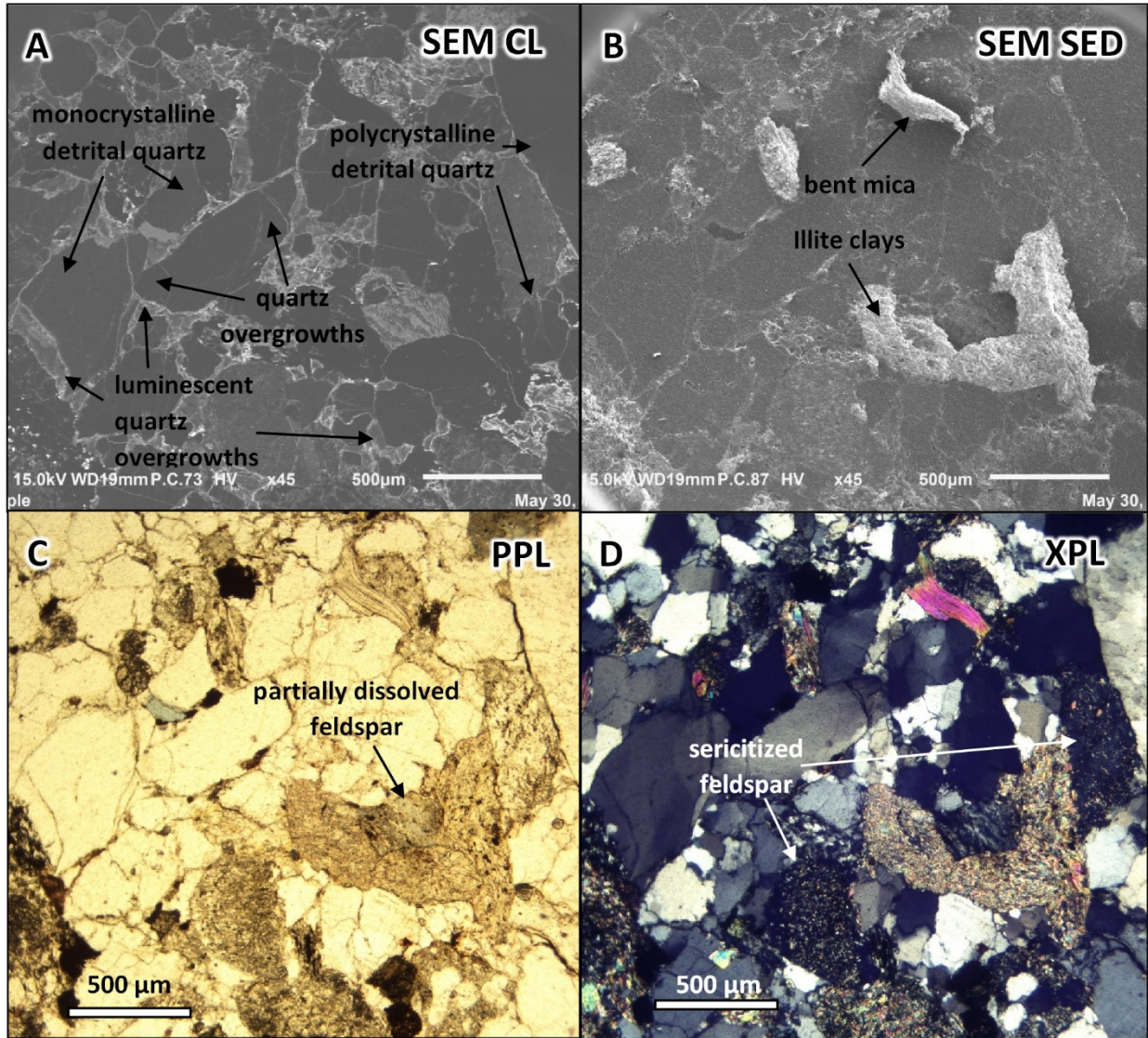


Figure 41. Photomicrographs of Polesville Member sample G. A, Scanning electron microscope cathodoluminescence (SEM CL). B, Scanning electron microscope secondary electrons (SEM SED). C, Plane-polarized light (PPL). D, Cross-polarized light (XPL). Scale same for all. Images show both non-luminescent and luminescent quartz overgrowths, altered feldspar, and ductile grains such as mica and illite clays.

Basin	Unit	Average % Composition (from modal analysis)			Stratigraphic position in basin	Porosity (%) (image analysis)	Porosity Types
		Quartz	Feldspar	Lithics			
Gettysburg	Conewago Member	90	2	8	middle	6.35	intergranular intragranular (dissolution) fracture
	New Oxford Formation	56	28	16	lower	0.36	intergranular intragranular (dissolution)
Culpeper	Poolesville Member	65	25	10	lower	0.73	intergranular intragranular (dissolution)
Taylorsville	Doswell Formation	58	24	18	Lower to middle	1.54	intergranular intragranular (dissolution)

**Table 5. Average framework grain composition, stratigraphic position, average percent porosity, and porosity types for each basin and section in the study.**

**Taylorsville Basin, Doswell Formation:** The compositions of sandstones from the Doswell Formation along Stagg Creek in the southern Taylorsville Basin includes sublitharenites, subarkoses, and arkosic arenites (Figure 39). Putative provenance is recycled orogenic terrane (Figure 40). Grain size ranges from very fine to very coarse sand, with granule and pebble conglomerates locally present (Figures 46 and 47). Plagioclase and microcline feldspar (often sericitized), polycrystalline quartz, mica, biotite, schist grains, shale clasts, and zircon are common (Figure 48). Samples from the Stagg Creek and Newfound Members are much coarser than those from the Vinita Member and range in porosity from 0.5-7.4% (Appendix IA). The fine sandstones of the Vinita Member (samples G, H, I) are better sorted and lower in porosity (0.1-0.3%).

**Porosity Types:** Samples with higher present-day porosity values from PPL scanned image analysis exhibit three types of porosity: intergranular, dissolution, and fracture. Porosity in the Conewago Member samples is comprised of both intergranular pore space (smaller pores between the framework grains) that is likely preserved primary porosity, and oversized pores (pores larger than the framework grains) that are likely secondary, due to dissolution of cements or feldspar grains (Figure 49A). The Poolesville Member, New Oxford Formation, and Doswell Formation samples have a combination of oversize intergranular pore space and smaller intragranular secondary porosity due to partial dissolution of feldspar (Figure 49B). Fracture porosity is not common, but results in 17% porosity for the Conewago Member sample D (Figure 49C).

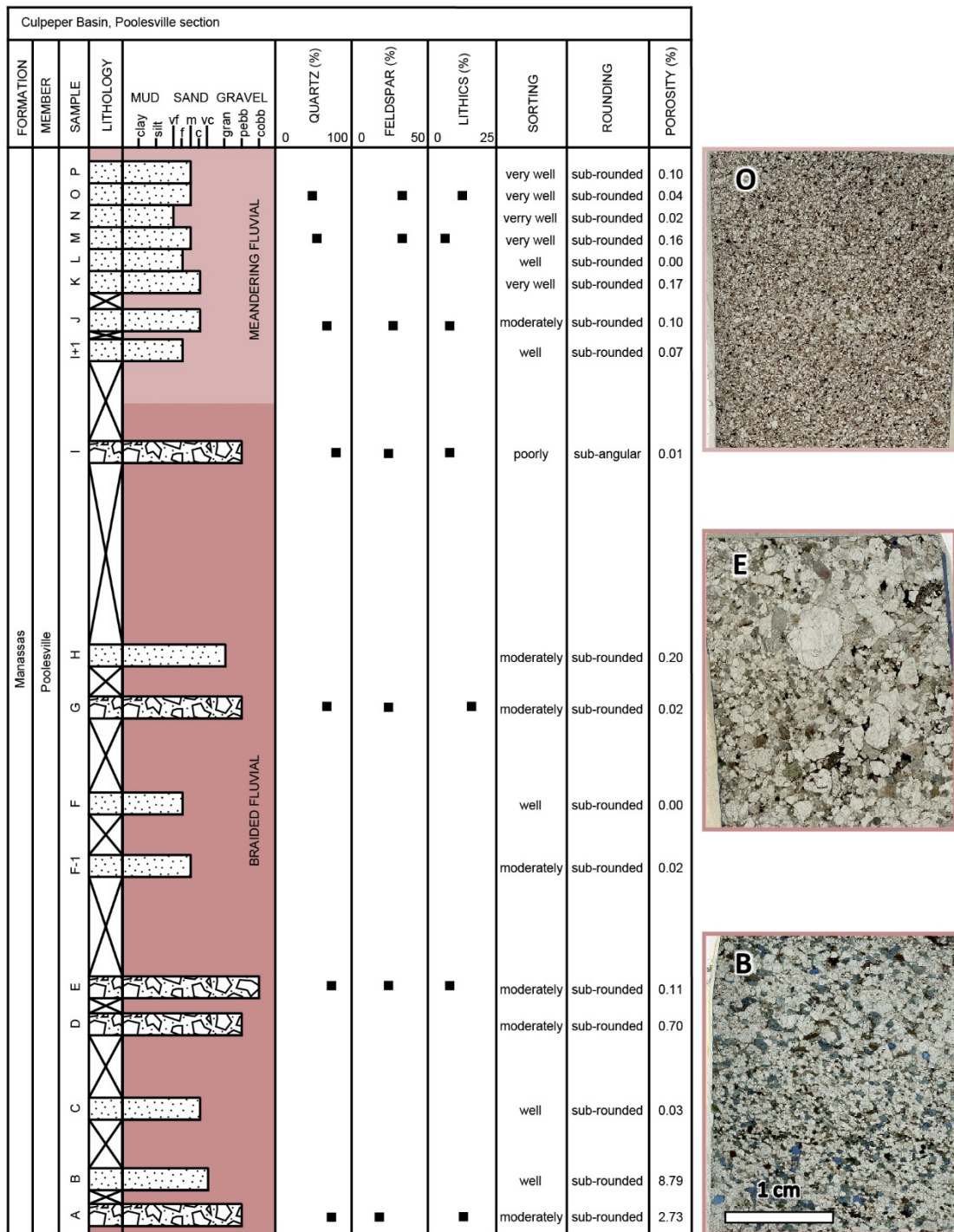
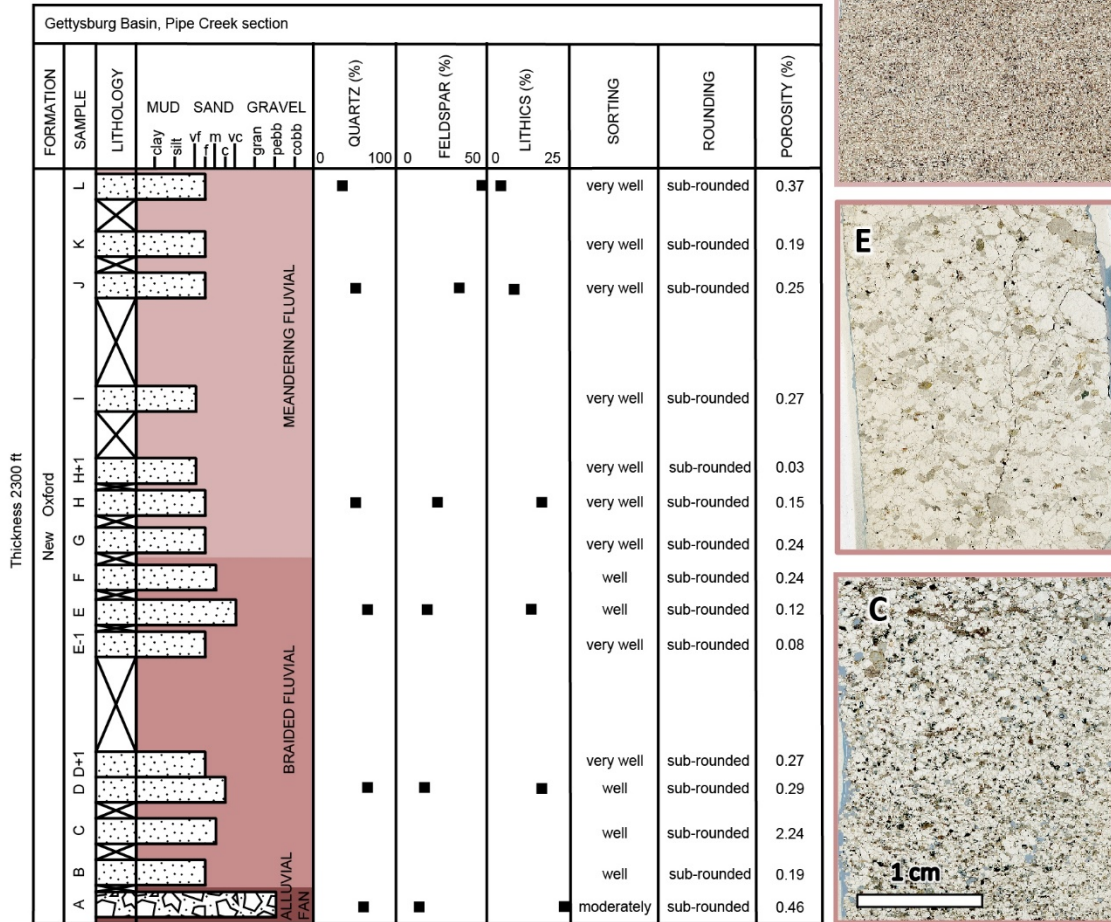


Figure 42. Stratigraphic variations in sample composition, grain size, sorting, roundness, and porosity for sandstone samples from the Culpeper Basin, Poolesville Member, Poolesville section. Column color reflects lithofacies associations from which samples were collected. Scanned thin sections in plane-polarized light (PPL) are shown for samples B, E, and O. All thin sections at same scale.



**Figure 43. Stratigraphic variations in sample composition, grain size, sorting, roundness, and porosity for sandstone samples from the Gettysburg Basin, New Oxford Formation, Pipe Creek section. Column color reflects lithofacies associations from which samples were collected. Scanned thin sections in plane-polarized light (PPL) are shown for samples C, E, and L. All thin sections at same scale.**

Feldspar dissolution is an important component of samples with higher present-day porosity values in the Doswell Formation of the Taylorsville Basin. In samples C, K+1, and L, partial to total dissolution of medium to very coarse sand-sized feldspar grains is evident in thin section (Figures 50 and 51).

**Porosity Reduction:** Image analysis of epoxy-impregnated thin sections was chosen for estimates of present-day porosity due to the efficiency and

reproducibility of this method over point counts. While porosity percentage from image analysis correlates with porosity percentage from point counts in a relative sense, it produces consistently lower values (Appendices IA, B). This may be due to limitations of scanned image resolution (Bowen et al., 2011) and automated IHS pixel selection. Furthermore, it does not quantify primary porosity or its reduction during diagenesis. Therefore, point counts and SEM image analysis were used to

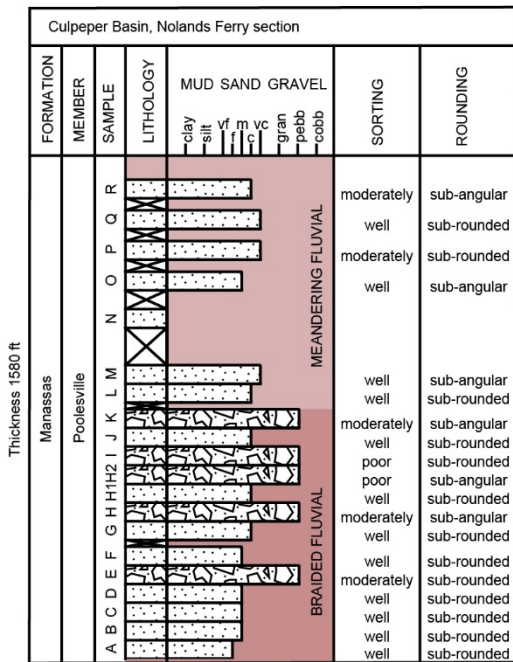


**Figure 44. Stratigraphic variations in grain size, sorting, and roundness for sandstone samples from the Culpeper Basin, Poolesville Member, Nolands Ferry section. Column color reflects lithofacies associations from which samples were collected.**

quantify diagenetic reduction in porosity (Appendix IB, Table 4).

Cementation and compaction appear to be the two main factors in the reduction of primary pore space. Point counts of thin sections under a polarizing microscope and analysis of SEM photomicrographs indicate that original primary porosity was greater than present-day porosities measured in scanned PPL image analysis because

of filling of original pore space by cementation (Table 4). The percentages given for primary porosity suggest pore space reduction of 18% by cement in the Poolesville Member sample G and 29% in the Conewago Member sample A, respectively. The reduction of pore space by compaction has not been quantified, but qualitative observation suggests that it is more important in the Poolesville Member sample G than in the Conewago Member sample A. Poolesville Member sample G contains abundant bent mica grains, crushed illite clays, and partially dissolved plagioclase feldspar between the quartz grains (Figure 41). Ductile grains are largely absent in Conewago Member sample A and quartz grains are typically surrounded by quartz overgrowths that may have resisted compaction.

**Cements:** Three cements were observed in thin section: hematite, quartz overgrowths, and calcite (Figure 52). Hematite cement is abundant in samples from all sections, commonly rimming grains and filling oversized pores (Figure 52A). Quartz overgrowths are present in all sections, but most continuous in the Conewago Member samples (Figure 52B). In the Poolesville Member sample G, SEM CL images reveal both luminescent and non-luminescent quartz overgrowths, suggesting at least two generations of quartz cement (Figure 41A). Calcite cement is limited to samples from the upper portion of the Poolesville Member, where it is patchy (Figure 52C) (samples I-P). There is one calcareous sandstone in the Vinita Member of the Doswell Formation (sample TYPE). Feldspar overgrowths also occur, but are uncommon, possibly because they are difficult to distinguish using standard petrographic techniques (Bowen et al., 2011).

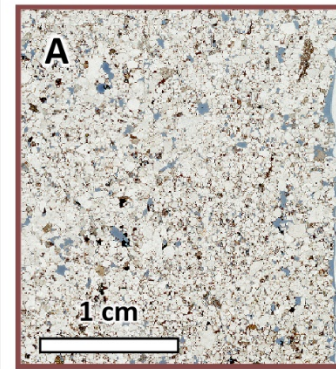
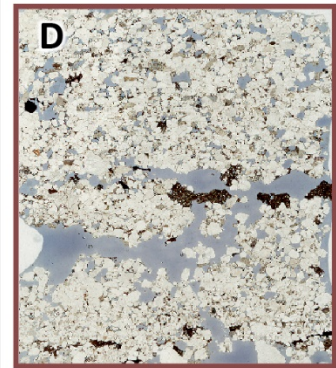
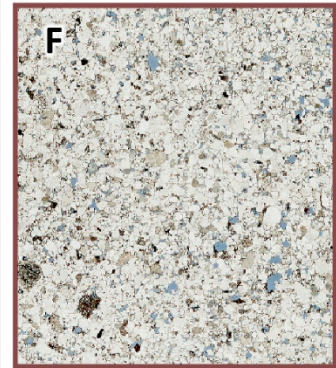
**Figure 45. Stratigraphic variations in sample composition, grain size, sorting, roundness, and porosity for sandstone samples from the Gettysburg Basin, Gettysburg Formation, Conewago Member, Conewago section. Column color reflects lithofacies associations from which samples were collected. Scanned thin sections in plane-polarized light (PPL) are shown for samples A, D, and F. Note high porosity values in this section. All thin sections at the same scale.**

→

Gettysburg Basin, Conewago section												
FORMATION	MEMBER	SAMPLE	LITHOLOGY	MUD SAND GRAVEL			QUARTZ (%)	FELDSPAR (%)	LITHICS (%)	SORTING	ROUNDING	POROSITY (%)
				clay	silt	fine med coarse						
Gettysburg	Conewago	G	[Lithology bar: mostly sand]							well	rounded	4.13
		F	[Lithology bar: mostly sand]				■	■	■	poorly	sub-rounded	6.19
		E	[Lithology bar: mostly sand]							very well	rounded	2.15
		D	[Lithology bar: mostly sand]				■	■	■	moderately	rounded	17.11
		C	[Lithology bar: mostly sand]				■	■	■	well	sub-rounded	7.46
		B	[Lithology bar: mostly sand]				■	■	■	well	rounded	3.12
		A	[Lithology bar: mostly sand]				■	■	■	well	sub-rounded	4.32

Thickness 4100 ft

ALLUVIAL FAN



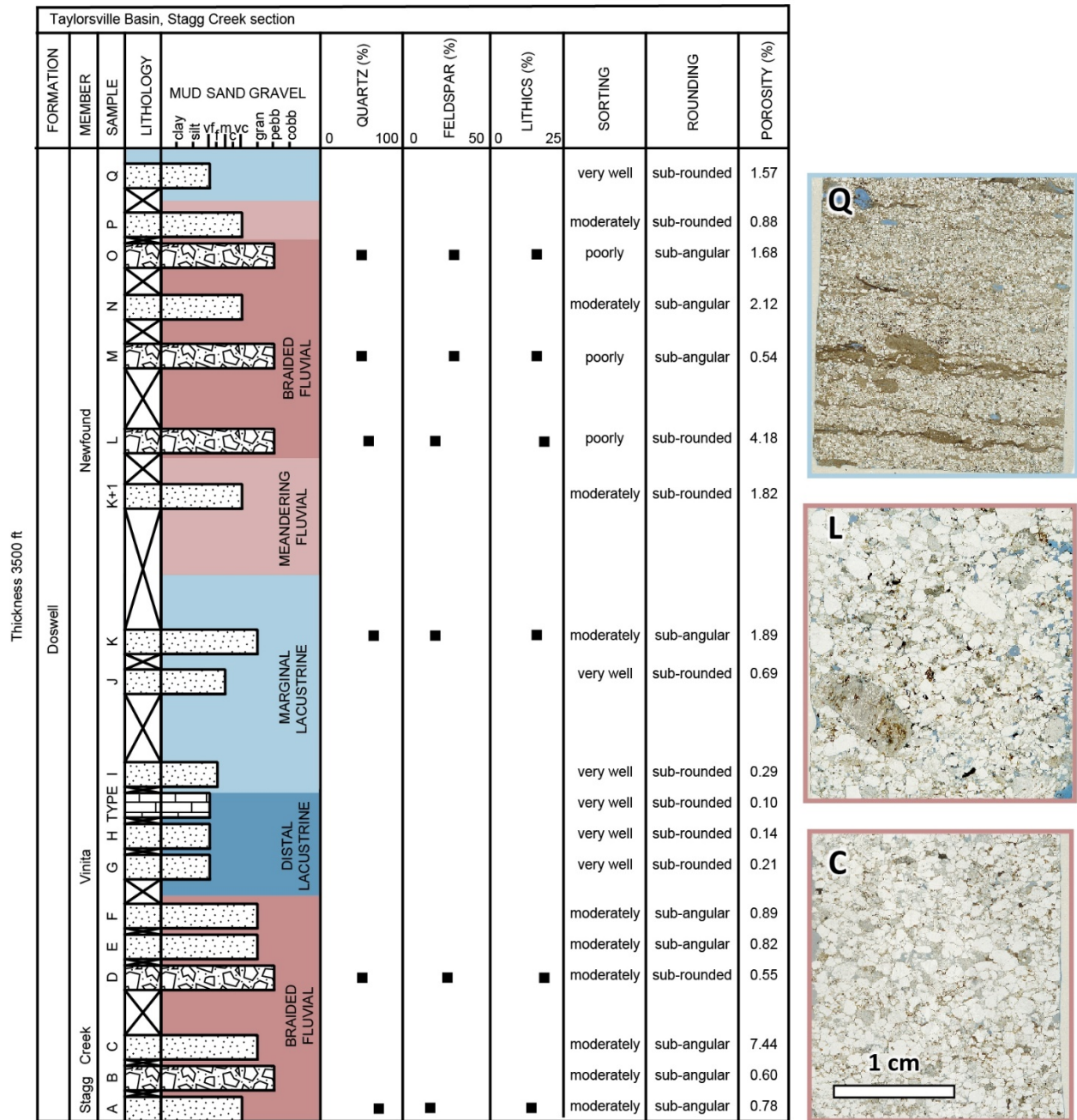


**Figure 46. Stratigraphic variations in sample composition, grain size, sorting, roundness, and porosity for sandstone samples from the Taylorsville Basin, Doswell Formation, Stagg Creek section. Column color reflects lithofacies associations from which samples were collected. Scanned thin sections in plane-polarized light (PPL) are shown for samples C, L, and Q. All thin sections at same scale.**



Figure 47. Photograph of hand sample L, Doswell Formation, Newfound Member. This hand sample is typical of conglomeratic, braided fluvial lithofacies association (LA B) sandstones.

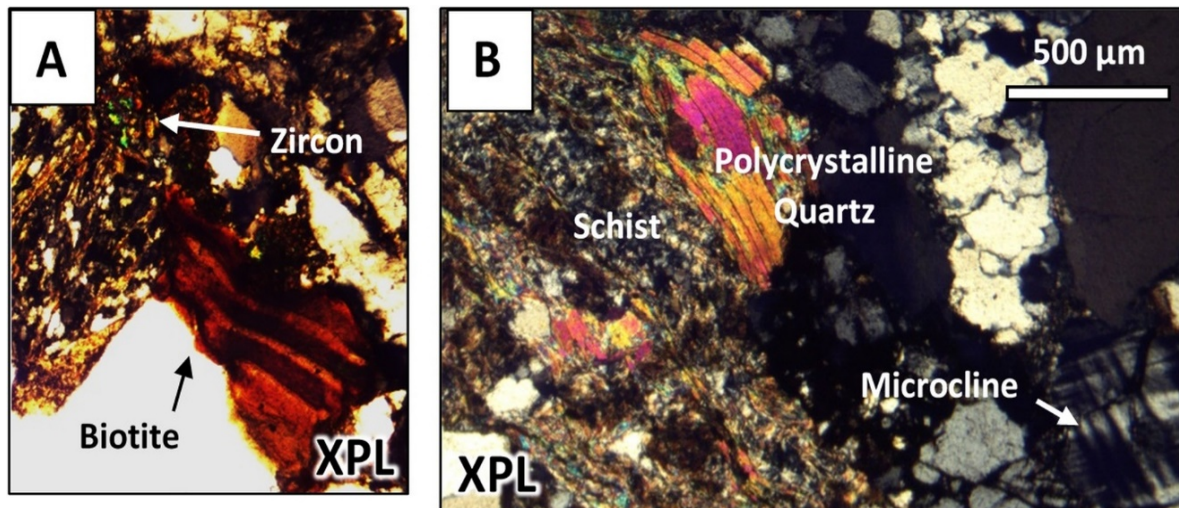


Figure 48. Photomicrographs (XPL) of Doswell Formation samples. A, Biotite and zircon accessory minerals of sample Q. B, Compositional grains of schist, polycrystalline quartz, and microcline in sample B. Scale same for both illustrations.

Lithofacies Assoc.	Porosity % (image analysis)	Porosity Range (%)		Average maximum grain size (mm)	# of samples
		Min.	Max.		
A	5.6	0.5	17.1	3.7	8
B	1.3	0.00	8.8	5.4	30
C	0.3	0.00	1.9	0.6	17
D	0.2	0.1	0.2	0.1	3
E	0.3	0.3	0.3	0.3	1

Table 6. Average percent porosity, range of porosity, average maximum grain size, and number of samples for each lithofacies association.

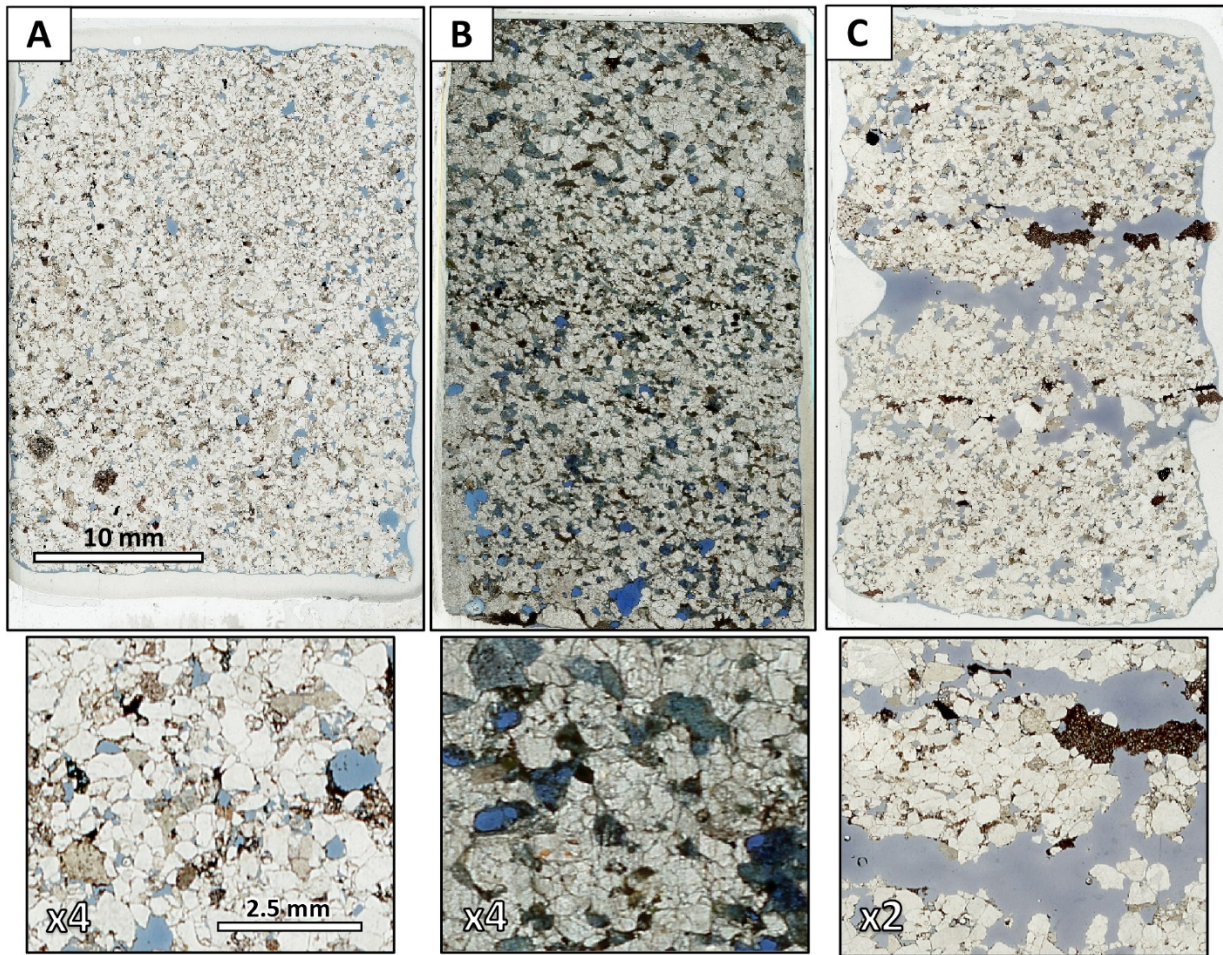
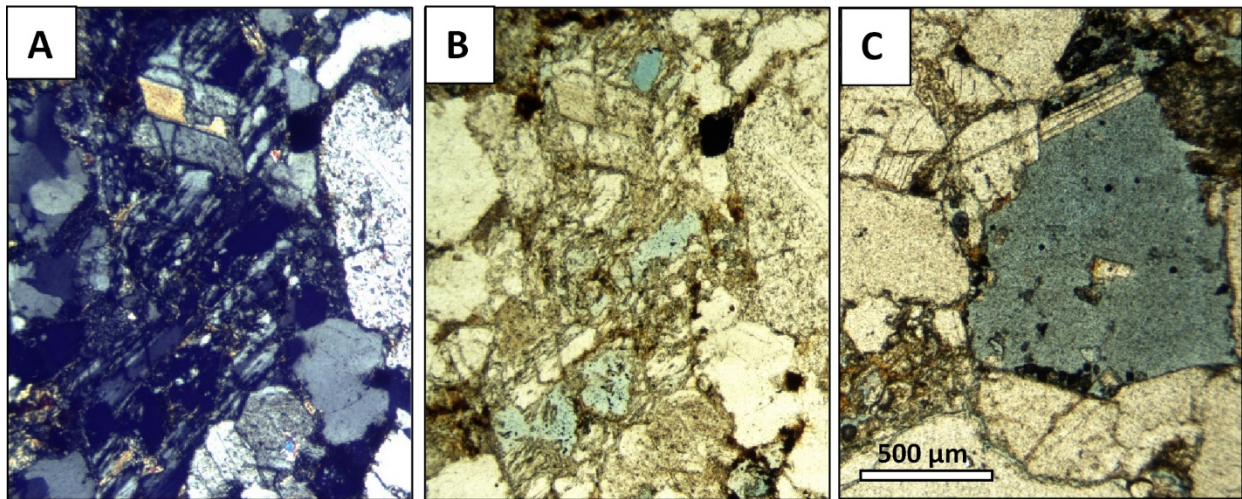


Figure 49. Scanned thin sections (PPL) showing types of present-day porosity assessed by image analysis. A, Intergranular pores (blue), both small and large, in Conewago Member sample F. Assessed at 6.2% porosity. B, Intergranular (bright blue) and intragranular dissolution porosity (muted blue) in Poolesville Member sample B. Assessed at 8.2% porosity. C, Fracture porosity in Conewago Member sample O. Assessed at 17.1% porosity.



**Figure 50. Photomicrographs showing secondary porosity due to feldspar dissolution. A, Dissolved feldspar grain in Doswell Formation, Stagg Creek Member, sample K+1 thin section (XPL). B, Same area of thin section as A in PPL. Small, intragranular pores (blue) due to partial feldspar dissolution. C, Large, intergranular pore (blue) likely caused by dissolution of entire feldspar grain, Doswell Formation, Stagg Creek Member, sample L thin section (PPL). Scale same for all.**

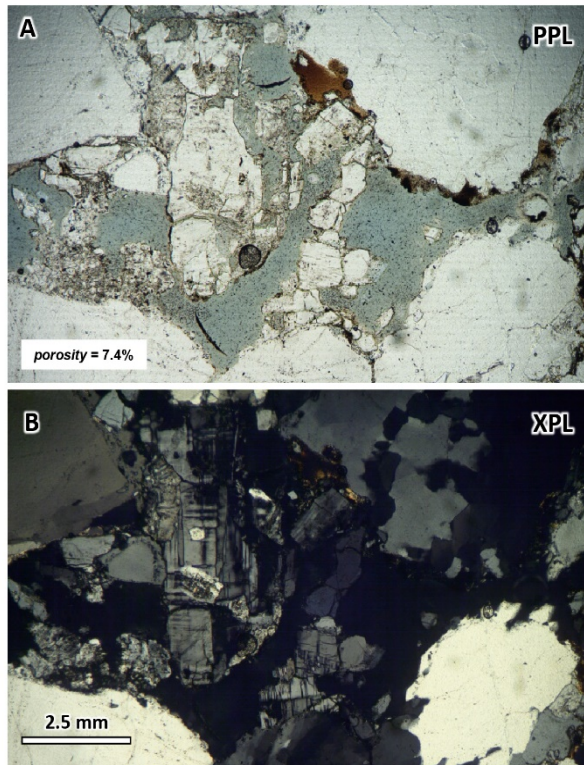
**Compaction:** Compaction processes reduce primary pore space by packing and deformation of grains. Greater compaction occurs in samples with abundant ductile grains such as mica and illite clays because they are easily crushed (Figure 41B, D). Samples with higher percentages of lithic and feldspar clasts, such as those from the Poolesville Member, New Oxford Formation, and Doswell Formation, are strongly compacted, with elongated sutured grain boundaries and deformed mica and illite clays. In contrast, the Conewago Member samples lack ductile grains; consequently, the quartz framework grains and early quartz overgrowths appear to have resisted compaction (Figure 52B).

Heterogeneity in the form of rip-up clasts, clay zones 1-5 cm thick, and laminae is observed in three thin sections prepared for this study. One heterogenous sample was found each in the Newfound Member of the Doswell Formation, the New Oxford Formation, and Poolesville Member of the Manassas Formation (Figures 53, 54). Poolesville Member sample I contains large (5 mm), sub-angular shale clasts. New Oxford Formation sample D+1 has a 2 cm layer of clay at the base of the sample that grades upward into sand

within a clay-rich matrix and then into sand without clay (Figure 53). These samples have very low porosity values that are due to the filling of pores and increased compaction from the abundance of clay. However, clay laminae in sample Q of the Newfound Member of the Doswell Formation, are the dominant location of present-day porosity, and occur every 2-5 mm throughout the sample (Figure 54). In thin section, it can be seen that these laminae alternate with sand and contain both oversized pores and thin bands of porosity.

### Discussion

Sandstones from the Culpeper, Gettysburg, and southern Taylorsville basins display a clear relationship between present day porosity and depositional environment, texture, and sorting (Figures 42-46). These data demonstrate that alluvial fan and braided fluvial deposits have coarser grain size and higher porosity values than meandering fluvial, shallow lacustrine, or deep lacustrine facies deposits (Table 6). Conglomeratic sandstones in the New Oxford Formation of the Gettysburg Basin, the Hammer Creek (Glaeser,



1966) and Stockton formations of the Newark Basin (Smoot, 2010), and the Wolfville Formation of the Fundy Basin (Hubert and Forlenza, 1988; Leleu and Hartley, 2010) have previously been interpreted to reflect high-energy depositional environments, such as those found on alluvial fans or in braided river channels.

**Figure 51. Photomicrographs showing secondary porosity due to feldspar dissolution in Doswell Formation, Stag Creek Member, sample C. A, Abundant pore space (blue) surrounding dissolved feldspar (PPL). B, Same area of thin section as A in XPL showing tartan microcline twinning on remaining portion of feldspar grain. Scale same for both.**

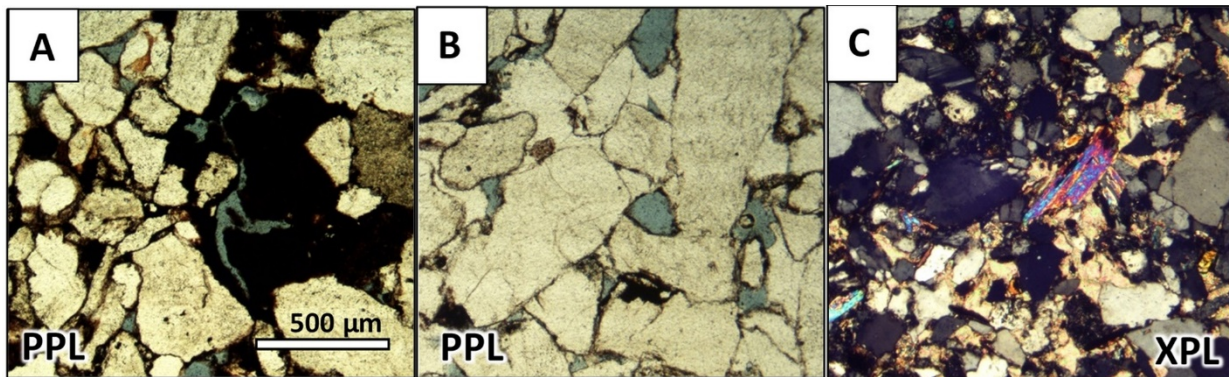


**Figure 52. Photomicrographs showing pore-filling cements. A, Hematite cement (dark brown) in Conewago Member, sample A (PPL). B, Quartz overgrowths (light tan) in Conewago Member, sample F (PPL). C, Patchy, poikilotopic calcite cement (peach-pink) in Poolesville Member, sample L (XPL). Scale same for all.**

Higher values for present-day porosity from PPL image analysis in braided versus meandering stream channel deposits are most likely the result of grain size differences rather than composition since sandstone from these environments have comparable framework grain compositions. Samples of these facies come from three studied

sections: the New Oxford Formation (Gettysburg Basin), the Manassas Formation (Culpeper Basin), and the Doswell Formation (Taylorsville Basin) (Table 7). Within a single basin, the porosity difference between braided and meandering fluvial lithofacies is greatest within the Culpeper, where grain size difference is also greatest. This may be

due to winnowing of finer, silt- and clay-size grains in the high-energy braided fluvial environments. Previous work on sandstones of the Stockton Formation (Newark Basin) showed porosity values were highest in medium-grained sandstones, due to a lack of pore-filling clays (Rima et al., 1962). Well-sorted sandstones with high porosity also have been identified recently as potential carbon sequestration targets in the Passaic Formation of the Newark Basin (Collins, 2017; Olsen et al., 2016; Slater et al., 2013).

The higher porosity values recorded in the alluvial fan deposits more strongly reflect composition of the source area rather than depositional environment. Seven of the eight alluvial fan samples come from the Conewago Member (Table 7), and thin sections show them to be quartz-rich sandstones that lack ductile grains. In contrast, braided and meandering fluvial sandstone samples from the New Oxford Formation, Poolesville Member, and Doswell Formation have abundant feldspar and lithic fragments. Previous workers have suggested a northern sedimentary source area for other quartz-rich conglomerates of the Gettysburg Basin (Hammer Creek Formation (Glaeser, 1966)) and a southern high-grade metamorphic source area for the New Oxford, Stockton, and Wolfsville formations of the Gettysburg, Newark, and Fundy basins, respectively (Glaeser, 1966; Hubert and Forlenza, 1988; Oshchudlak and Hubert, 1988). These compositional differences, resulting from source area, appear to be the reason for the Conewago Member samples being more resistant to compaction.

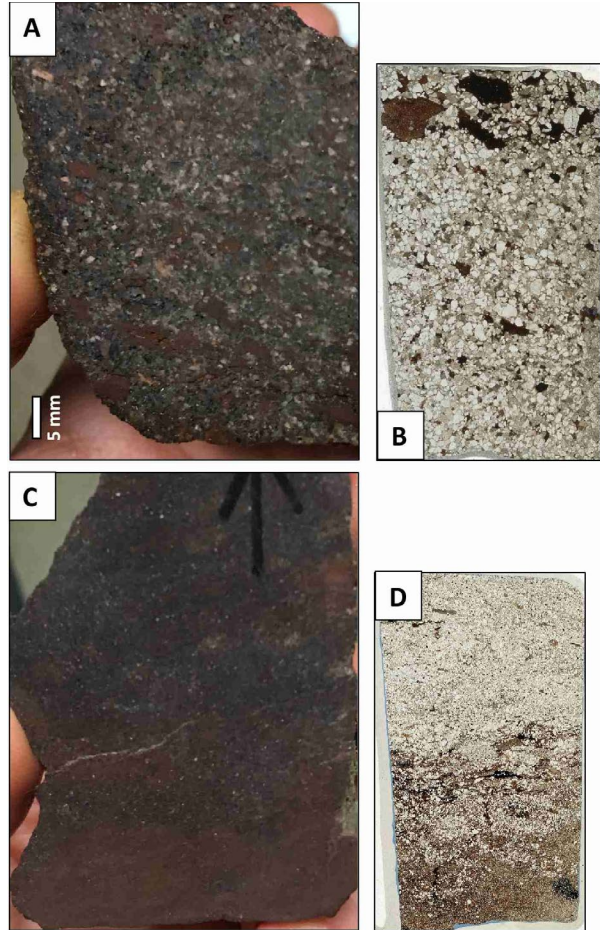


**Figure 53. Heterogeneity within Poolesville Member and New Oxford Formation sandstones due to layers and clasts (both dark red). A, Poolesville Member hand sample I. B, Scanned (PPL) thin section Poolesville Member sample I. C, New Oxford Formation hand sample D+1. D, Scanned (PPL) thin section New Oxford Formation sample D+1. Scale same for all.**

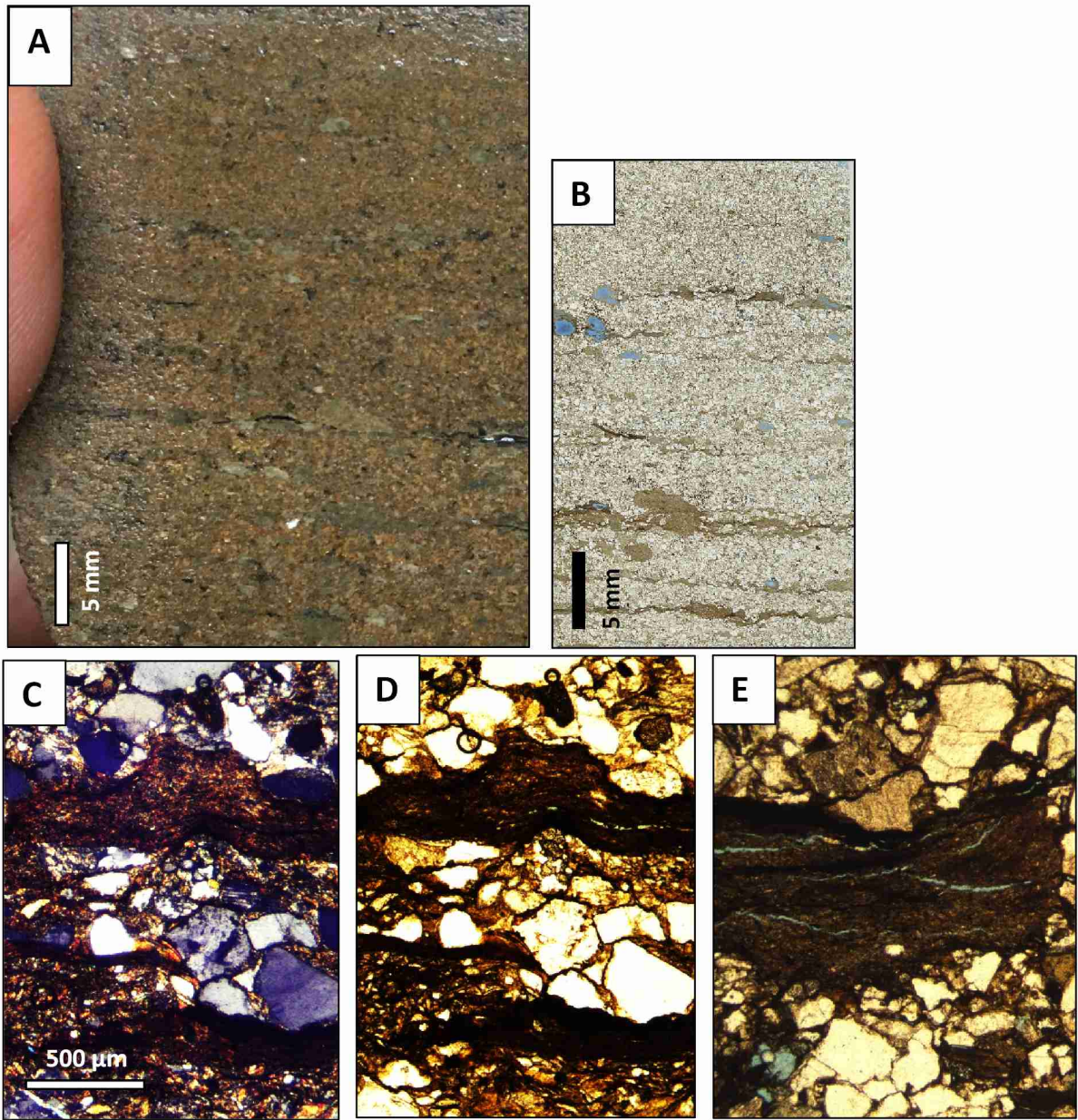


**Figure 54. Heterogeneity within Doswell Formation sample Q. A, Hand sample. B, Scanned thin section. C, Photomicrograph (XPL). D and E, Photomicrographs (PPL). Lamina with higher mica and clay-rich matrix (dark brown to reddish brown) alternate with coarser grains. Thin bands of porosity occur within these zones (E). Scale same for C, D, and E.**

The Conewago Member represents a middle depositional episode within the Gettysburg Formation (Smoot, 1999) and may not have been buried as deeply as other sandstones sampled in this study. The New Oxford Formation, Poolesville Member, and Doswell Formation sandstones are early rift filling deposits that may

have been buried beneath as much as 21,000 (Craddock et al., 2012), 27,000 (Olsen et al., 1989), and 8,000 to 13,000 (Milici et al., 1991; Malinconico, 2003) feet of sediment, respectively. The differences in depth of burial may partially account for the differences in compaction and thus porosity. Similarly, porosity values were found to

be higher in outcrop samples from the upper part of the Wolfville Formation as compared to core samples from a depth of 3,600 feet (Kettanah et al., 2014). This difference was attributed largely to

compaction, and existed despite a higher percentage of quartz and lack of lithics in the more deeply buried core samples.

Basin	Section	Average composition (from modal analysis)			Lithofacies Association	Image Analysis Porosity	Range of % Porosity		Avg. Max Grain size (mm)	No. of samples
		Q	F	L			Min	Max		
		Gettysburg	Conewago Member	90			2	8		
B	-									0
C	-									0
D	-									0
E	-									0
New Oxford Member	56		28	16	A	0.5	0.5	0.5	12.0	1
					B	0.5	0.1	2.2	0.7	7
					C	0.2	0.0	0.4	2.5	7
					D	-				0
					E	-				0
Culpeper	Pooleville Member	65	25	10	A	-				0
					B	1.3	0.0	8.8	6.8	10
					C	0.1	0.0	0.2	0.5	8
					D	-				0
					E	-				0
Taylorsville	Doswell Formation	58	24	18	A	-				0
					B	2.0	0.5	7.4	7.1	13
					C	1.3	0.7	1.9	2.3	2
					D	0.2	0.1	0.2	0.1	3
					E	0.3	0.3	0.3	0.3	1

**Table 7. Average framework grain composition for each basin compared to porosity and grain size for lithofacies within that basin.**

Feldspar dissolution resulted in higher porosity values in meandering fluvial, braided fluvial, and marginal lacustrine deposits in the Doswell Formation. Samples with higher porosity occur throughout the formation, so there is not a simple

decrease in porosity with depth as might be expected. Increased porosity at depth due to feldspar dissolution also has been documented in deposits interpreted as distal alluvial fan and braided fluvial in the basal Mount Simon

Sandstone (Bowen et al., 2011). Carbon sequestration in the Illinois Basin has successfully targeted this lower arkosic sandstone (Leetaru et al., 2019). Like the Doswell Formation, the basal Mount Simon Sandstone overlies granitic basement rock, which shed sediment from topographic highs associated with Cambrian rifting (Leetaru and McBride, 2009; Lovell and Bowen, 2013). Similarly, the source area for abundant

feldspar in the Doswell Formation may be the Petersburg Granite, which underlies the rift basin to the south/southeast. Records from exploratory wells drilled in the Taylorsville Basin in the 1980's contain thin section imagery and porosity values (Figure 55) that show dissolved feldspar and high porosity values in braided fluvial lithofacies on the southeast side of the basin.

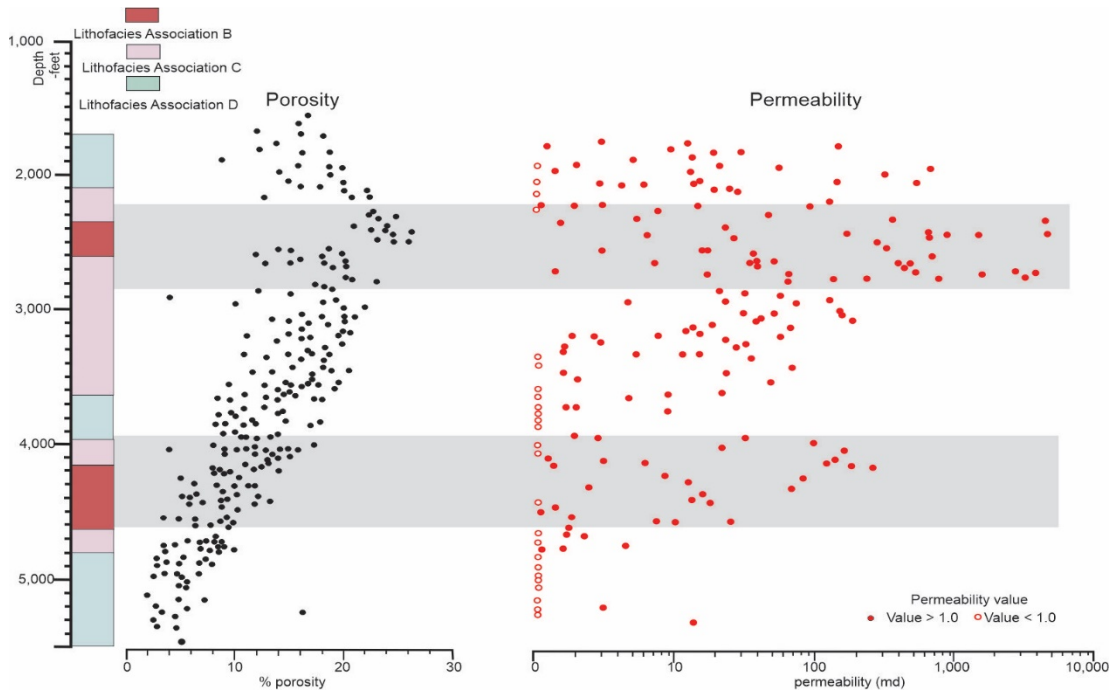


**Figure 55. Stratigraphic changes in porosity and permeability within the Ellis well of the Taylorsville Basin as determined from geophysical logs. Gray shaded areas reflect elevated porosity and permeability intervals coincident with LAs B and C.**

Lastly, millimeter- to centimeter-scale clay zones in sandstone beds of both braided fluvial and meandering fluvial deposits appear to increase porosity locally within the Newfound Member (Taylorsville Basin), and decrease porosity in the New Oxford Formation (Gettysburg Basin) and Manassas Formation (Culpeper Basin). Grain-size heterogeneity in sandstones has previously been attributed to fluvial distribution of detrital clays in point bar and overbank environments (Henares et al., 2016; Bowen et al., 2011). Clay layers may reduce porosity due to increased compaction (Fawad et al., 2010), but in contrast, can increase

porosity by inhibiting the growth and movement of pore-filling cements (Milliken, 2001). The impact of these heterogeneous clay-rich zones on porosity and permeability within sandstone beds of the Culpeper, Gettysburg, and Taylorsville basins requires better understanding of their extent and abundance within lithofacies associations.

### CARBON SEQUESTRATION POTENTIAL

The extensional tectonism associated with rift basin formation typically generates highly fractured bedrock surrounding isolated

depositional basins with interior drainage (Smoot, 1999, 2010). These controlling factors tend to produce broadly replicated facies within each basin (Schlische et al., 2003). Within these sedimentary packages there are numerous intervals that may have potential as either high-porosity reservoirs or relatively impermeable seals necessary for geologic sequestration of CO<sub>2</sub> (Craddock et al., 2012; Brezinski and Adams, 2019). Furthermore, NAM rift basins underlie extensive areas of the Atlantic Coastal Plain and Piedmont physiographic provinces. These broad areas are in near proximity and/or juxtaposed to a wide range of point source carbon producers (Figure 56).

### Potential for Traditional CO<sub>2</sub> Reservoirs

Depositional factors within rift basins produce a rock succession that exhibits an initial fining-upward profile followed by one that is upward-coarsening. The basal, coarse-grained fluvial deposits characteristically fine upward into lacustrine deposits, that ultimately are followed by progradation of alluvial fan successions. This tripartite depositional motif (fluvial-lacustrine-alluvial fan) provides a level of predictability in the arrangement of potential reservoir and seal units. The vertical arrangement of lithologies had long been considered congruent with the distribution of Triassic basin reservoir and seal beds (Root, 1988; Milici et al., 1991). Although extensional tectonics produce high-relief basin margins conducive to the formation of coarse-grained clastic deposits and the extensive brittle fracturing that characterizes the associated faulting, and may provide increased reservoir potential, the extension of these faults to the surface in many basins may preclude long-term carbon storage.

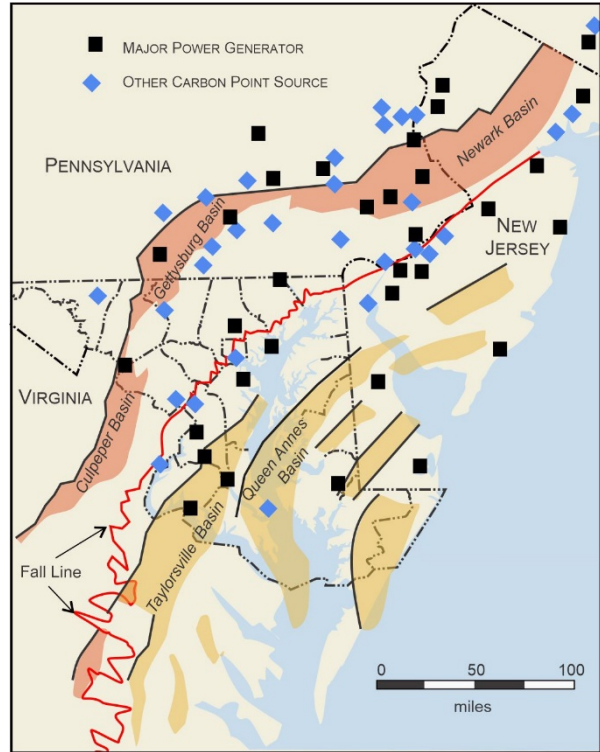


**Figure 56. Distributional relationship between Mid-Atlantic carbon point source producers and exposed and buried Triassic rift basins. Brown areas are exposed rift basins, beige areas are buried basins.**

### Culpeper and Gettysburg Basins

Triassic rift basins of the Atlantic margin of North America present the widespread potential for CO<sub>2</sub> storage within high population areas. As discussed earlier in this report, the upward-fining then -coarsening depositional successions of the Culpeper and Gettysburg basins reflect depositional processes that are repeated between other rift valley successions (Schlische and Olsen, 1990) (Figure 35). Within these sequences sandstone intervals provide porous and permeable potential reservoirs, while fine-grained lacustrine sediments represent thick sealing layers.

Because CAM basin successions invariably rest upon metamorphosed pelitic and granitic rocks of the western Piedmont Physiographic Province, their basal sealing capability may be considerable. Intuitively, it should be expected that the fracturing associated with the half-graben border faulting may provide a transmissive zone for injected fluids.

Furthermore, these brittle-deformed structures are laterally continuous and interconnections occur along cross strike structures (Root, 1988; Schlische, 1993).

The basal and marginal fluvial strata in the Culpeper and Gettysburg basins contain coarse-grained lithologies that are potential storage intervals for CO<sub>2</sub> (Figure 57). The basal Irishtown Member in the Gettysburg Basin, and Reston and Tuscarora Creek members (LA A) in the Culpeper Basin contain thin, discontinuous intervals of conglomerate and interbedded mudstone. Because of their lateral discontinuous character, these units do not present significant opportunity for CO<sub>2</sub> storage.

Above these basal conglomerates, both the Culpeper and Gettysburg basins contain thick successions of coarse-grained, braided fluvial deposits (LA B). These strata contain numerous poorly cemented, pebbly sandstone intervals up to 45 feet thick. However, porosity values for these sandstone intervals are highly variable and range from less than 1% to more than 8% (Appendix IA). Above this interval, finer grained, meandering fluvial deposits (LA C) yield porosity values that characteristically are less than 1%. These strata tend to be lenticular, localized, and fine-grained. Because of their laterally discontinuous character, fine-grained nature, and low porosity, these sandstone units exhibit a poor reservoir potential.

The alluvial and fluvial parts of the Triassic basin successions are supplanted upward and basinward by very thick intervals of red and gray shale, mudstone, and shale-rich limestone in the Gettysburg Formation in the Gettysburg Basin, and the Bull Run Formation within the Culpeper Basin (Craddock et al., 2012). These fine-grained intervals are as much as 20,000 feet thick in the Gettysburg Basin (Root, 1988), with equivalent thicknesses in the Culpeper Basin. Even though Craddock et al. (2012) did not believe that the fine-grained components of the lower Gettysburg Formation represent quality sealing units similar to those of the Lockatong Formation of the Newark Basin, those parts of the Gettysburg Formation appear to be sufficiently fine-grained and thick to serve as a confining unit (Figure 57).

The fan-delta deposits of the upper Culpeper and Gettysburg basins, deposited along the western border fault of each basin, also may provide potential as CO<sub>2</sub> reservoirs. Where these deposits are composed of carbonate clasts, calcareous cement occludes pore space. However, where these conglomerates consist of non-carbonate rock fragments, and especially rounded rock fragments, extensive porosity and permeability are present. Porosity values of the conglomeratic sandstones of the Conewago Member of the Gettysburg basin range from 2% to more than 17 % (Appendix IA). While no porosity values were determined for the debris flow intervals in the Millbrook Quarry Member of the Waterfall Formation (Culpeper Basin), these rocks exhibited modest levels of porosity in outcrop view.

### **Taylorsville Basin**

Within the exposed area of the Taylorsville rift basin, potential reservoir intervals suggest abundant capacity for carbon storage. In addition, the buried parts of the basin are concealed beneath hundreds, or even thousands, of feet of overlying sediments (Figure 26, 34) (Milici et al., 1991, p. 10).

Coastal Plain sediments that overlie the Taylorsville Basin range from more than 2,000 feet in thickness along its eastern margin to 0 feet at the Fall Line (see Figure 26 for location). These sediments consist of intercalated intervals of porous sandstone aquifers alternating with relatively impermeable intervals of clay and silt. Many of these aquifers have high transmissivity and contain increasingly high chloride levels in the down-dip areas (Meng and Harsh, 1991), making them potential sequestration intervals. Within Maryland six separate confining layers overlie the Taylorsville Basin; Arundel, Patapsco, Magothy, Matawan, Nanjemoy, and Calvert formations. The maximum combined thickness of these confining units is 650 feet (Andreasen et al., 2013). In Virginia, four separate confining intervals overlie the Triassic rocks of the Taylorsville Basin. These are the Potomac, Nanjemoy-Marlboro, Calvert, and St. Marys confining units (McFarland and Bruce, 2006, fig. 2). Some of these confining units

only partially overlie the Taylorsville Basin; each unit averages 100 feet in thickness. However, the combined maximum thickness of these four units is 550 feet (McFarland and Bruce, 2006).

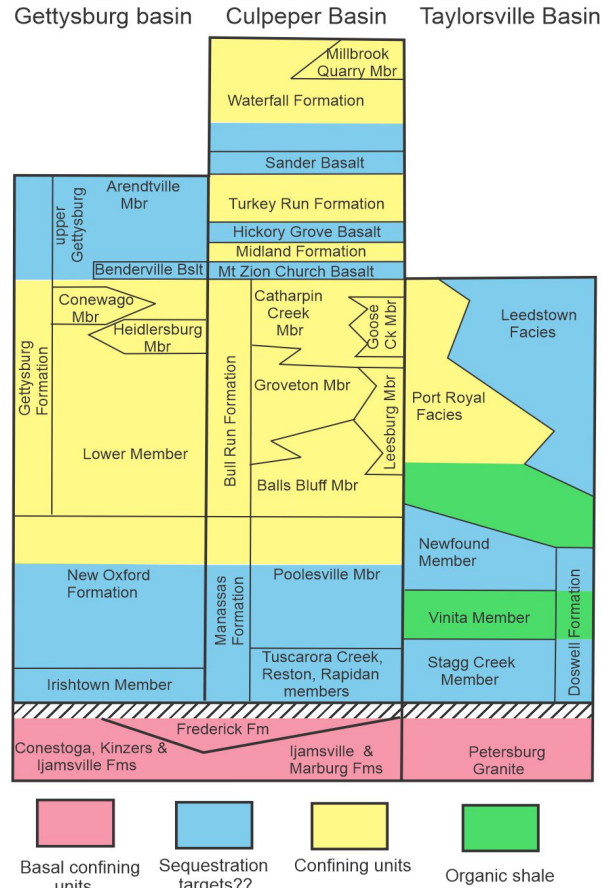


**Figure 57. Potential intervals that could serve as reservoir or seal units for CO<sub>2</sub> sequestration within the Gettysburg, Culpeper, and Taylorsville basins.**

In the Taylorsville Basin, Triassic strata are confined both above and below by unconformable surfaces. The lower contact juxtaposed coarse-grained fluvial sandstones and conglomerates of the basal Doswell Formation against weathered Carboniferous igneous rocks of the Petersburg Granite. Where the Doswell Formation is exposed, one can observe varying amounts (>50%) of unlithified, large clasts of the underlying weathered granite incorporated within the Doswell beds. Although no local topographic relief is evident, the

contact interval certainly constitutes, at least in part, a lithified paleosol.

The contact between the top of the Doswell Formation and overlying Cretaceous sediments was not observed during this study. Based on well cutting descriptions, the contact is placed at the top of the red siltstone and sandstone characteristic of Triassic strata (Milici et al., 1991). These red strata are replaced upsection by well-rounded, quartz-pebble conglomerates and glauconitic sandstones of the Lower Cretaceous (Milici et al., 1991). This change in texture and color reflects the dramatic shift from the arid Late Triassic climates to the more humid early Cretaceous climates (Frakes et al., 1992). Furthermore, there is considerable evidence for an angular discordance between the upper Taylorsville Basin strata and the basal Cretaceous sediments (LeTourneau, 2003, fig. 3.8) (Figure 34), and indications that a considerable thickness of Triassic strata was removed prior to basin burial (Malinconico, 2003).

When studying the Taylorsville Triassic succession, it is assumed that the deposits were formed under similar conditions as those that occurred in the Culpeper and Gettysburg basins. Therefore, the exposures of the Stagg Creek Member in the Taylorsville Basin are considered depositionally equivalent to the braided stream deposits (LA B) within the lower Poolesville Member in the Culpeper Basin and the New Oxford Formation in the Gettysburg Basin. These coarse-grained strata represent an interval with likely reservoir potential (Craddock et al., 2012). Outcrop samples taken through this stratigraphic interval tend to be poorly cemented, pebbly sandstones up to 45 feet thick. Porosity values for these outcrop sandstones range from less than 1% to more than 7% (Table 7). Above this interval, fine-grained, meandering fluvial and lake-margin deltaic sandstones (LA C) yield porosity values that characteristically are less than 1% (Table 7). These strata also tend to be localized, lenticular, and finer grained. Because of their laterally discontinuous extent and fine-grained character, these sandstone units provide an unknown and unlikely reservoir potential.

The exposed lake deposits of the Vinita Member that overlie the Stagg Creek Member consist predominantly of greenish gray to dark gray shales with few sandstone intervals greater than 20 feet thick. These sandstone intervals are fine- to medium-grained, argillaceous, and relatively impervious, with outcrop porosity values at less than 0.5% (Table 7). The preponderance of shale and claystone, some organic-rich, make this interval a potential seal interval above the Stagg Creek Member. Although this interval is less than 1,000 feet thick in outcrop, it appears to thicken dramatically into the center of the basin (>6,000 feet) (Figure 32,33).

Overlying the Vinita Member are coarse-grained strata of the Newfound Member. This succession of interbedded porous sandstone and intervening shale presents an additional interval of potential storage near the southern margin of the basin. Considering that the sandstone units in this interval have outcrop porosity values over 2%, it appears that they may provide an area with reservoir potential (Figure 57).

Although the exposed strata of the southwestern margin of the Taylorsville Basin present a stratigraphic succession that has strong potential for CO<sub>2</sub> sequestration, this stratigraphy may be only partially representative of the basin's entire sequence. Well data show that up to 8,000 feet of fluvial and lacustrine rocks are preserved near the basin center (Figure 33). This study indicates that the relationship between the coarse-grained fluvial facies and fine-grained lacustrine facies differs substantially between the basin center and basin margin. This can be shown in the Ellis well where higher porosity values are confined to marginal coarse-grained deposits (Figure 55). Vertical trends through this well suggest that LAs B and C display higher porosity and permeability values consistent with reservoir intervals, while intervening lacustrine strata (LA E) have very low permeability values and could serve as confining layers. This alternation of lithofacies associations suggests that there is good potential for storage targets in the buried Taylorsville Basin.

### **Concordant Igneous bodies as Reservoirs**

Within many NAM rift basins, diabase and basalt could serve as a CO<sub>2</sub> reservoir (Goldberg et al., 2010). Hypabyssal diabase and extrusive basalts are extensive in the Culpeper and Gettysburg basins, and are known from many other rift basins. These igneous deposits represent an important episode of igneous activity throughout the Mid-Atlantic region, near the end of rift basin formation. These igneous events have been dated, and appear to coincide with the Triassic-Jurassic transition (Schlische et al., 2003; Whiteside et al., 2007). They are the result of crustal attenuation concomitant with protracted rift basin development. This widespread episode of igneous activity is known from deposits throughout eastern North America and western Africa, and is commonly portrayed by the acronym, CAMP (Central Atlantic Magmatic Province) (Marzoli et al., 1999). The CAMP igneous activity is widely known from swarms of narrow discordant dikes, but may be best known for thick concordant sills such as the Palisades Sill of New York and New Jersey. Preliminary study has suggested that both the intrusive and extrusive concordant bodies of Triassic rift basins may offer potential suitability as CO<sub>2</sub> reservoirs (Goldberg et al., 2010).

Both the sills and flows exhibit prolific fracturing resulting from rapid cooling and contraction of the magma. Fracture spacing within exposed parts of the Gettysburg sill varies from less than an inch to more than 3 feet, and tends to pervade the entire diabase body (Figure 58).

In addition to the fracture porosity that characterizes both intrusive and extrusive deposits, extrusive flow units exhibit porous intervals that are concentrated near the top of individual lava flows. These layers of interconnecting pores represent vesicular intervals produced by gas escaping the liquid magma during flow emplacement. Some of these vesicle layers display porosity values in excess of 30% (Goldberg et al., 2010). Furthermore, these porous, flow-top horizons tend to be interconnected by the pervasive fracture porosity and columnar jointing.

Thick mafic bodies such as these provide potential as nonconventional CO<sub>2</sub> reservoirs.

Matter et al. (2007) and Matter and Kelemen (2009) have shown that CO<sub>2</sub> injected into these types of rocks can initiate a remineralization reaction with the constituent mafic minerals. The product of this reaction is inter-cavity deposition of carbonate minerals. Carbon dioxide chemically reacts with the mafic (iron- and magnesium-rich) minerals, resulting in the precipitation of various carbonate minerals (Olsen et al., 2016), and thus locking the CO<sub>2</sub> within a stable mineral lattice.

The presence of fracture porosity within diabase and basalt layers may not seem initially to be a significant factor in the potential of CO<sub>2</sub> reservoirs. However, when one considers the extensive area encompassed by these igneous bodies in Triassic rift basins, the capacity of the reservoir is impressive. Figure 59 illustrates the area of both the exposed and buried parts of the diabase sills within the Gettysburg and Culpeper basins. Total area for the Gettysburg sills is 930 km<sup>2</sup>, while that of the Culpeper Basin is 1145 km<sup>2</sup>. For both basins, potential reservoir areas exceed 200 x 10<sup>7</sup> m<sup>2</sup>. Therefore, based upon the generalized thicknesses described above, potential reservoir volume within the Gettysburg basin is 5.6 x 10<sup>11</sup>m<sup>3</sup>, and within the Culpeper Basin 1.1 x 10<sup>12</sup>m<sup>3</sup>.

Another significant aspect of these concordant igneous bodies within Triassic rift basins is that a preponderance of these units is contained within the lacustrine deposits (LAs D and E). The reason for this relationship is not currently understood, but the typically fine-grained lake deposits could serve to encase and seal all of these main igneous bodies. The fine-grained character of these surrounding rocks may serve as confining layers that help contain injected CO<sub>2</sub> (Figure 60). This also may be important when considering that the thermal

metamorphism associated with these bodies has further hardened these surrounding fine-grained deposits into hornfels (Collins, 2017). Collins suggested that these contact metamorphism zones represent impermeable layers surrounding the diabase intrusion. Within the exposed larger Triassic basins of eastern North America, thick



**Figure 58. A, B, Spaced fracturing of diabase of the Gettysburg sill, Adams County, Pennsylvania. C, Highly fractured columnar character of the Sander Basalt at Vulcan Materials', Warrenton, Virginia quarry. D. Intense and fine level of fracturing within contact metamorphosed lake deposits of the Balls Bluff Member of the Bull Run Formation, Loudoun County, Virginia. →**

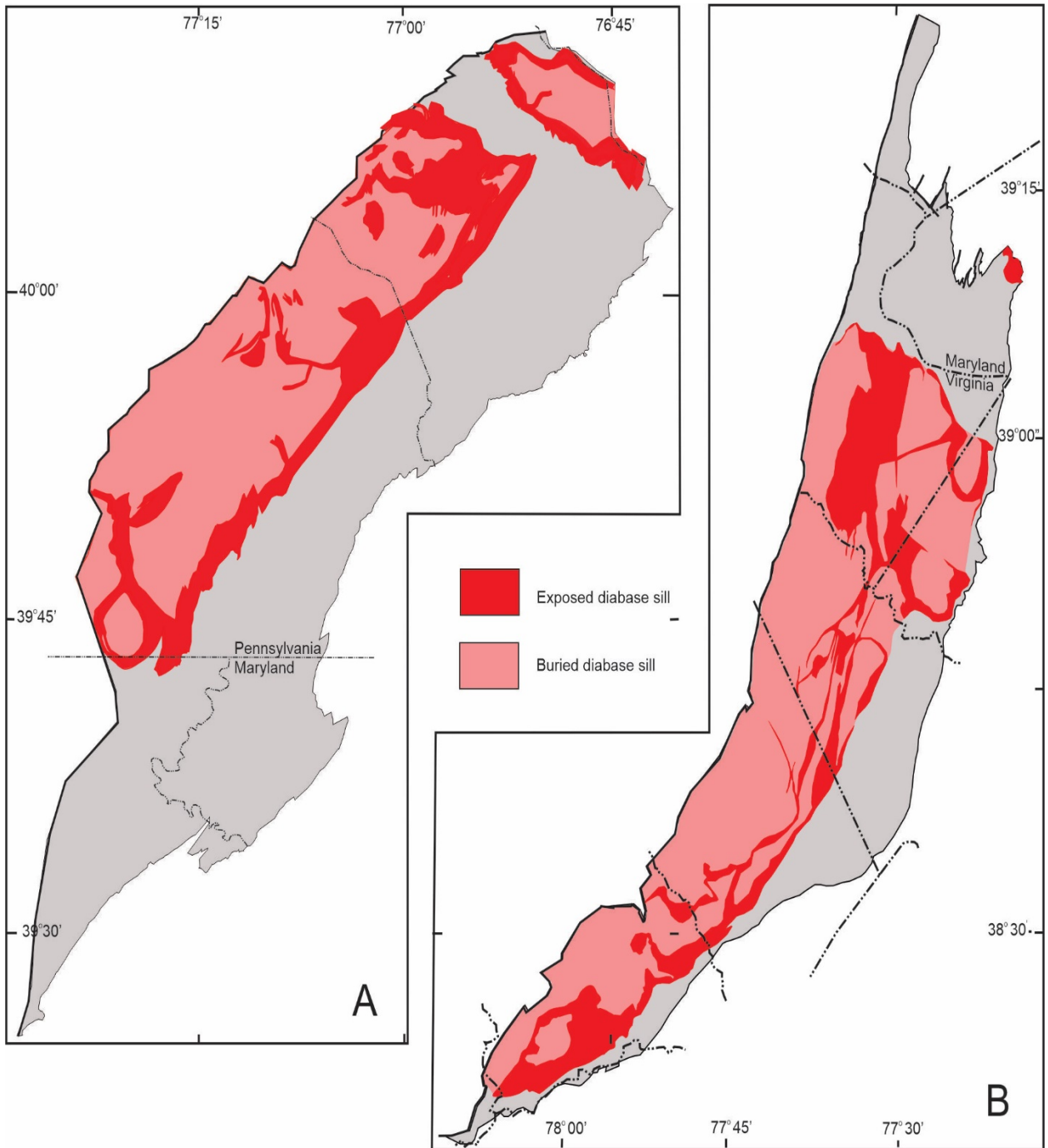


**Figure 59. Areal distribution of diabase in the Gettysburg (A) and Culpeper (B) basins. Deep red areas indicate diabase in outcrop, while pink areas represent areas inferred to be buried mafic beneath lake deposits. Diabase outcrop areas for the Culpeper Basin from Leavy et al. (1983), and for the Gettysburg Basin from Stose (1932), and Stose and Jonas (1939).**

mafic intrusive and extrusive bodies are widespread. Moreover, these types of bodies also can be shown to exist within the buried basins. Within the Butler well of the Taylorsville Basin, nearly 1,000 feet of mafic, presumably intrusive, rocks occupy the interval between the depths of 2,800 to 1,800 feet. Consequently, this interval appears to be a favorable target for CO<sub>2</sub> storage.

In summary, Triassic rift basins present a broad range of non-marine clastic facies that provide potential capacity for conventional CO<sub>2</sub> sequestration. Furthermore, the typical upward-fining character of rift basins provides a natural arrangement of lithologies in which the impervious lacustrine rocks serve as a thick seal layer over the porous and permeable marginal and basal coarse-grained clastics. Lastly, the thick, highly fractured extrusive and hypabyssal igneous rocks that are encapsulated within the lake sediments provide thick, extensive reservoirs with sequestration potential.

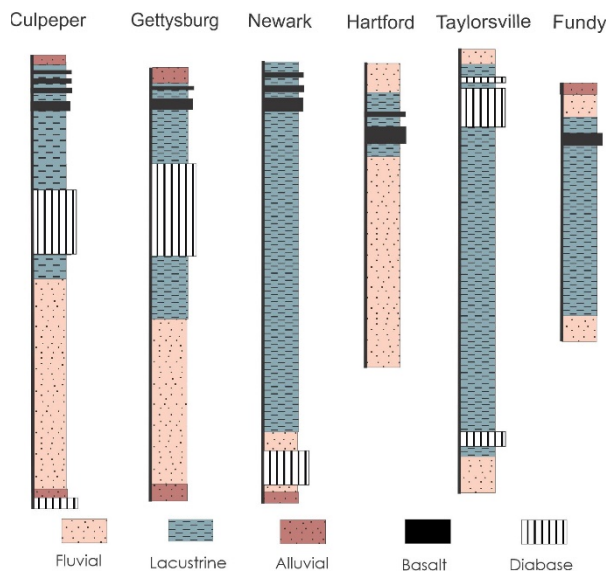


**Figure 60. Generalized stratigraphy and levels of potential igneous reservoirs within several NAM rift successions. No vertical scale implied, and lithofacies are generalized.**

## ACKNOWLEDGEMENTS

This study was partially funded by Battelle Memorial Institute of Columbus through a research grant from the U.S. Department of Energy. We would like to thank Patrick O'Brien of LDEO for providing access to Taylorsville Basin data and to C. Connallon (MGS) for his efforts in obtaining that available subsurface data. Beth Moore and Rusty Franklin kindly provided access to the Vulcan Materials quarry exposures of the Sander Basalt at Warrenton, Virginia. We would also like to thank D. Harris and M. Parris of the Kentucky Geological Survey/University of Kentucky for generating SEM images, as well as providing comments on the petrography of several samples. L. Cummings, (Battelle), M. KunleDare, P.P. and McLaughlin (DGS), A.W. Staley (MGS), W. Lassetter, Virginia DMME, and C.A. Kertis (USGS) provided helpful suggestions to versions of this report.

## REFERENCES CITED

- Andreasen, D.C., Staley, A.W., and Achmad, G., 2013, Maryland Coastal Plain aquifer information system: Hydrogeologic framework: Maryland Geological Survey, Open-File Report 12-02-20, 121 p.
- Barnes, D.A., and Ellet, K.M., 2014, Geological carbon sequestration storage resource estimates for the Ordovician St. Peter Sandstone, Illinois and Michigan Basins, USA: DOE Cooperative Agreement No. DE-FE002068, topical report, 63 p.
- Benson, R., 1992, Map of exposed and buried early Mesozoic rift basins/synrift rocks of the U.S. Middle Atlantic Continental Margin: Delaware Geological Survey, Miscellaneous Map Series 5.
- Berg, T.M., Edmunds, W.E., and Geyer, A.R., 1980, Geologic map of Pennsylvania: Pennsylvania Topographic and Geologic Survey, (4th Series), Map 1, scale 1:250,000.
- Berg, T.M., McInerney, M.K., Way, J.H., and MacLachlan, D.B., 1983, Stratigraphic Correlation Chart of Pennsylvania: Pennsylvania Topographic and Geologic

- Survey (4th Series), General Geology Report 75.
- Blair, T., 1987, Tectonic and hydrologic controls on cyclic alluvial fan, fluvial, and lacustrine rift-basin sedimentation, Jurassic-lowermost Cretaceous Todos Santos Formation, Chiapas, Mexico: *Journal of Sedimentary Petrology*, 57:845-862.
- Bobyarchick, A.R., and Glover, L., 1979, Deformation and metamorphism in the Hylas zone and adjacent parts of the eastern Piedmont in Virginia: *Geological Society of America Bulletin*, 70:739-752.
- Bowen, B.B., Ochoa, R.I., Wilkens, N.D., Brophy, J., Lovell, T.R., Fischietto, N., Medina, C.R., and Rupp, J.A., 2011, Depositional and diagenetic variability within the Cambrian Mount Simon Sandstone: Implications for carbon dioxide sequestration: *Environmental Geosciences*, 18:69-89.
- Brezinski, D.K., 2004, Stratigraphy of the Frederick Valley and its relationship to karst development: Maryland Geological Survey, Report of Investigations 75, 101 p.
- Brezinski, D.K., 2021, Geologic map of the Emmitsburg and Taneytown Quadrangles, Frederick and Carroll Counties, Maryland. Maryland Geological Survey Geological Map, scale 1:24,000.
- Brezinski, D.K., and Edwards, J., 2004, Geologic map of the Woodsboro quadrangle, Carroll and Frederick Counties, Maryland: Maryland Geological Survey, scale 1:24,000.
- Burggraf, D.R., and Vondra, C.F., 1982, Rift Valley Facies and Paleoenvironments: An example from the East African Rift system of Kenya and southern Ethiopia, in: Brunnacker, K., and Taieb, M., eds., Graben geology and geomorphogenesis: *Zeitschrift für Geomorphologie Supplement* 42, p. 43-73.
- Cohen, A.S., 1989, Facies relationship and sedimentation in large rift lakes and implications for hydrocarbon exploration: Examples from Lake Turkana and Tanganyika: *Palaeogeography, Palaeoclimatology, Palaeoecology*, 70:65-80.
- Collins, D.J., 2017, Characterization of the Triassic Newark Basin of New York and New Jersey for geologic storage of carbon dioxide: United States Department of Energy final report, 1902 p.
- Collinson, J.D., 1978, Lakes, in: Reading, H.G., ed., *Sedimentary Environments and Facies*: Elsevier, New York, p. 61-79.
- Cornet, B. 1977, The palynostratigraphy and age of the Newark Supergroup: Ph.D. dissertation, Pennsylvania State University, 505 p.
- Cornet, B., and Olsen, P.E., 1990, Early to middle Carnian (Triassic) flora and fauna of the Richmond and Taylorsville basins, Virginia and Maryland, U.S.A: *Virginia Museum of Natural History Guidebook*, Volume 1, 87 p.
- Craddock, W.H., Merrill, M.D., Roberts-Ashby, T.L., Brennan, S.T., Buursink, M.L., Drake, R.M. II, Warwick, P.D., Cahan, S.M, DeVera, C.A., Freeman, P.A., Gosai, M.A., and Lohr, C.D., 2012, Geologic framework for the national assessment of carbon dioxide storage resources—Atlantic Coastal Plain and eastern Mesozoic rift basins, in: Warwick, P.D. and Corum, M.D., eds., *Geologic Framework for the National Assessment of Carbon Dioxide Storage Resources*: U.S. Geological Survey Open-File Report 2012-1024-N, Chapter N 32 p.
- Demars, C., Pagel, M., Deloule, E., and Blanc, P., 1996, Cathodoluminescence of quartz from sandstones: Interpretation of the UV range by determination of trace element distributions and fluid-inclusion P-T-X properties in authigenic quartz. *American Mineralogist*, 81:891-901.
- Dickinson, W.R., 1970, Interpreting detrital modes of graywacke and arkose: *Journal of Sedimentary Research*, 40:695-707.
- Dickinson, W.R., Beard, L.S., Brakenridge, G.R., Erjavec, J.L., Ferguson, R.C., Inman, K.F., Knepp, R.A., Lindberg, F.A., and Ryberg, P.T., 1983, Provenance of North American Phanerozoic sandstones in relation to tectonic setting: *Geological Society of America Bulletin*, 94:222-235.

- Dunagan, S.P., and Turner, C.E., 2004, Regional paleohydrologic and paleoclimatic setting of wetland/lacustrine depositional systems in the Morrison Formation (Upper Jurassic), Western Interior, USA: *Sedimentary Geology*, 167:269–296.
- Fail, R., 2008, The Gettysburg Basin, in: Fleeger G.M., ed., *Geology of the Gettysburg Mesozoic basin and geology of the Gettysburg Campaign: 73rd Annual Field Conference of Pennsylvania Geologists*, p. 1-7.
- Fawad, M., Mondol N.H., Jahren J., and Bjørlykke K., 2010, Microfabric and rock properties of experimentally compressed silt-clay mixtures: *Marine and Petroleum Geology*, 27:1698–1712.
- Frakes, L.A., Francis, J.E., and Syktus, J.I., 1992, *Climate modes of the Phanerozoic*: Cambridge University Press, Glasgow, 274 p.
- Glaeser, J.D., 1966, Provenance, dispersal, and depositional environments of Triassic sediments in the Newark-Gettysburg Basin: *Pennsylvania Topographic and Geologic Survey, (4th Series) General Geology Report G 43*, 170 p.
- Goldberg, D.S., Kent, D.V., and Olsen, P.E., 2010, Potential on-shore and off-shore reservoirs for CO<sub>2</sub> sequestration in Central Atlantic magmatic province basalts: *Proceedings of the National Academy of Sciences*, 107:1327–1332.
- Gore, P.J.W., 1988, Late Triassic and Early Jurassic lacustrine sedimentation in the Culpeper basin Virginia, in: Fleet, A.J., Kelts, K., and Talbot, M.R., eds., *Lacustrine Petroleum Source Rocks*: Geological Society of London Special Publication 40, p. 247-278.
- Hansen, H.J., 1988, Buried rift basin underlying Coastal Plain sediments, central Delmarva Peninsula, Maryland: *Geology*, 16:779–782.
- Hansen, H.J., and Edwards, J.J., 1986, The lithology and distribution of pre-Cretaceous basement rocks beneath the Maryland Coastal Plain: *Maryland Geological Survey Report of Investigations 44*, 27 p.
- Henares, S., Caracciolo, L., Viseras, C., Fernández, J., and Yeste, L.M., 2016, Diagenetic constraints on heterogeneous reservoir quality assessment: A Triassic outcrop analogue of meandering fluvial reservoirs: *American Association of Petroleum Geologists Bulletin*, 100:1377–1398.
- Hentz, T.F., 1985, Early Jurassic sedimentation of a rift-valley lake: The Culpeper Basin of northern Virginia: *Geological Society of America Bulletin*, 96:92-107.
- Horton, B.K., and Schmitt, J.G., 1996, Sedimentology of a coalescing fan-delta system, Miocene Horse Camp Formation, Nevada, U.S.A.: *Sedimentology*, 43:133-155.
- Hubert, J.F., and Forlenza, M.F., 1988, Sedimentology of braided-river deposits in Upper Triassic Wolfville redbeds, southern shore of Cobequid Bay, Nova Scotia, in: Manspeizer, W., ed., *Triassic-Jurassic rifting, continental breakup and the origin of the Atlantic Ocean and passive margin*: Elsevier Science Publishers, Amsterdam, p. 231-247.
- Hubert, J.F., Feshbach-Meriney, P.E. and Smith, M.E., 1992, The Triassic-Jurassic Hartford rift basin, Connecticut and Massachusetts: Evolution, sandstone diagenesis and hydrocarbon history: *American Association of Petroleum Geologists Bulletin*, 76:1710-1734.
- Ingersoll, R. V., Bullard, T. F., Ford, R. L., Grimm, J. P., Pickle, J. D., and Sares, S. W., 1984, The effect of grain size on detrital modes: a test of the Gazzi-Dickinson point-counting method: *Journal of Sedimentary Research*, 54:103-116.
- Kettanah, Y.A., Kettanah, M.Y., and Wach, G.D., 2014, Provenance, diagenesis, and reservoir quality of the Upper Triassic Wolfville Formation, Bay of Fundy, Nova Scotia, Canada: in: Scott, R.A., Smyth, H.R., Morton, A.C. and Richardson, N., eds., *Sediment provenance studies in hydrocarbon exploration and production*: Geological Society of London Special Publications 386, p. 75-110.
- Kostelnik, K., and Carter, K.M., 2009, Unraveling the stratigraphy of the Oriskany Sandstone: A necessity in assessing its site-specific carbon sequestration potential: *Environmental Geosciences*, 16:187–200.

- Lambiase, J., 1990, A model for tectonic control of lacustrine stratigraphic sequences in continental rift basins, in: Katz, B., and Rosendahl, B., eds., Lacustrine exploration: case studies and modern analogues: American Association of Petroleum Geologists Memoir 50, p. 265-276.
- Larsen, V and Steel, R.J., 1978, The sedimentary history of a debris flow dominated Devonian alluvial fan-A study of textural inversion: *Sedimentology*, 5:37-59.
- Leavy, B.D., Froelich, A.J., and Abram, A.C., 1983, Bedrock map and geotechnical properties of rocks of the Culpeper Basin and vicinity, Virginia and Maryland: U.S. Geological Survey, Miscellaneous Investigations Series Map I-1313.
- Lee, K.Y., 1977, Triassic-Jurassic geology of the northern part of the Culpeper Basin, Virginia and Maryland: U.S. Geological Survey Bulletin 1422, p. C1-C17.
- Lee, K.Y., and Froelich A.J., 1989, Triassic-Jurassic stratigraphy of the Culpeper and Barbourville Basins, Virginia and Maryland: U.S. Geological Survey Professional Paper 1472, 52 p.
- Leetaru, H.E., and McBride, J.H., 2009, Reservoir uncertainty, Precambrian topography, and carbon sequestration in the Mt. Simon Sandstone, Illinois Basin: *Environmental Geosciences*, v. 16, no. 4, p. 235-243.
- Leetaru, H. E., Korose, C., and Whittaker, S., 2019, CarbonSAFE – Illinois: Illinois State Geological Survey, Prairie Research Institute, 26 p.
- Leleu, S., and Hartley, A.J., 2010, Controls on the stratigraphic development of the Triassic Fundy Basin, Nova Scotia: Implications for the tectonostratigraphic evolution of Triassic Atlantic rift basins. *Journal of the Geological Society London*, 167:437-454.
- LeTourneau, P.M., 2003, The stratigraphy and structure of the buried Late Triassic Taylorsville basin, Virginia and Maryland, in: LeTourneau, P.M. and Olsen, P.E., eds., The great rift valleys of Pangea in eastern North America, V.2, *Sedimentology, Stratigraphy, and Paleontology*: Columbia University Press, New York, p. 12-58.
- Lindholm, R.C., 1979, Geologic history and stratigraphy of the Triassic-Jurassic Culpeper Basin, Virginia: *Geological Society of America Bulletin*, 90:995-97.
- Lovell, T. R., and Bowen, B. B., 2013, Fluctuations in sedimentary provenance of the Upper Cambrian Mount Simon Sandstone, Illinois Basin, United States: *The Journal of Geology*, v. 121, no. 2, p. 129-154.
- Luttrell, G.W., 1989, Stratigraphic nomenclature of the Newark Supergroup of eastern North America: U.S. Geological Survey Bulletin 1572, 136 p.
- McFarland, E.R., and Bruce, T.S., 2006, The Virginia Coastal Plain hydrogeologic framework: U.S. Geological Survey Professional Paper 1731, 118 p.
- Malinconico, M.L., 2003, Estimates of eroded strata using borehole vitrinite reflectance data, Triassic Taylorsville rift basin, Virginia: Implications for duration of syn-rift sedimentation and evidence of structural inversion, in: LeTourneau, P.M., and Olsen, P.E., eds., The great rift valleys of Pangea in eastern North America: Columbia University Press, New York, p. 80-103.
- Marzoli, A., Renne, P.R., Piccirillo, E.M., Ernesto, M., Bellieni, G., and DeMin, A., 1999, Extensive 200 million-year-old continental flood basalts of the central Atlantic magmatic province: *Science*, 284:616-618.
- Matter, J.M., and Kelemen, P.B., 2009, Permanent storage of carbon dioxide in geologic reservoirs by mineral carbonation: *Nature Geoscience* (online), doi: 10.1038/NGE0683.
- Matter, J.M., Takahashi, T., and Goldberg, D., 2007, Experimental evaluation of in situ CO<sub>2</sub>-water-rock reactions during CO<sub>2</sub> injection in basaltic rocks: Implications for geological CO<sub>2</sub> sequestration: *Geochemistry, Geophysics, Geosystems* 8, 19 p.
- Medina, C.R., and Rupp, J.A., 2012 Reservoir characterization and lithostratigraphic division of the Mount Simon Sandstone (Cambrian): Implications for estimations of geologic

- sequestration storage capacity: *Environmental Geosciences*, 19:1-15.
- Meng, A.A., and Harsh, J.F., 1991, Hydrogeologic framework of the Virginia Coastal Plain: U.S. Geological Survey Professional Paper 1404 C, 85 p.
- Miall, A.D., 1977, Lithofacies type and vertical profile models in braided river deposits: A summary, in Miall A.D., ed., *Fluvial Sedimentology: Canadian Society of Petroleum Geologists Memoir 5*, p. 597–604.
- Milici, R.C., Bayer, K.C., Pappano, P., Costain, A.J., Coruh, K.C., and Nolde, J.E., 1991, Preliminary geologic section across the buried part of the Taylorsville Basin, Essex and Caroline Counties, Virginia: Virginia Division of Mineral Resources, Open File Report 91–1, 31 p.
- Milliken, K.L., 2001, Diagenetic heterogeneity in sandstone at the outcrop scale, Breathitt Formation (Pennsylvanian), eastern Kentucky: *American Association of Petroleum Geologists Bulletin*, 85:795–815.
- Nutter, L.J., 1975, Hydrogeology of the Triassic Rocks of Maryland. Maryland Geological Survey: Report of Investigations 26, 37 p.
- Nemec, W., and Steel, W.R., 1984, Alluvial and coastal conglomerates: Their significant features and some comments on gravelly mass-flow deposits: in: Koster, E.H., and Steel, R.J., eds., *Sedimentology of gravels and conglomerates: Canadian Society of Petroleum Geologists, Memoir 10*, p.1-31.
- Olsen, P. E., 1980, Triassic and Jurassic formations of the Newark Basin, in Manspeizer, W. ed., *Field Studies in New Jersey Geology and Guide to Field Trips: 52nd Annual Meeting*, New York State Geological Association, Newark College of Arts and Sciences, Newark, Rutgers University, p. 2-39.
- Olsen, P. E., 1986, A 40-million-year lake record of early Mesozoic climatic forcing: *Science*, 234:842–848.
- Olsen, P.E., 1997, Stratigraphic record of the early Mesozoic breakup of Pangea in the Laurasia-Gondwana rift system: *Annual Reviews of Earth and Planetary Science*, 25:337–401.
- Olsen, P.E., and Kent, D.V., 1999 Long-period Milankovitch cycles from the Late Triassic and Early Jurassic of eastern North America and their implications for the calibration of the Early Mesozoic time-scale and long term behavior of the planets: *Philosophical Transactions of the Royal Society of London*, 367:1761-1786.
- Olsen, P.E., Schlische, R.W., and Gore, P.J.W., 1989, Field guide to the tectonics, stratigraphy, sedimentology, and paleontology of the Newark Supergroup, eastern North America: *International Geological Congress, Guidebooks for Field Trips T351*, p. 59-68.
- Olsen, P.E., Kent, D.V., Cornet, B., Witte, W.K., and Schlische, R.W., 1996. High-resolution stratigraphy of the Newark rift basin (Early Mesozoic), eastern North America: *Geological Society of America Bulletin*, 108:40-77.
- Olsen, P.E., Reid, J.C., Taylor, K.B., Whiteside, J.H., Kent, D.V., 2015 Revised stratigraphy of the Late Triassic age strata of the Dan River Basin (Virginia and North Carolina, USA) based on drill core and outcrop data: *Southeastern Geology*, 51:1-31.
- Olsen, P.E., Kinney, S.T., Zakharova, N.V., Schlische, R.W., Withjack, M.O., Kent, D.V., Goldberg, D.S., and Slater, B.E., 2018, New insights on rift basin development and the geological carbon cycle, mass extinction, and carbon sequestration from outcrops and new core, drill holes, and seismic lines from the northern Newark Basin (New York and New Jersey), in: Gates, A.E., ed., *Geologic Diversity in the New York Metropolitan Area: 88th Annual New York State Geological Field Conference, Guidebook*, p. 190-274.
- Oshchudlak, M.E., and Hubert, J.F., 1988, Petrology of Mesozoic sandstones in the Newark basin, central New Jersey and adjacent New York, in: Manspeizer, W., ed., *Triassic-Jurassic rifting, continental breakup and the origin of the Atlantic Ocean and passive margins: Developments in Geotectonics 22: Amsterdam: Elsevier*, p. 333-352.

- Pettijohn, F. J., Potter, P.E., and Siever, R., 1987, Sand and sandstone: Springer-Verlag, New York, 2nd ed., 553 p.
- Picard, M.D. and High, L.R., 1981, Physical stratigraphy of ancient lacustrine deposits, in Ethridge, F.G., and Flores, R.M., eds., Recent and ancient nonmarine depositional environments: Models for Exploration: Society of Economic Paleontologists and Mineralogists Special Publication 31, p. 233–259.
- Reger, J.P., and Edwards, J., 2006, Geologic map of the Union Bridge quadrangle, Carroll and Frederick Counties, Maryland: Maryland Geological Survey Digital Geologic Map, scale 1:24,000.
- Reinemund, J.A., 1955, Geology of the Deep River coal field, North Carolina: U.S. Geological Survey Professional Paper 246, 159 p.
- Ressetar, R., and Taylor, G.K., 1988, Late Triassic depositional history of the Richmond and Taylorsville basins, eastern Virginia, in: Manspeizer, W., ed., Triassic–Jurassic rifting: continental breakup and the origin of the Atlantic Ocean and the passive margins: Developments in Geotectonics 22, Amsterdam: Elsevier, p. 423–443.
- Retallack, G.J., 2001, Soils of the past: An introduction to paleopedology: Blackwell Science, Oxford, 600 p.
- Rima, D.R., Meisler, H., and Longwill, S., 1962, Geology and hydrology of the Stockton Formation in southeastern Pennsylvania: Pennsylvania Topographical and Geological Survey (4th series), Water Resources Report 14, 111 p.
- Roberts, J.K., 1928 The geology of the Virginia Triassic: Virginia Geological Survey, Bulletin 29, 205 p.
- Root, S.I., 1988, Structure and hydrocarbon potential of the Gettysburg Basin, Pennsylvania and Maryland, in: Manspeizer, W., ed., Triassic–Jurassic Rifting, continental breakup, and the origin of the Atlantic Ocean and passive margins: Developments in Geotectonics 22, Elsevier, Amsterdam, p. 353–367.
- Schlische, R.W. 1992, Structural and stratigraphic development of the Newark extensional basin, eastern North America; implications for the growth of the basin and its bounding structures: Geological Society of America Bulletin, 104:1246–1263.
- Schlische, R.W., 1993, Anatomy and evolution of stratigraphic record of Triassic–Jurassic continental rift system, eastern North America: Tectonics, 12:1026–1042.
- Schlische, R.W., and Olsen, P.E., 1990, Quantitative filling model for continental extensional basins with applications to early Mesozoic rifts of eastern North America: Journal of Geology, 98:135–155.
- Schlische, R.W., Withjack, M.O., and Olsen, P.E., 2003, Relative timing of CAMP, rifting, continental breakup, and basin inversion: Tectonic significance, in: Hame, W.E., McHomes, G.C., Renne, P.R., and Ruppel, C., eds., The central Atlantic magmatic province: American Geophysical Union Monographs, p. 1–15.
- Slater, B.E., Smith, L., Tymchak, M.P., and Collins, D.J., 2013, Preliminary results from the TriCarb deep stratigraphic well drilled into the Newark Rift Basin, Rockland County, NY: Annual AAPG Meeting, (Abst 90163), Pittsburgh, Pennsylvania.
- Smoot, J.P., 1991, Sedimentary facies and depositional environments of early Mesozoic Newark Supergroup basins, eastern North America: Palaeogeography, Palaeoclimatology, Palaeoecology, 84:369–423.
- Smoot, J.P., 1985, A closed-basin hypothesis and its use in facies analysis of the Newark Supergroup. in: Robinson, G.R. and Froelich, A.J., eds., Proceeding so the second U.S. Geological Survey workshop on early Mesozoic basins of the eastern United States: U.S. Geological Survey Circular 946, p. 4–9.
- Smoot, J.P., 1989, Fluvial and lacustrine facies of the Early Mesozoic Culpeper Basin, Virginia and Maryland: Fieldtrip T213, 28th International Geological Congress,

- Washington D.C., American Geophysical Institute, 15 p.
- Smoot, J.P., 1999, Early Mesozoic. Chapter 12, in: Schultz, C. ed., *The Geology of Pennsylvania: Pennsylvania Geological Survey Special Publication 1*, p. 178-201.
- Smoot, J., 2009, Newark Supergroup exposed basins, in: Lassiter, W.L., ed., *Proceedings of the 2009 southeastern U.S. Mesozoic basins energy workshop: Division of Geology and Mineral Resources Open File Report 09-03*.
- Smoot, J.P., 2010, Triassic depositional facies in the Newark basin, Chapter A, in: Herman, G.C. and Serfes, M.E., eds., *Contributions to the geology and geohydrology of the Newark Basin: New Jersey Geological and Water Survey Bulletin 77A*, 108 p.
- Smoot, J.P., 2016, Early Mesozoic geology of Virginia, in: Bailey, C.M., Sherwood, W.C., Eaton, L.S., and Powars, D.S., eds., *The Geology of Virginia: Virginia Museum of Natural History Special Publication 18*, p. 159-192.
- Smoot, J.P. and Olsen, P.E., 1994, Climatic cycles as sedimentary controls of rift basin lacustrine deposits in the early Mesozoic Newark basin based on continuous core, in: Lomando, A.J. and Harris, M., eds., *Lacustrine Depositional Systems: SEPM Core Workshop Notes*, 19:201-237.
- Southworth, S., Burton, W.C., Schindler, J.S., and Froelich, A.J., 2006, *Geologic map of Loudoun County, Virginia: U.S. Geological Survey, Geologic Investigations Series Map I-2553*.
- Southworth, S., Brezinski, D.K., Drake, A.A., Jr., Burton, W.C., Orndorff, R.C., Froelich, A.J., Reddy, J.E., Denenny, D., and Daniels, D.L., 2007, *Geologic map of the Frederick 30' × 60' quadrangle, Maryland, Virginia, and West Virginia: U.S. Geological Survey, Scientific Investigations Map 2889, scale 1:100,000*.
- Stose, G.W., 1932, *Geology and mineral resources of Adams County, Pennsylvania; Pennsylvania Topographic and Geologic Survey (4th Series), Bulletin C-1*.
- Stose, G.W., and Bascom, F., 1929, *Description of the Fairfield and Gettysburg quadrangles, Pennsylvania: U.S. Geological Survey, Geologic Atlas Folio 225*, 22 p.
- Stose, G.W., and Jonas, A.I., 1939, *Geology and mineral resources of York County, Pennsylvania: Pennsylvania Topographic and Geologic Survey (4th Series), County Report 67*, 19 p.
- Suhaimi, A.A., 2016, *Pore characterization and distribution within Niagran-Lower Silurian reef complex reservoirs in the Silurian northern pinnacle reef trend, Michigan Basin: Unpublished Masters thesis, Western Michigan University, Kalamazoo*, 179 p.
- Thayer, P.A., 1970, *Stratigraphy and geology of the Dan River Triassic basin: Southeastern Geology*, 12:1-31.
- Turner-Peterson, C., 1980, *Sedimentology and uranium mineralization in the Triassic-Jurassic Newark Basin, Pennsylvania, and New Jersey, in: Turner-Peterson, C., ed., Uranium in Sedimentary Rocks, Application and the Facies Concept in Exploration: SEPM Rocky Mtn. Section, Short Course Notes*, p. 149-175.
- Turner-Peterson, C.E., and Smoot, J.P., 1985, *New thoughts on facies relationships in the Triassic Stockton and Lockatong Formations, Pennsylvania and New Jersey, in: Robinson, G.R., and Froelich, A.J., eds., Workshop on the Early Mesozoic basins of the eastern United States: U.S. Geological Survey Circular 946*, p. 10-17.
- Van Houten, F.B., 1962, *Cyclic sedimentation and the origin of analcime-rich Upper Triassic Lockatong Formation, west-central New Jersey and adjacent Pennsylvania: American Journal of Science*, 260:561-576.
- Van Houten, F. B., 1977, *Triassic-Liassic deposits of Morocco and eastern North America: comparison: American Association of Petroleum Geologists*, 61:79-99.
- Virginia Division of Mineral Resources, 1993, *Geologic map of Virginia: Virginia Division of Mineral Resources, scale 1:500,000*.
- Vroblesky, D.A., and Fleck, W.B., 1991, *Hydrogeologic framework of the Coastal Plain of Maryland, Delaware, and District of*

- Columbia: U.S. Geological Professional Paper 1404-E, 52 p.
- Wade, J.A., Brown, D.E., Traverse, A., and Fensome, R.A., 1996, The Triassic-Jurassic Fundy Basin, eastern Canada: regional setting, stratigraphy and hydrocarbon potential: *Atlantic Geology*, 32:189-231.
- Walker, R.G., and Cant, D.J., 1978, Facies Models 3. Sandy fluvial systems, in: Walker, R.G., ed., *Facies Models: Geoscience Canada Reprint Series 1*, p. 23-31.
- Weems, R.E., 1980, Geology of the Taylorsville Basin, Hanover County, Virginia: *Contributions to Virginia Geology 4*. Virginia Division of Mineral Resources Publication 27, 23-38.
- Weems, R.E., 1981, Geology of the Hanover Academy Quadrangle, Virginia: Virginia Division of Mineral Resources Publication 30, scale 1:24,000.
- Weems, R.E., 1986 Geology and mineral resources of the Ashland Quadrangle, Virginia: Virginia Division of Mineral Resources Publication 64, scale 1:24,000.
- Weems, R.E., and Olsen, P.E., 1997, Synthesis and revision of groups within the Newark Supergroup in eastern North America: *Geological Society of America Bulletin*, 109:195-209.
- Weems, R.E., Tanner, L.H., and Lucas, S.G., 2016, Synthesis and revision of the lithostratigraphic groups and formations in the Upper Permian?–Lower Jurassic, Newark Supergroup of eastern North America: *Stratigraphy*, 13:111–153.
- Whiteside, J.H., Olsen, P.E., Kent, D.V., Fowell, S.J., Et-Touhami, M., 2007. Synchrony between the CAMP and the Triassic-Jurassic mass-extinction event? *Palaeogeography, Palaeoclimatology, Palaeoecology*, 244:345-367.
- Wickstrom, L.H., Venteris, E.R., Harper, J.A., McDonald, J., Slucher, E.R., Carter, K.M., Greb, S.F., Wells, J.G., Harrison, W.B. III., Nuttal, B.C., Riley, R.A., Drahovzal, J.A., Rupp, J.A., Avary, K.L., Lanham, S., Barnes, D.A., Gupta, N., Baranoski, M.A., Radhakrishnan, P., Solis, M.P., Baum, G.R., Powers, D., Hohn, M.E., Parris, M.P., McCoy, K., Grammer, M., Pool, S., Luckhardt, C., Kish, P., 2005, Characterization of geologic sequestration opportunities in the MRCSP region phase I task report period of performance: October 2003–September 2005. MRCSP Phase I Report, 152 p.
- Withjack, M.O., Schlische, R.W., and Olsen, P.E., 1998, Diachronous rifting, drifting, and inversion on the passive margin of central eastern North America: analog for other passive margins: *American Association of Petroleum Geologists Bulletin*, 82:817–835.
- Withjack, M.O., Schlische, R.W., and Olsen, P.E., 2002, Rift-basin structure and its influence on sedimentary systems, in: Renaut, R.W. and Ashley, G.M., eds., *Sedimentation in continental rifts: SEPM Special Publication 73*, ISBN 1-56576-082-4, p. 57–81.
- Withjack, M.O., Schlische, R.W., and Olsen, P.E., 2012. Development of passive margin of eastern North America: Mesozoic rift, igneous activity, and breakup. in: Roberts, E.D., and Bally, A.W., eds., *Regional geology and tectonics: Phanerozoic rift systems and sedimentary basins*. p. 301-335. DOI/10:1016/B978-00444-56356-9000012-2.
- Withjack, M.O., Schlische, R.W., Malinconico, M.L., and Olsen, P.E., 2013, Rift-basin development: Lessons from the Triassic-Jurassic Newark basin of eastern North America, in: Mohriak, W.U., Danforth, A., Post, P.J., Brown, D.E., Tari, G.C., Nemcok, M., and Sinha, S.T., eds., *Conjugate divergent margins: Geological Society of London, Special Publication 369:301-321*.
- Yager, R.M., and Ratcliffe, N.M., 2010, *Hydrogeology and simulation of groundwater flow in fractured rock in the Newark basin, Rockland County, New York: U.S. Geological Survey, Scientific Investigations Report 2010–5250*, 139 p.
- Yuretich, R.F., 1979, Modern sediments and sedimentary processes in Lake Rudolf (Lake Turkana), Kenya: *Sedimentology*, 26: 313-331.

## APPENDIX I

Appendix IA. Results of porosity assessment from PPL scanned thin section image analysis.

<b>Basin</b>	<b>Culpeper</b>																	
<b>Formation</b>	<b>Manassas</b>																	
<b>Member</b>	<b>Poolesville</b>																	
<b>Sample</b>	A	B	C	D	E	F-1	F	G	H	I	I+1	J	K	L	M	N	O	P
<b>Porosity (%)</b>	2.7	8.8	0.0	0.7	0.1	0.0	0.0	0.0	0.2	0.0	0.1	0.1	0.2	0.0	0.2	0.0	0.0	0.0

<b>Basin</b>	<b>Gettysburg</b>															
<b>Formation</b>	<b>New Oxford</b>															
<b>Member</b>	<b>N/A</b>															
<b>Sample</b>	A	B	C	D	D+1	E-1	E	F	G	H	H+1	I	J	K	L	
<b>Porosity (%)</b>	0.5	0.2	2.2	0.3	0.3	0.1	0.1	0.2	0.2	0.1	0.0	0.3	0.2	0.2	0.4	

<b>Basin</b>	<b>Gettysburg</b>						
<b>Formation</b>	<b>Gettysburg</b>						
<b>Member</b>	<b>Conewago</b>						
<b>Sample</b>	A	B	C	D	E	F	G
<b>Porosity (%)</b>	4.3	3.1	7.5	17.1	2.2	6.2	4.1

<b>Basin</b>	<b>Taylorsville</b>																			
<b>Formation</b>	<b>Doswell</b>																			
<b>Member</b>	<b>Stagg Creek</b>						<b>Vinita</b>					<b>Newfound</b>								
<b>Sample</b>	A	B	C	D	E	F	G	H	TYPE	I	J	K	K+1	L	M	N	O	P	Q	
<b>Porosity (%)</b>	0.8	0.6	7.4	0.6	0.8	0.9	0.2	0.1	0.1	0.3	0.7	1.9	1.8	4.2	0.5	2.1	1.7	0.9	1.6	

Appendix IB. Results of modal analysis using PPL and XPL microscopy of sandstone thin-sections.

Formation	Member	Sample	Q F L grains - Gazzi-Dickenson method				other		
			mono-crystalline quartz	poly-crystalline quartz	feldspar (undifferentiated)	lithics	accessory minerals	opaques	matrix
Gettysburg	Conewago	A	43%	17%	0%	4%	0%	1%	0%
		B	40%	21%	0%	4%	0%	0%	0%
		C	46%	9%	1%	5%	0%	1%	0%
		D	35%	11%	3%	3%	0%	0%	3%
		F	40%	13%	2%	9%	0%	0%	0%
Doswell	Stagg Creek	A	32%	18%	12%	11%	4%	0%	0%
		D	17%	25%	21%	15%	1%	1%	0%
	Vinita	K	20%	30%	15%	13%	3%	0%	0%
	Newfound	L	21%	24%	16%	15%	1%	1%	0%
		M	28%	10%	23%	13%	4%	2%	0%
		O	23%	18%	26%	15%	0%	0%	0%
Manassas	Poolesville	A	18%	37%	12%	10%	0%	0%	0%
		E	17%	36%	17%	5%	1%	0%	0%
		G	18%	34%	15%	13%	2%	0%	0%
		I	29%	23%	14%	5%	3%	1%	0%
		J	20%	19%	15%	5%	10%	1%	0%
		M	27%	12%	25%	4%	2%	0%	0%
		O	21%	12%	23%	8%	2%	0%	0%
New Oxford	N/A	A	12%	37%	10%	22%	3%	0%	0%
		D	15%	36%	11%	16%	4%	3%	0%
		E	26%	31%	15%	12%	2%	1%	0%
		H	24%	11%	17%	13%	8%	1%	0%
		J	18%	18%	28%	8%	4%	0%	0%
		L	15%	5%	30%	3%	3%	1%	0%

Formation	Member	Sample	cement				porosity (i.e. epoxy filled spaces)			total count
			illite-feldspar**	quartz over-growth	hematite	calcite	inter-particle	intra-particle (dissolution)	fracture	
Gettysburg	Conewago	A	0%	10%	19%	0%	7%	0%	0%	315
		B	0%	14%	15%	0%	6%	0%	0%	316
		C	0%	13%	18%	0%	8%	0%	0%	315
		D	0%	9%	14%	0%	3%	0%	19%	315
		F	0%	15%	16%	0%	5%	0%	0%	315
Doswell	Stagg Creek	A	0%	5%	17%	0%	1%	0%	0%	316
		D	0%	3%	17%	0%	0%	0%	0%	315
	Vinita	K	0%	1%	17%	0%	1%	0%	0%	315
		L	0%	2%	12%	0%	7%	0%	0%	315
	Newfound	M	0%	1%	19%	0%	1%	0%	0%	315
		O	3%	1%	6%	0%	7%	0%	0%	315
Manassas	Poolesville	A	0%	1%	1%	1%	18%	0%	0%	312
		E	0%	3%	2%	0%	16%	1%	0%	315
		G	0%	5%	10%	3%	1%	1%	0%	315
		I	7%	1%	5%	10%	0%	0%	0%	315
		J	5%	5%	18%	0%	1%	0%	0%	315
		M	1%	4%	10%	6%	7%	0%	0%	312
		O	1%	6%	13%	2%	11%	3%	0%	322
New Oxford	N/A	A	1%	4%	11%	0%	0%	0%	0%	315
		D	5%	3%	7%	0%	0%	0%	0%	315
		E	0%	7%	5%	0%	0%	0%	0%	315
		H	4%	3%	18%	0%	0%	0%	0%	315
		J	3%	6%	15%	0%	0%	0%	0%	315
		L	7%	3%	30%	0%	3%	0%	0%	315

## APPENDIX II

### Glossary of Geologic terms

- Alleghanian** - Referring to the mountain building episode that created the Appalachian Mountains, circa 250 Mya.
- Alluvial fan** - A wedge of sediment, typically shaped like a fan, that accumulates where streams emerge from a steep canyon onto a flat area.
- Anticline** - A convex upward bend in rock, the central part of which contains the oldest section of rock.
- Anticlinorium - A broad upward bend in the Earth's crust made up of a series of anticlines and synclines that, taken together, has the general outline of an arch.
- Arkosic** - A sandstone type where feldspar makes up more than 25% of the detrital grains.
- Argillaceous** - Containing significant amounts of clay.
- Bedding** - Original or depositional layering in sedimentary rocks. Also called stratification.
- Bedrock** - Solid rock that underlies unconsolidated material, such as soil.
- Bioturbation** - The destruction of layering in strata by movement of biota in the soft sediment.
- Breccia** - A clastic rock composed of particles more than 2 millimeters in diameter and marked by the angularity of its component grains and rock fragments.
- Carbonate** - One of several minerals containing one central carbon atom with strong covalent bonds to three oxygen atoms and typically having ionic bonds to one or more positive ions.
- Caliche** - A soil layer composed of small carbonate nodules. Characteristic of arid climates.
- Chert** - A fine-grained rock made of microcrystalline quartz.
- Chronostratigraphic** - Aspect of stratigraphy dealing with the study of the age of rock strata in a region and their temporal relationship with other strata.
- Colluvium** - A sedimentary deposit formed by the movement of unconsolidated material down steep slopes.
- Clastic rock** - A sedimentary rock composed of fragments of pre-existing rocks.
- Cross-bedding** - The arrangement of sedimentary beds tilted at different angles to each other, indicating that the beds were deposited by flowing wind or water.
- Conglomerate** - A clastic rock composed of particles more than 2 millimeters in diameter and marked by the roundness of its component grains and rock fragments.
- Dolomite** - A carbonate rock made up of more than 50 percent of the mineral calcium-magnesium carbonate  $\text{CaMg}(\text{CO}_3)_2$ .
- Evaporite** - A sedimentary rock or mineral formed by precipitation from evaporating waters.
- Fanglomerate** - Stratified alluvial fan material composed of pebbles to cobbles and deposited in the shape of a fan.
- Fault** - A fracture dividing a rock into two sections that have visibly moved relative to each other.
- Ferruginous** - A rock rich in iron minerals.
- Fracture** - A crack or break in rock.
- Graben** - A down dropped block of rocks formed by normal faulting.
- Grainstone** - A limestone composed of carbonate grains or sand-sized clasts.
- Graywacke** - A sandstone composed of fragments of preexisting rocks.
- Interbedded** - Alternations of layers of rock with beds of a different kind of rock.
- Intraclast** - A limestone clast that has been broken by depositional processes.
- Lacuna** - A gap in deposition, formation or time.
- Listric** - A fault whose angle decreases with depth and may turn horizontal.
- Lithology** - Referring to the composition and character of a specific rock type.
- Lithofacies** - A laterally continuous body of rock of similar character.

**Lithosome** – A body of rock with roughly the same character.

**Metasediment** – Sedimentary rocks that have been metamorphosed.

**Metavolcanic** – Metamorphosed volcanic deposits.

**Orogeny** - An episode of mountain building or deformation.

**Packstone** - A limestone composed of a mixture of lime mud and carbonate grains.

**Pedogenic** – Created during soil formation.

**Phyllite** - A fine grained rock formed by the metamorphism of shale.

**Poikilotopic** - fabric of a crystalline cement in which the constituent crystals are multisized and enclose smaller detrital grains

**Polymictic** – A clastic rock, usually a conglomerate, composed of clasts of varying multiple lithologies.

**Quartzite** - An extremely durable, nonfoliated metamorphic rock derived from pure sandstone and consisting primarily of quartz.

**Rift** - A zone where the Earth's crust is being pulled apart, usually forming grabens.

**Sandstone** - A clastic sedimentary rock composed of particles that range in diameter from 1/16 millimeter to 2 millimeters in diameter. Sandstones make up about 25% of all sedimentary rocks.

**Shale** - A clastic sedimentary rock composed of clay particles.

**Siliciclastic** - Referring to a rock composed of clasts made of quartz.

**Slickensides** - A polished rock surface created by frictional movement of rocks.

**Strata** - An individual layer of a sedimentary rock.

**Stratigraphic** - Referring to the study of multiple strata.

**Subarkosic** – A sandstone with less than 25% feldspar.

**Synclinorium** - A regional series of synclines and anticlines grouped together that have the general outline of a trough.

**Thalweg** – The area of deepest development of a trough or channel.



Larry Hogan

*Governor*

Boyd K. Rutherford

*Lt. Governor*

Jeannie Haddaway-Riccio

*Secretary*

A message to Maryland's citizens

The Maryland Department of Natural Resources (DNR) seeks to balance the preservation and enhancement of the living and physical resources of the state with prudent extraction and utilization policies that benefit the citizens of Maryland. This publication provides information that will increase your understanding of how DNR strives to reach that goal through the earth science assessments conducted by the Maryland Geological Survey.

MARYLAND DEPARTMENT OF NATURAL RESOURCES

Resource Assessment Service

Tawes State Office Building

580 Taylor Avenue

Annapolis, Maryland 21401

Toll free in Maryland: 877-620-8DNR

Out of State call: 410-260-8021

TTY users: Call via the Maryland Relay

[Internet Address: dnr.Maryland.gov](http://dnr.Maryland.gov)

MARYLAND GEOLOGICAL SURVEY

2300 St. Paul Street

Baltimore, Maryland 21218

Telephone Contact Information: 410-554-5500

[Internet Address: mgs.md.gov](http://mgs.md.gov)

DNR Publication No. 12-041720-225-2020



*The facilities and services of the Maryland Department of Natural Resources are available to all without regard to race, color, religion, sex, sexual orientation, age, national origin or physical or mental disability. This document is available in alternative format upon request from a qualified individual with a disability.*